2mit

SQT

(NASA-CR-133810) PRELIMINARY DESIGN OF A MINI-BRAYTON COMPRESSOR-ALTERNATOR-TURBINE (CAT) Final Report (AiResearch Mfg. Co., Phoenix, Ariz.) 103 p HC $7.25 CSCL 13I G3/15

N73-30463

Unclas 12884

# FINAL REPORT

## PRELIMINARY DESIGN OF A MINI-BRAYTON COMPRESSOR-ALTERNATOR-TURBINE (CAT)

## CONTRACT NAS3-16739

PREPARED BY
CLOSED CYCLE POWER PROJECT
AIRESEARCH MANUFACTURING COMPANY
PHOENIX, ARIZONA 85034

PREPARED FOR
NASA-LEWIS RESEARCH CENTER
CLEVELAND, OHIO 44135



APS-5440-R MARCH 12, 1973

FINAL REPORT
PRELIMINARY DESIGN OF A MINI-BRAYTON
COMPRESSOR-ALTERNATOR-TURBINE
(CAT)
CONTRACT NAS3-16739

APS-5440-R March 12, 1973

**Prepared by:** Engineering Staff/DLA

**Approved by:** A. Pietsch
A. Pietsch, Closed Cycle
Power Project

AIRESEARCH MANUFACTURING COMPANY OF ARIZONA
A DIVISION OF THE GARRETT CORPORATION

REPORT NO. APS-5440-R

TOTAL PAGES 100

ATTACHMENTS:

| REV | BY | APPROVED | DATE | PAGES AND/OR PARAGRAPHS AFFECTED |
| --- | --- | --- | --- | --- |
| | | | | |

# TABLE OF CONTENTS

# FINAL REPORT
# PRELIMINARY DESIGN OF A MINI-BRAYTON COMPRESSOR - ALTERNATOR - TURBINE (CAT)
# CONTRACT NAS3-16739

## 1. INTRODUCTION AND SUMMARY

This report, prepared by AiResearch Manufacturing Company of Arizona, A Division of The Garrett Corporation, is presented in fulfillment of the data requirements of the Mini-Brayton Contract NAS3-16739. This program consists of the following four tasks pertaining to the study of a 0.5 to 2.0 $kw_e$ closed Brayton cycle power system.

Task I - Parametric Study
Task II - Off-Design Study
Task III - Preliminary Design
Task IV - Reporting

Many space missions encompassing near earth orbit, interplanetary and deep space vehicles are planned for the next twenty years. These missions will require an electrical power source which can supply from several hundred watts to a few thousand watts of power. Among the leading candidate power systems are isotope-Brayton, reactor thermoelectric (RTG) and solar-plus storage battery systems.

In the required power range, isotopic fuels offer the most promise as a heat source from which to make electricity. Since isotopes are costly, it follows that the efficiency of the power conversion system must be high. Of the three systems mentioned, the Brayton system has the best potential for high efficiency.

Missions of many years duration require a power conversion system of unprecedented reliability. The system must be able to operate without human attendance, must supply uninterrupted power, and must operate in the harsh environment of outer space. As simple a system design as possible with few moving parts and, if possible, no rubbing parts would be desirable if this high reliability is to be attained.

An extensive study was performed during 1972 by the NASA-Lewis Research Center to evaluate the isotope-Brayton electric power system. This system was compared, for several typical missions, on indices such as cost effectiveness, reliability, and performance, with other power system approaches.

The results of the study were reported in NASA TM X-68072 and presented at the Seventh IECEC in San Diego, California, on September 25-29, 1972. It was concluded that the cost effectiveness of the Brayton system depends upon the nature of the mission. For a number of unmanned satellite missions requiring from 600 to 3000 watts electric, the isotope-Brayton system cost, on a "dollars-per-watt" basis, was comparable to solar array/battery systems and about one-fourth that of RTG systems. These favorable economic considerations, combined with a 10 year Brayton technology base established at NASA-Lewis, stimulated further investigation of the mini-Brayton concept.

## 1.1 General Program Description

The purpose of this mini-Brayton study was to further develop design philosophy for low power level isotope-Brayton systems and to conduct a preliminary design for the rotating component of the system. The study has stressed, during Tasks I and II, the following design criteria:

(a) Simplicity of design

(b) High reliability

(c) Long life (five to ten years)

(d) High efficiency at low power level

(e) Minimum extrapolation of proven technology

(f) System versatility

Also an important goal for the design presented herein was mission versatility. It is desirable, particularly from a cost standpoint, to select one system that may be easily adapted to various mission power requirements.

The schedule for the study program is shown in Figure 1-1. The contract start date was June 26, 1972. The results of the study have, to date, been very encouraging and some important design philosophy relative to very small Brayton systems has been postulated, explored, and defined. The reference cycle and system components are described in Section 1.3 of this report.

The balance of the study, Task III, was devoted to a preliminary design of the mini-Brayton (a schematic is presented in Figure 1-2 and a cross section is shown in Figure 1-3). The unique design features incorporated into the design include:

(a) Hydrodynamic (self-pressurized) foil gas bearings

(b) Gas cooling of the alternator and bearings (liquid loops not required anywhere in the power system--a direct or gas flow radiator is used)

(c) A solid rotor Rice alternator

(d) Motor start up of the CRU (combined rotating unit)

# MINI-BRAYTON STUDY PROGRAM SCHEDULE

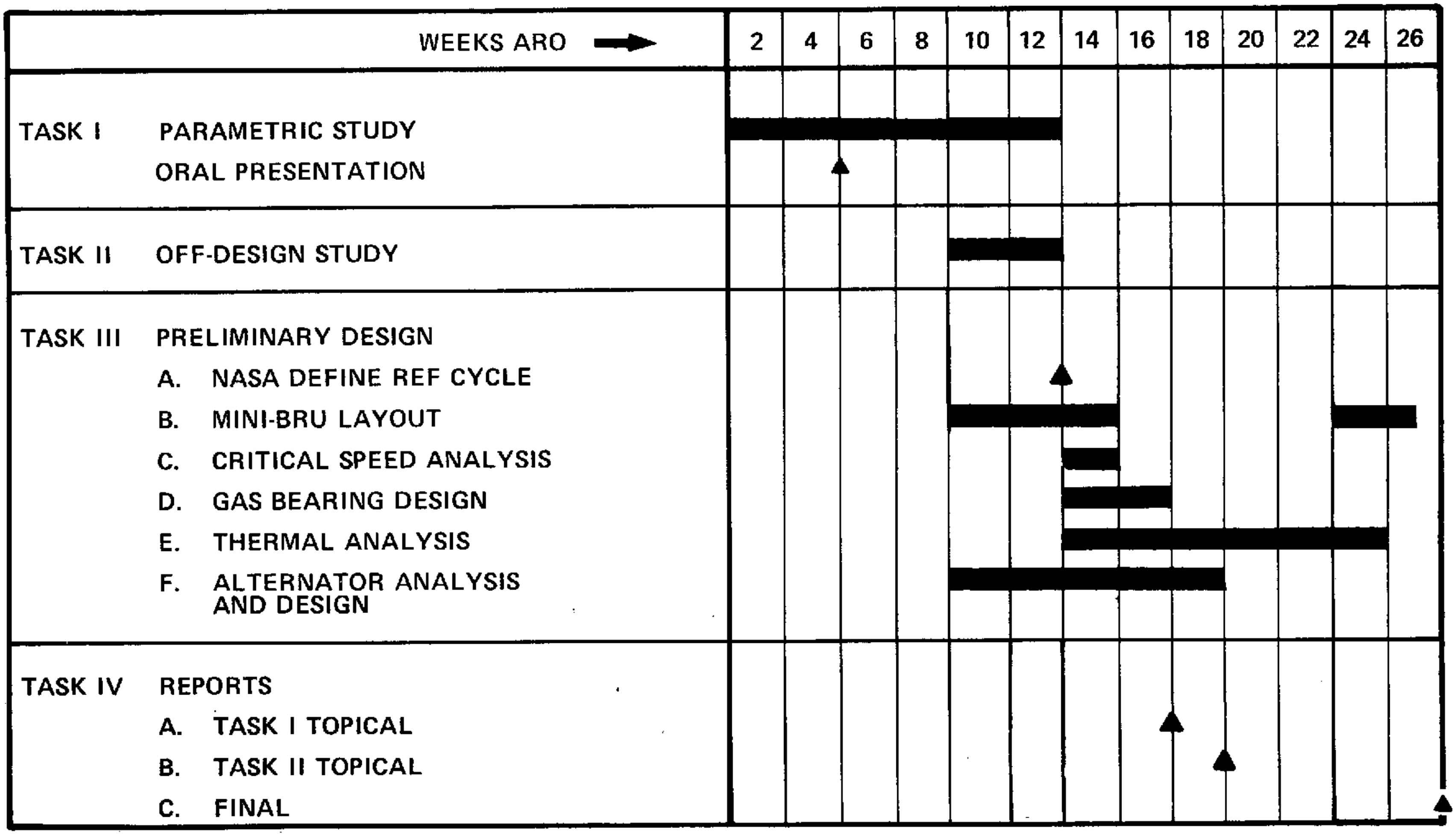


MS 3011-1

TASK I START DATE JUNE 26, 1972

FIGURE 1-1

# MINI-BRU CYCLE SCHEMATIC

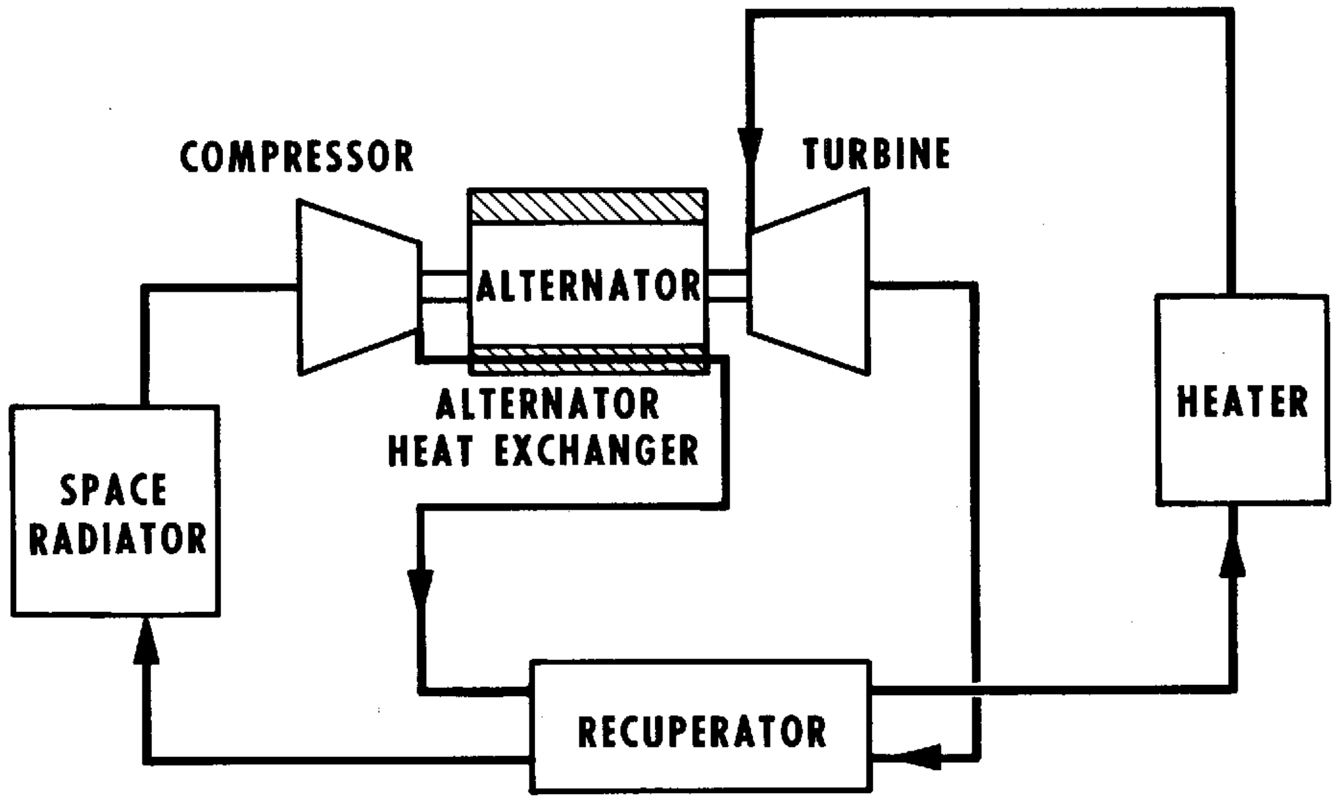


MS 3063-1

FIGURE 1-2

# MINI-BRAYTON ENGINE

## 0.5 TO 2.0 KWe

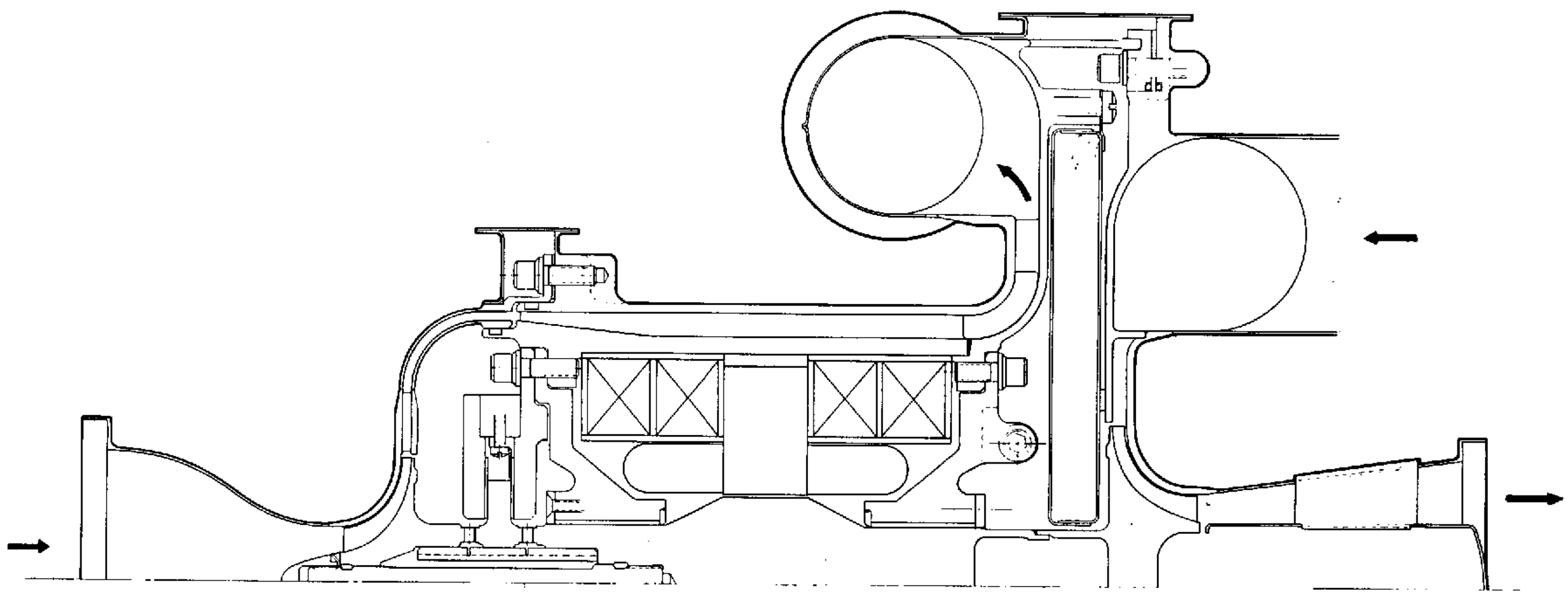


MS 3063-7

FIGURE 1-3

Further discussion of the study objectives and guide lines is included in Section 1.2.

## 1.2 Program Objectives

Table 1-1 lists the program design goals. Optimum system characteristics over the entire power output range were determined by performing a wide-range parametric study. Mathematical models, in the form of a series of digital computer programs are used during the optimization procedure. These models, whose accuracy has been proven through correlation with test data for components and also for complete systems, provide the capability to explore design questions in great scope and depth in a short period of time.

A further important objective of Task I was, having defined component design characteristics, to assess the ability to develop those components to the degree necessary within the limitations of present technology. This is done by comparing the design requirements to those already proven with existing hardware.

Task II was performed using a sophisticated off-design performance computer program. With this program, the off-design performance of a fixed hardware system (i.e. a particular and unique system design) can be predicted. This program has been verified by comparison to actual systems in operation. Important conclusions were drawn from the Task II study relative to the number and type of systems required to cover the power spectrum of interest.

An additional important facet of the study was the determination of system performance sensitivity to the various individual design parameters. This question was studied in two parts. The first was the impact on system optimization of constraints placed on component performance. The second was the evaluation of the impact on system performance and/or weight of a component unable to meet its design goal (assuming this was discovered during the development program).

TABLE 1-1

PROGRAM OBJECTIVES

TASK I: <u>Parametric Study Over Power Range</u>

- o Define optimum system characteristics
- o Determine system performance sensitivity to individual design parameters
- o Assess compatibility of system designs and existing technology base

TASK II: <u>Off-Design Performance</u>

- o Determine reference system design point
- o Select reference system components
- o Determine the number of unique engine designs required to cover power level spectrumm

TASK III: <u>Preliminary Design</u>

- o Compressor design integration with alternator heat exchanger
- o Gas bearings (minimize losses)
- o Thermal design (gas cooling)
- o Alternator - EM design and motor starting capability

The objectives of the program were to be pursued while constraining the study within certain fundamental guidelines. These guidelines were specified by the NASA, by the contract, and by technical directive during the conduct of the study. These are summarized in Table 1-2.

TABLE 1-2

MINI-BRAYTON STUDY GUIDELINES

General

- System heat derived from 1, 2 or 3 isotope heat source capsules, each having a 2400 watt capacity
- Component sizing and performance predictions based upon emperical data base
- System fixed weights supplied by the NASA
- System parasitic losses (electronic) supplied by the NASA
- Meteoroid criteria defined in NASA SP-8013
- Armor protection--(Refer to Astronautics and Aeronautics, Power Systems for Space Flight Volume II, Academic Press, 1962, Pages 551-579)

Specific

- Assume turbine inlet temperature = 1600°F
- Assume use of a gas radiator with stainless steel tubes
- Assume use of foil gas bearings
- Alternator hot spot limit = 400°F
- Radiator sink temperature = -10°F

## 1.3 Conclusion and Summary Data

### 1.3.1 Conclusions

The conclusions drawn from this study have been quite encouraging. All of the key design goals, summarized in Table 1-3, were achieved.

Table 1-4 shows the results of the study to determine development risk. Forced variation in individual parameters were made by using the off-design computer model of the system. In every instance, a performance loss was prevented by assuming that the radiator surface area would be increased (resulting in a lower compressor inlet temperature). Hence, radiator size and weight can be used as a common index for assessing system weight penalty. It can be seen that for all of the parameters, the resulting weight penalty is modest.

All Task III key design goals were achieved, as summarized in Table 1-5.

TABLE 1-3

TASK I AND TASK II CONCLUSIONS

- A single set of hardware would operate efficiently over the entire power range
- The best design point was at the three heat source capsule condition
- Any mission requiring up to approximately 2500 watts could be satisfied with a single system comprised of the reference recuperator and Brayton Rotating Unit (BRU) hardware and the reference radiator or a space radiator sized specifically for the mission. (The reference components are described in Section 1.3.2).
- The development risk involved in the selected design is low, both in terms of compatibility of design with existing technology and in program impact due to component performance variation.

TABLE 1-4

DEVELOPMENT RISK ASSESSMENT

| | Design Value | Potential Deviation | *Penalty (lbs) |
|---|---|---|---|
| $T_1$ | 536 | -- | -- |
| $\eta_c$ | 76.1 | -2% | 16 |
| $\eta_t$ | 83.2% | -2% | 32 |
| $\beta$ | 0.980 | -0.012 | 11 |
| $E_r$ | 0.975 | -0.010 | 12 |
| $r_c$ | 1.50 | -- | -- |
| N | 52000 rpm | -- | -- |
| $\eta_g$ | 0.917 | -0.010 | 2 |
| $N_{sc}$ | 0.07 | -- | -- |
| $T_{SINK}$ | 450 | +10°R | 5 |

*Weight increase due to enlarging radiation surface

TABLE 1-5

TASK III CONCLUSIONS

- HIGH LEVEL OF CONFIDENCE IN DESIGN
  - Gas cooling of alternator
  - No critical speed problems
  - Hydrodynamic gas bearings
- ONE ROTATING UNIT CAN COVER 0.5 - 2.0 $KW_e$ APPLICATIONS
- HIGH RELIABILITY
- HIGH EFFICIENCY
- LOW COST DESIGN

### 1.3.2 Summary Data

The initial part of the study was intended to not only result in selection of a specific reference cycle but to also define the general characteristics of low output closed Brayton cycle systems. Figure 1-4 shows the general case data. The line which is an envelope of and is tangent to the lines defining the minimum specified weight for a fixed number of heat source capsules itself defines the minimum specific weight achievable at any power level if the system is optimized at that power level. A real system, designed according to the constraints and guidelines imposed by this study, cannot be designed to fall below the general boundary shown.

Figure 1-5 shows the results of a study to define systems using a basic configuration (fixed hardware) of CRU and recuperator, combined with various numbers of multi-hundred watt heat sources and radiators of various sizes and configurations. In this study, the radiator parameters that were varied were surface area and radiator core pressure drop. This data is very useful for mission planning. For a given mission, one can determine the power conversion system weight and the number of heat source capsules required to produce the desired electrical power.

The reference cycle resulting from the study is also plotted in Figure 1-5. The complete definition of the reference cycle is shown in Figure 1-6. The off design performance and weight summaries of the reference design are presented in Table 1-6 and 1-7, respectively.

# SYSTEM SENSITIVITY TO RECUPERATOR EFFECTIVENESS

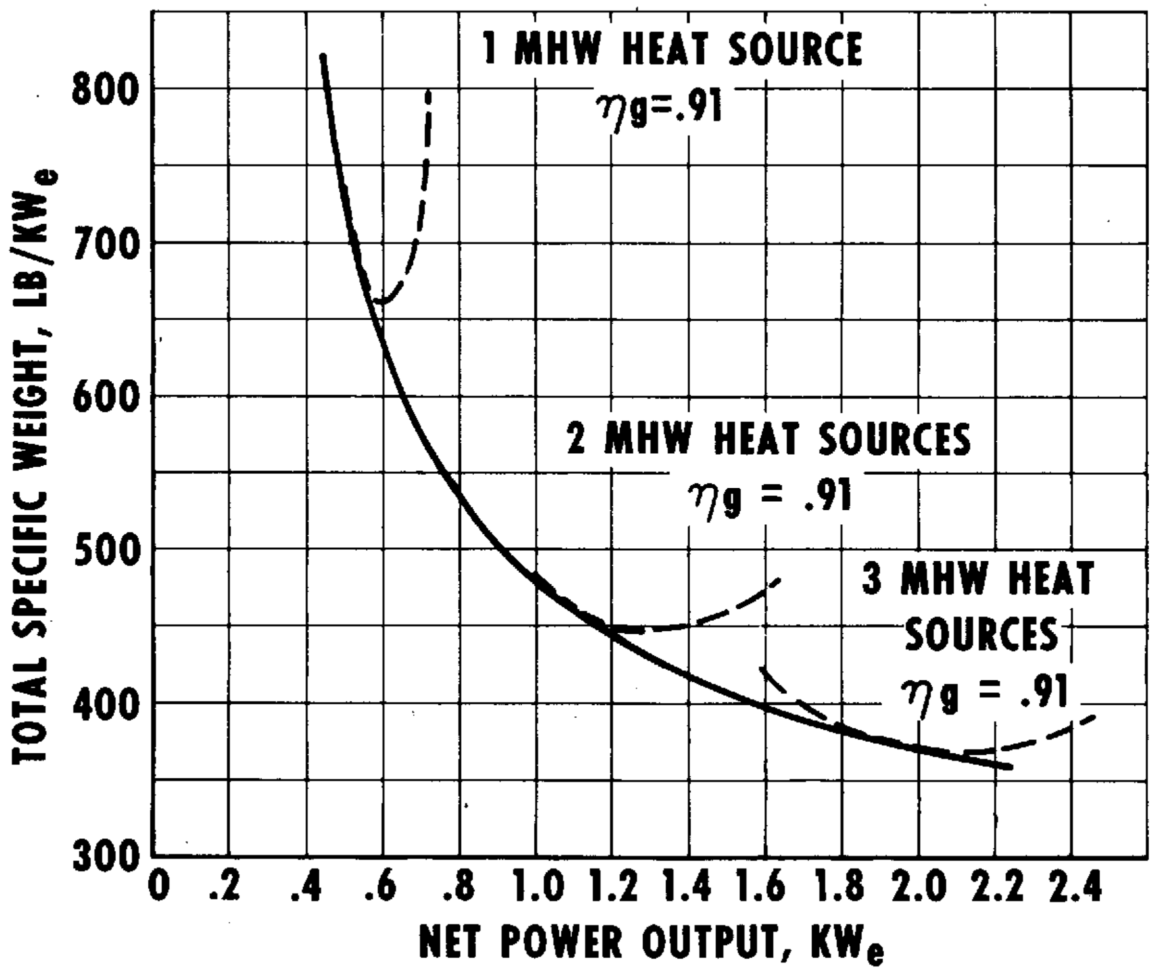


MS 3063-8

FIGURE 1-4

# RADIATOR CONFIGURATION OPTIMIZATION

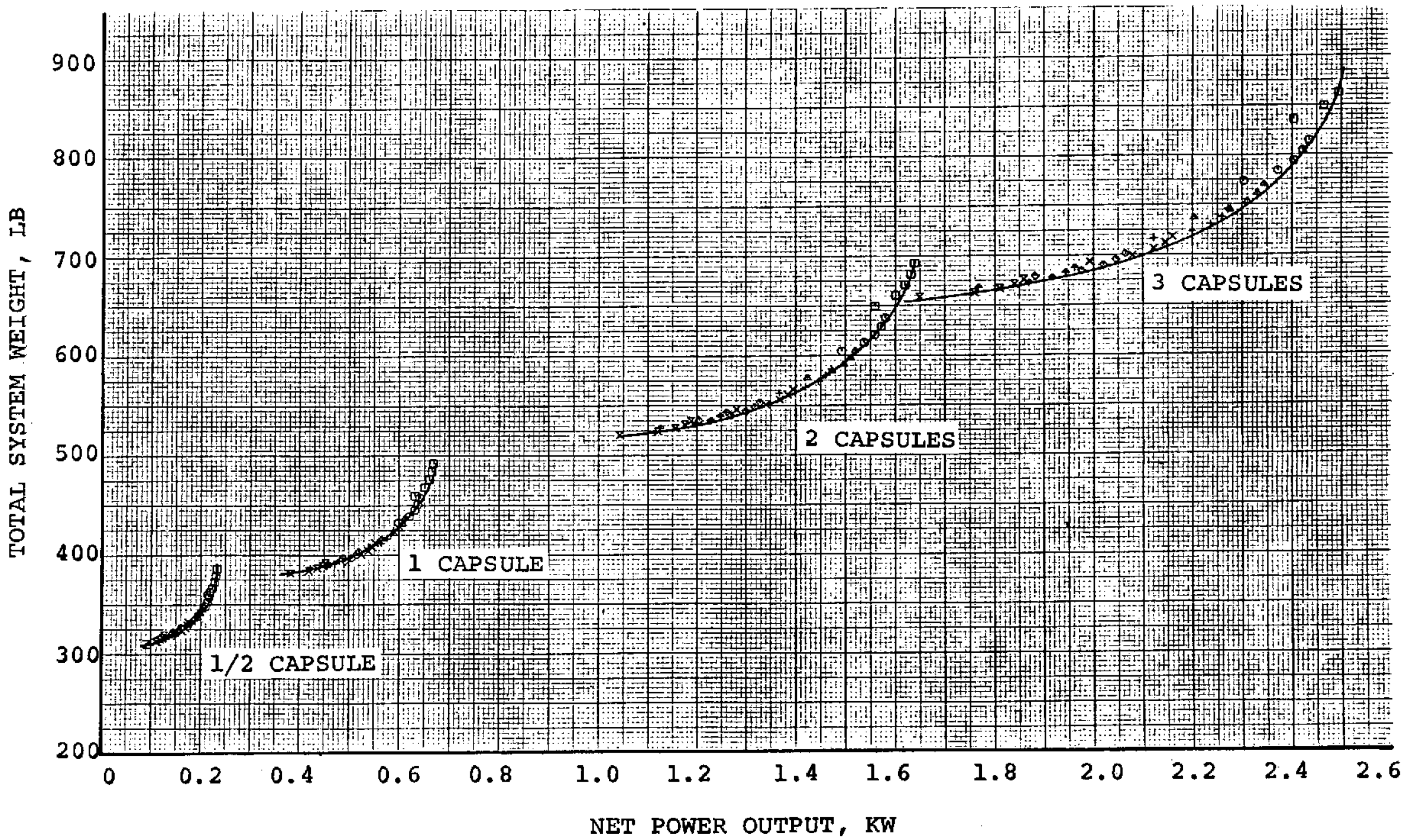


FIGURE 1-5

# THREE CAPSULE MINIMUM SPECIFIC WEIGHT REFERENCE CYCLE

| | |
|---|---|
| SHAFT SPEED | 52,000 RPM |
| BEARING LOSS | 241 WATTS |
| ALT. WINDAGE | 68 WATTS |
| ALT. EFFICIENCY | 91.7% |

| | |
|---|---|
| RADIATOR AREA | 125 $FT^2$ |
| CONTROL POWER | 81 WATTS |
| NET OUTPUT | 2013 WATTS |

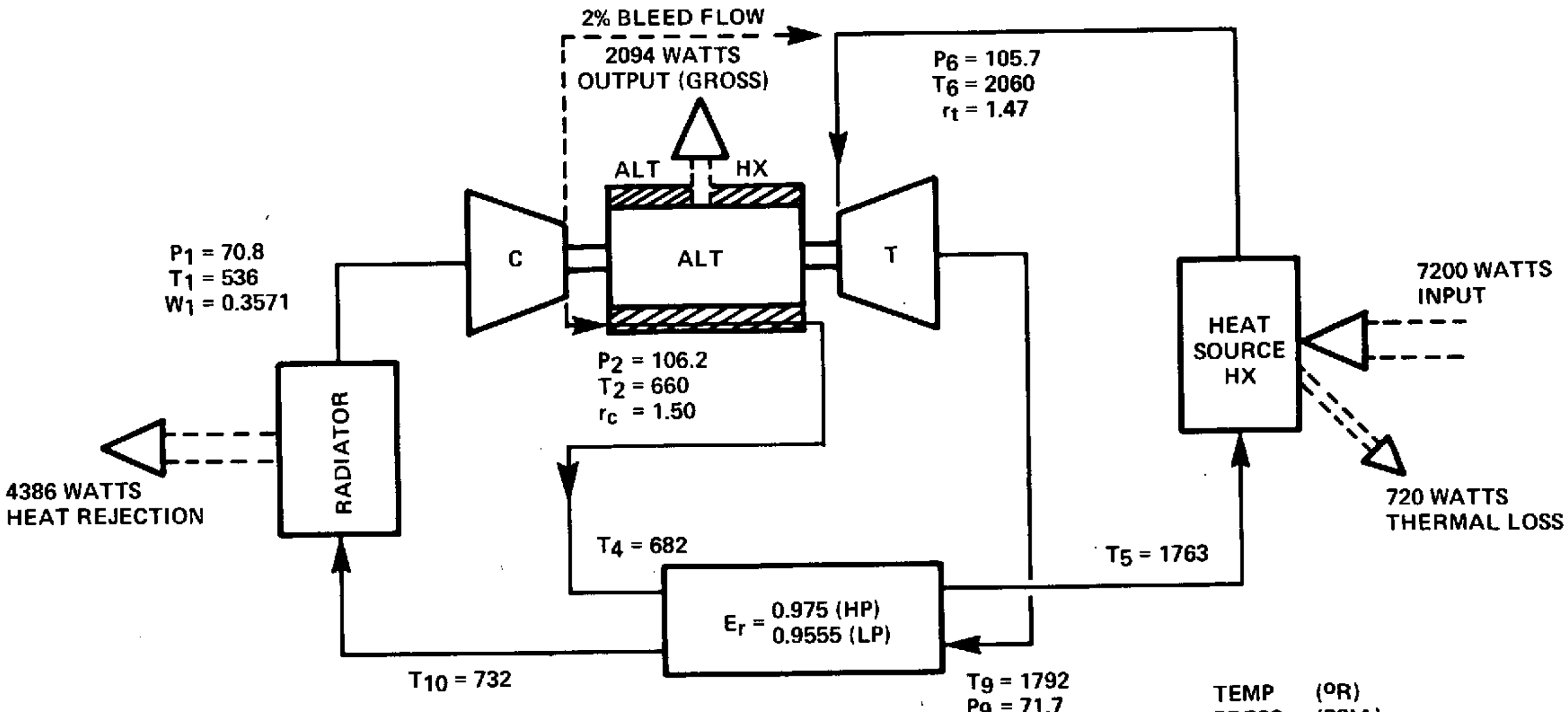


| | |
|---|---|
| TEMP | ($^oR$) |
| PRESS. | (PSIA) |
| FLOW | (LBS/SEC) |

MS 3063-9

FIGURE 1-6

The design and performance details for the reference system radiator, recuperator, and CRU are summarized in Tables 1-8, 1-9, and 1-10.

TABLE 1-6

SYSTEM PERFORMANCE AT THREE POWER LEVELS

| | Number of Capsules | | |
|---|---|---|---|
| | 3 | 2 | 1 |
| Alternator output power, kw | 2.094 | 1.443 | 0.633 |
| Control power, kw | 0.082 | 0.069 | 0.053 |
| Net cycle efficiency, percent | 28.0 | 28.6 | 24.2 |
| Compressor efficiency, percent | 76.1 | 76.1 | 75.8 |
| Turbine efficiency, percent | 83.2 | 82.0 | 79.7 |
| Alternator efficiency, percent | 91.7 | 92.1 | 90.2 |
| Lost pressure ratio parameter ($\beta$) | 0.98 | 0.975 | 0.961 |
| Recuperator effectiveness ($E_r$) | 0.975 | 0.980 | 0.981 |
| Compressor inlet temperature, °R | 536 | 502 | 469 |
| Compressor inlet pressure, psia | 70.8 | 44.2 | 21.0 |
| Compressor pressure ratio | 1.5 | 1.54 | 1.59 |
| Bearing loss, kw | 0.241 | 0.209 | 0.180 |
| Windage loss, kw | 0.068 | 0.047 | 0.025 |
| Compressor flow rate, lb/sec | 0.357 | 0.236 | 0.117 |
| Turbine inlet temperature, °R | 2060 | 2060 | 2060 |
| CRU speed, rpm | 52,000 | 52,000 | 52,000 |

TABLE 1-7

SYSTEM WEIGHT FOR THREE POWER LEVELS

| | Number of Capsules (wt in lbs) | | |
|---|---|---|---|
| | 3 | 2 | 1 |
| Combined rotating unit | 31 | 31 | 31 |
| Recuperator | 106 | 106 | 106 |
| Radiator | 160 | 160 | 160 |
| Ducting (hot end only) | 12 | 10 | 8 |
| Capsule and HSHX | 306 | 204 | 102 |
| Super insulation | 78 | 72 | 66 |
| Structure | 55 | 53 | 51 |
| PLR | 20 | 15 | 10 |
| Electronics | 15 | 15 | 15 |
| TOTAL | 783 | 666 | 549 |

Fixed weights to be used in system specific weight estimates are:

| Number of MHW capsules | 1 | 2 | 3 |
|---|---|---|---|
| Capsule and HSHX weight (lb) | 102 | 204 | 306 |
| Super insulation weight (lb) | 66 | 72 | 78 |
| Structure weight (lb) | 51 | 53 | 55 |
| Parasitic load resistor weight (lb) | 10 | 15 | 20 |
| Electonrics weight (lb) | 15 | 15 | 15 |

Cycle effiency and system specific weight had been defined as:

Gross cycle efficiency =

$$\frac{\text{Gross power at alternator terminals}}{\text{Heat input to cycle working fluid}}$$

System specific weight (lb/kw) =

$$\frac{\text{Total of variable weights}}{\text{Gross power at alternator terminals}}$$

To achieve consistency in reporting efficiency and specific weight, the following terminology and computing methods were adopted:

Buss bar efficiency =

$$\frac{\text{Power at alternator terminals - electronic losses}}{\text{2400 watts X number of MHW capsules}}$$

Specific weight (lb/kw) =

$$\frac{\text{Total weight (including fixed weights)}}{\text{Power at alternator terminals - electronic losses}}$$

TABLE 1-8

MINI-BRU REFERENCE RADIATOR
STAINLESS STEEL/ALUMINUM ARMOR AND FINS

| | | |
|---|---|---|
| Total area, $ft^2$ | 125.3 | |
| Gas flow rate, lb/sec | 0.3573 | (XeHe 83.8) |
| Tube length, ft | 8.3205 | |
| Radiator diameter, ft | 4.8 | |
| Inlet temperature, °F | 733.1 | |
| Outlet temperature, °F | 536 | |
| SS tube wall thickness, in. | 0.030 | |
| Fin thickness, in. | 0.040 | |
| Armor thickness, in. | 0.0716 | |
| Number of tubes | 41 | |
| Tube spacing, in. | 4.4 | |
| Header dimension, in. | 1.5224 | |
| Header weight, lb | 33.1 | |
| Core weight, lb* | 117.6 | |
| Total weight, lb | 160.3 | |
| Sink temperature, °F | 450 | |

*Includes stainless steel tubes, fins, coating, and armor.

TABLE 1-9

MINI-BRAYTON
REFERENCE RECUPERATOR
STAINLESS-STEEL/NICKEL
PLATE-FIN CONFIGURATION

| | |
|---|---|
| Weight, lb | 106 |
| Width, in. | 5.023 |
| Height, in. | 9.646 |
| Core length, in. | 24.427 |
| Overall length, in. | 28.777 |
| Splitter plate thickness, in. | 0.008 |
| Side plate thickness, in. | 0.100 |
| Low pressure side | |
| Splitter plate spacing, in. | 0.101 |
| Fin thickness, in. | 0.004 |
| Fin length, in. | 0.100 |
| Number of fins per in. | 20 |
| High pressure side | |
| Splitter plate spacing, in. | 0.101 |
| Fin thickness, in. | 0.004 |
| Fin length, in. | 0.100 |
| Number of fins per in. | 20 |
| Total fractional pressure drop | 0.006968 |

TABLE 1-10

REFERENCE CRU DATA

| | |
|---|---|
| Total CRU weight, lb | 31 |
| CRU rotating speed, rpm | 52,000 |
| <u>Turbine Data</u> | |
| Diameter, in. | 3.0 |
| Pressure ratio | 1.47 |
| Efficiency | 0.832 |
| <u>Compressor Data</u> | |
| Diameter, in. | 2.3 |
| Pressure ratio | 1.50 |
| Efficiency | 0.761 |
| Foil journal bearing diameter, in. | 1.0 |
| Thrust bearing ID, in. | 1.0 |
| Thrust bearing OD, in. | 1.75 |
| <u>Alternator Physical Data</u> | |
| Total weight, lb | 10.42 |
| Rotor weight, lb | 1.053 |
| Rotor diameter, in. | 1.5 |
| Rotor length, in. | 3.72 |
| Frame OD, in. | 4.14 |
| Frame width, in. | 3.38 |
| Stack length, in. | 0.72 |
| <u>Alternator EM Efficiency</u> | 0.917 |

# 2. TASK I - PARAMETRIC STUDY AND TASK II - OFF DESIGN STUDY

## 2.1 Summary of Analytical Approach

Details of the Task I and Task II analyses, including the method used to achieve system optimization and a description of the analytical tools employed are described in this section. The rationale leading to the selection of the reference system and many design approaches investigated prior to the final selection are also discussed. The component selection justification is documented, as well as a review of the important design considerations for the various components.

The data generated during this part of the study is the result of the application of a cascading series of the most sophisticated computer design tools existing in the aerospace industry. The automated procedure goes from basic thermodynamic cycle optimization to detail component sizing to automatic machine plotting of the results.

### 2.1.1 System Specifications

The specifications designated by the NASA defined the parametric and geometric ranges to be covered in the study. These were:

(a) Compressor

(1) Cycle temperature ratio: $T_1/T_2$

(2) Pressure ratio: 1.6 through 2.2

(3) Slip factor (defined as $\frac{\text{tangential gas velocity}}{\text{wheel tip speed}}$)

(b) Turbine

(1) Specific speed

(2) Lost pressure ratio: $\beta$ factor, where $\beta = r_t/r_c$
$r_t/r_c = 0.92, 0.94, 0.96$

(c) Working Fluid

(1) He/Xe, Mw = 60, 83.8, 39.94

(2) Argon

(3) Krypton

(d) Rotating speed = 48,000 rpm - 60,000 rpm

(e) Recuperator

(1) Various core geometries

(2) Effectiveness = 0.90, 0.925, 0.95

(f) Radiator

(1) With and without internal fins in tubes

(2) Various internal fin geometries

(3) All aluminum construction

(4) Stainless steel tubes and headers with aluminum armor and fins

(g) Heat source H/X (*): Vary cores

(h) Alternator H/X: Vary cores

### 2.1.2 Data Requirements

The study results were to include but not be limited to the following system and component characteristics:

(a) Turbine and Compressor

(1) Size and weight

(2) Efficiency

(3) Pressure ratio

(4) Specific speed

(b) Alternator

(1) Physical dimensions

(2) Electromagnetic performance

(c) System

(1) Overall efficiency

(2) Component weights and sizes

*Sketches and design considerations for the heat source were furnished by the NASA.

(3) Molecular weights (fluid)

(4) Duct sizes

(5) Flow rates

(6) State points (pressure and temperature)

(d) Windage Losses

(e) Bearing Losses

### 2.1.3 Analytical Procedure or Methodology

The study progresses from wide range parametric studies in the initial phases, resulting in later elimination by inspection of a large number of systems.

After the envelope was defined for minimum weight systems over the entire power level range (refer to Figure 1-4), only specific system designs lying close to that envelope were investigated further.

Several of AiResearch's component and cycle design computer programs were merged in order to define the geometry and performance of a complete closed, recuperated Brayton cycle power system. During the Task I study, literally tens-of-thousands of complete systems were designed, sorted and machine-plotted in order to define the minimum envelope of weight and power. Figure 2-1 describes, schematically, the analytical procedure:

# POWER SYSTEM DESIGN METHODOLOGY

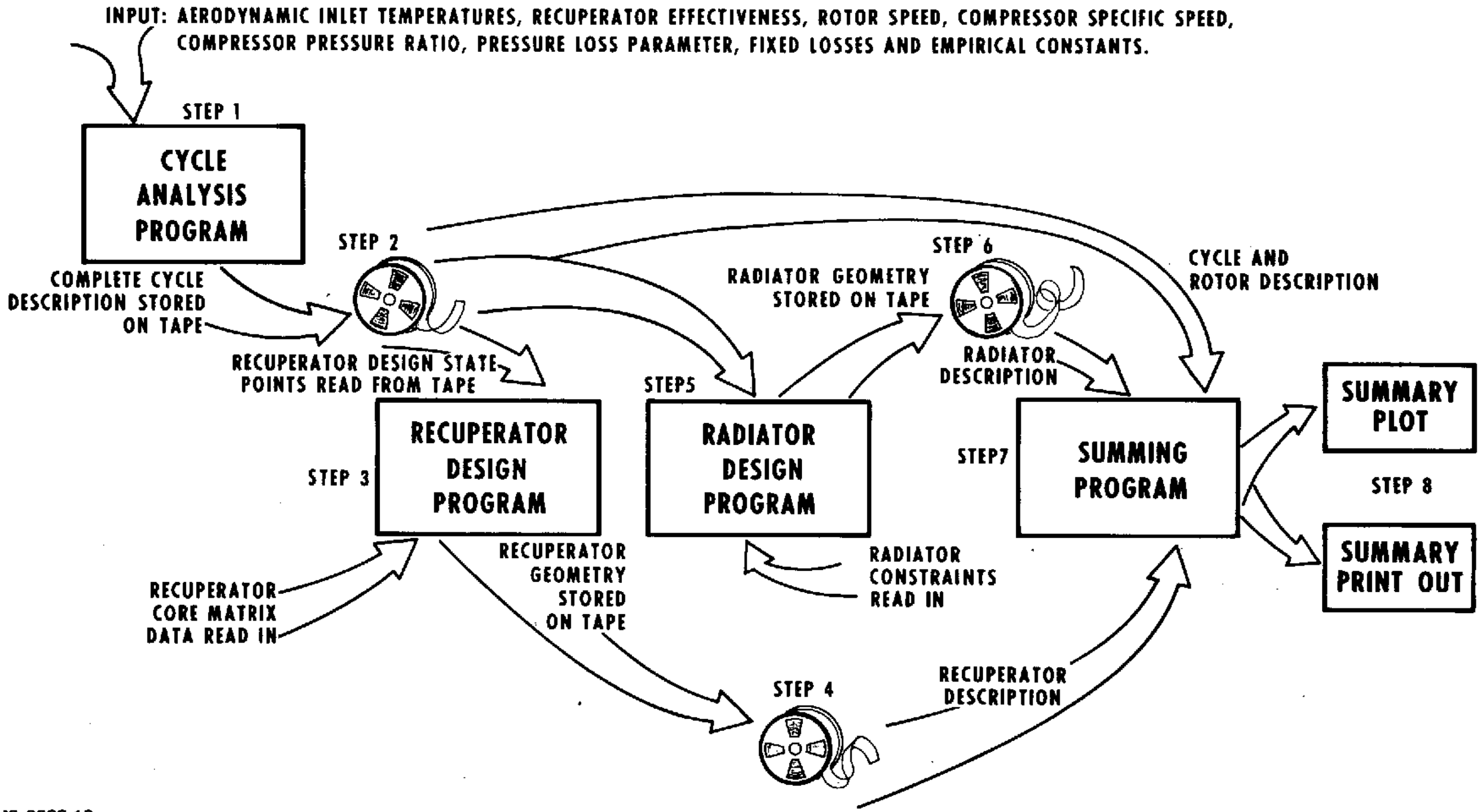


MS 3063-10

FIGURE 2-1

Step 1

As can be seen in Figure 2-1, the input to the cycle design portion of the analysis consists mainly of the aerodynamic, thermodynamic and empirical specifications of the desired systems. These values include:

- Desired recuperator effectivenesses (up to 12 values) - $E_r$
- Desired rotor speed (up to 12 values) - N
- Desired compressor specific speed (up to 12 values) - $N_{s_c}$
- Desired compressor pressure ratio (up to 12 values) - $r_c$
- Desired compressor inlet temperature (up to 12 values) - $T_1$
- Desired turbine inlet temperature - $T_6$
- Desired output power or input power (up to 12 values) - PWR
- Compressor bleed fraction (up to 12 values) - BL
- Desired pressure loss distribution (up to 12 values) - $\Delta P/P$
- Predicted alternator efficiency - $\eta g$
- Specification of working fluid properties
- Desired compressor slip factor, turbine velocity factor and turbine diffuser recovery - SC, $F_v$, CPR
- Bearing power loss - $PWR_b$
- Alternator sizing coefficient - $C_g$

Inherent to the cycle program are also empirical data bases for turbomachinery efficiency predictions (based on Reynold's number, size, pressure ratio and specific speed) and for alternator windage calculation.

When a cycle definition is complete, the following values have been generated:

- Compressor, turbine and alternator diameter
- Compressor, turbine and alternator efficiency
- Rotating group weight
- Gross alternator electrical output
- Alternator windage
- Gross cycle efficiency
- All state point temperatures, pressures and fractional pressure drops

Step 2

As the data compliation for each computed cycle is completed, the pertinent parameters are written out to magnetic tape storage for further processing upon completion of the cycle analysis. When the desired range of cycle parameters has been explored and the output from each stored, the analysis proceeds into the recuperator design program. The output for each cycle can also be printed at this point. A typical print-out is shown in Figure 2-2.

# TYPICAL CYCLE DESIGN PROGRAM OUTPUT

CASE NUMBER 3

| | | | | |
|---|---|---|---|---|
| GENERATOR OUTPUT (KW) .20772E+01 | GEN.ROTOR DIAMETER (IN.) .15000E+01 | GROSS SHAFT POW.OUT. (KW) .25849E+01 | GEN. WINDAGE LOSS (KW) .72613E-01 | CYCLE EFFICIENCY (----) .32068E+00 |
| RECUPERATOR EFFECT. (----) .97500E+00 | CRU ROTATION. SPEED (RPM) .52000E+05 | BLEED FLOW FRACTION (----) .20000E-01 | COMP.TOT.TEMP.RATIO (----) .12313E+01 | PRESS. LOSS FACTOR (PRT/PRC) .98000E+00 |
| COMP. ADIAB. EFF. (----) .76127E+00 | COMPR. ROTOR DIAM. (IN.) .23003E+01 | COMPR. PRESS. RATIO (----) .15000E+01 | REQD. SURFACE FINISH (MICRO IN.) .10226E+02 | COMPR. SPEC. SPEED (----) .70000E-01 |
| TURB. ADIAB. EFF. (----) .83160E+00 | TURB. ROTOR DIAM. (IN.) .28543E+01 | TURB. PRESS.RATIO (----) .14700E+01 | TURB. ROTOR TIP SPEED (FPS) .64762E+03 | TURB. SPEC. SPEED (----) .54408E-01 |
| COMPR. + TURB. WEIGHT (LB.) .14619E+00 | GEN. PER. REY. NO. (----) .30262E+05 | COMPR. MEAN SPEC.SP. (----) .44337E+02 | COMPR. EXPAN.EFF. (----) .87925E+00 | GEN. DISK REY. NO. (----) .11351E+07 |

| COMPONENT | FLOW (LB/SEC) | INLET TEMP. (R) | INLET PRESS. (PSIA) | OUTLET TEMP. (R) | OUTLET PRESS. (PSIA) |
|---|---|---|---|---|---|
| COMPRESSOR | .35730E+00 | .53600E+03 | .70826E+02 | .65998E+03 | .10624E+03 |
| RECUPERATOR | .35016E+00 | .68319E+03 | .10589E+03 | .17638E+04 | .10553E+03 |
| HEATER | .35016E+00 | .17638E+04 | .10553E+03 | .20600E+04 | .10535E+03 |
| TURBINE | .35016E+00 | .20600E+04 | .10535E+03 | .18152E+04 | .71669E+02 |
| RECUPERATOR | .35730E+00 | .17921E+04 | .71669E+02 | .73311E+03 | .71301E+02 |
| COOLER | .35730E+00 | .73311E+03 | .71301E+02 | .53600E+03 | .71063E+02 |

FIGURE 2-2

Step 3

The core matrix data (i.e., heat transfer and pressure drop maps) and the desired margin for heat transfer and pressure drop are read-in. From the data stored for each computed cycle, the variables pertinent to recuperator design effectiveness (inlet conditions and gas properties) are obtained. One or more recuperators are designed for each computed cycle.

Step 4

The recuperator design parameters for each design are, in turn, stored on another tape. The individual recuperator designs can be called for and printed at this point. A typical print-out is shown in Figures 2-3 and 2-3 Cont'd.

Step 5

The design of the gas flow radiators proceeds in a manner similar to that for the recuperator design.

Step 6

The radiator design program output is likewise stored on a third tape, and/or printed out in the format presented in Figure 2-4.

Step 7

The summation program serves the function of merging the individual component designs and cycles into a total system representation. The summation program also sizes the minor components, such as ducting, and controls, for each system.

# TYPICAL RECUPERATOR DESIGN PROGRAM OUTPUT

INPUT GEOMETRY FOR COUNTER FLOW HEAT EXCHANGER DESIGN PROGRAM

MINI-BRU RECUPERATOR

| | GAS | UA MARGIN (-----) | DP MARGIN (-----) | F MARGIN (-----) | J MARGIN (-----) |
|---|---|---|---|---|---|
| L.P. SIDE -------------------- | XE/HE83 | .2000 | .2000 | -0.0000 | -0.0000 |
| H.P. SIDE -------------------- | XE/HE83 | .2000 | .2000 | -0.0000 | -0.0000 |

| | NUMBER (PER INCH) | THICKNESS (INCHES) | SPACING (INCHES) | FQ. LENGTH (INCHES) | DENSITY (LB/CU-IN) | CONDUCTIVITY (BTU/HR-FT-R) |
|---|---|---|---|---|---|---|
| L.P. SIDE FINS --------------- | 20.00 | .004 | .101 | .050 | .297 | 6.000 |
| H.P. SIDE FINS --------------- | 20.00 | .004 | .101 | .050 | .297 | 6.000 |
| L.P. SIDE HEADER FINS --------- | 10.00 | .006 | | | .297 | |
| H.P. SIDE HEADER FINS --------- | 10.00 | .006 | | | .297 | |
| SPLITTER PLATES --------------- | | .008 | | | .297 | 10.000 |
| WRAP-UP MATERIAL -------------- | | .060 | | | .297 | 10.000 |
| SPACER BARS ------------------- | | .100 | | | .297 | 10.000 |
| BRAZE MATERIAL ---------------- | | .001 | | | .297 | 10.000 |

| | FLOW AREA RATIO (-----) | SURFACE AREA/VOLUME (1/IN.) | FIN AREA/VOLUME (1/IN.) | PLATE AREA/VOLUME (1/IN.) | HYDRAULIC DIAMETER (INCHES) |
|---|---|---|---|---|---|
| L.P. SIDE FINS --------------- | .40936 | 26.239 | 17.798 | 8.440 | .06241 |
| H.P. SIDE FINS --------------- | .40936 | 26.239 | 17.798 | 8.440 | .06241 |
| L.P. SIDE HEADER FINS --------- | .40963 | 17.339 | 8.716 | 8.624 | .09450 |
| H.P. SIDE HEADER FINS --------- | .40963 | 17.339 | 8.716 | 8.624 | .09450 |

| | ENTRY LOSS (-----) | TURNING LOSS (-----) | EXIT LOSS (-----) | TURNING ANGLE (DEGREES) |
|---|---|---|---|---|
| L.P. SIDE HEADER FINS --------- | .40400 | .18000 | 1.00000 | 30.00 |
| H.P. SIDE HEADER FINS --------- | .40400 | .60000 | 1.00000 | 60.00 |

FIGURE 2-3

# TYPICAL RECUPERATOR DESIGN PROGRAM OUTPUT

PLATE FIN COUNTERFLOW DESIGN

MINI-HRU RECUPERATOR

**LOW PRESSURE SIDE — GAS IS XE/HEA3**

| EFFECTIVENESS (-----) | INLET TEMPERATURE (DEG. R) | EXIT TEMPERATURE (DEG. R) |
|---|---|---|
| .95552E+00 | .17321E+04 | .73236E+03 |
| **FLOW RATE (LB/SEC)** | **INLET PRESSURE (PSIA)** | **PRESSURE DROP (DP/P)** |
| .35730E+00 | .71700E+02 | .47390E-02 |
| **FIN EFFECTIVENESS (-----)** | **REYNOLDS NO. (-----)** | **PRANDTL NO. (-----)** |
| .84645E+00 | .42745E+03 | .26637E+00 |
| **H.T. CONDUCTANCE (BTU/SEC. DEG.R)** | **VISCOSITY (LB/FT-SEC)** | **SPECIFIC HEAT (BTU/LB-DEG.F)** |
| .16418E+01 | .32873E-04 | .59200E-01 |
| **HEADER WEIGHT (LB)** | **FIN WEIGHT (LB)** | **FLUID WEIGHT (LB)** |
| .15485E+01 | .18205E+02 | .13520E+00 |

**HIGH PRESSURE SIDE — GAS IS XE/HEA3**

| EFFECTIVENESS (-----) | INLET TEMPERATURE (DEG. R) | EXIT TEMPERATURE (DEG. R) |
|---|---|---|
| .97500E+00 | .68300E+03 | .17644E+04 |
| **FLOW RATE (LB/SEC)** | **INLET PRESSURE (PSIA)** | **PRESSURE DROP (DP/P)** |
| .35016E+00 | .10589E+03 | .22373E-02 |
| **FIN EFFECTIVENESS (-----)** | **REYNOLDS NO. (-----)** | **PRANDTL NO. (-----)** |
| .84914E+00 | .42925E+03 | .26580E+00 |
| **H.T. CONDUCTANCE (BTU/SEC. DEG.R)** | **VISCOSITY (LB/FT-SEC)** | **SPECIFIC HEAT (BTU/LB-DEG.F)** |
| .16100E+01 | .32086E-04 | .59200E-01 |
| **HEADER WEIGHT (LB)** | **FIN WEIGHT (LB)** | **FLUID WEIGHT (LB)** |
| .15485E+01 | .18205E+02 | .20622E+00 |

| TOTAL WEIGHT (LB) | PLATE WEIGHT (LB) | SPACER BAR WEIGHT (LB) | WRAP UP WEIGHT (LB) | BRAZE WEIGHT (LB) | ASPECT RATIO (-----) |
|---|---|---|---|---|---|
| .10601E+03 | .24693E+02 | .14770E+02 | .16272E+02 | .70232E+01 | .20000E+01 |
| **CORE LENGTH (INCHES)** | **CORE WIDTH (INCHES)** | **CORE HEIGHT (INCHES)** | **OVERALL LENGTH (INCHES)** | **VOLUME (CU.IN.)** | **TOTAL PRESSURE DROP (DP/P)** |
| .24427E+02 | .50227E+01 | .96455E+01 | .28777E+02 | .12888E+04 | .69680E-02 |

FIGURE 2-3 CONT'D.

# TYPICAL RADIATOR DESIGN PROGRAM OUTPUT

CYCLE NUMBER 3

| | | | | | |
|---|---|---|---|---|---|
| MASS FLOW | CORE PRESSURE DROP | HEADER PRES. DROP | RET. DUCT PRES. DROP | SUP. DUCT PRES. DROP | INLET TEMP. |
| (LB/SEC) | --- | --- | --- | | (R) |
| .35730E+00 | .36000E-02 | .16660E-02 | .27800E-03 | .27800E-03 | .73311E+03 |
| OUTLET TEMP. | NO. INTERNAL FINS | SINK TEMP. | TUBE LENGTH | NO. HEADER PAIRS | EXTERNAL FIN EFF. |
| (R) | ---- | (R) | (FT) | ---- | ---- |
| .53600E+03 | -0. | .45000E+03 | .83205E+01 | .10000E+01 | .96455E+00 |
| TUBE INT. DIAM. | TOTAL WEIGHT | CORE WEIGHT | HEADER WEIGHT | DUCT WEIGHT | NUMBER OF TUBES |
| (IN) | (LB) | (LB) | (LB) | (LB) | ---- |
| .31667E+00 | .16029E+03 | .11764E+03 | .33086E+02 | .95645E+01 | .41044E+02 |
| RADIATOR AREA | TUBE SPACING | EXT. FIN THICK. | INLET WALL TEMP. | OUTLET WALL TEMP. | ARMOR THICKNESS |
| (SQ FT) | (IN) | (IN) | (R) | (R) | (IN) |
| .12526E+03 | .44014E+01 | .40000E-01 | .72142E+03 | .53395E+03 | .71583E-01 |
| HEADER FLOW DIM. | FIN BASE TEMP. | FILM COEFFICIENT | REYNOLDS NO. | RET. DUCT DIAM. | SUP. DUCT DIAM. |
| (IN) | (R) | (BTU/SEC SQ FT F) | ---- | (IN) | (IN) |
| .15224E+01 | .64777E+03 | .65653E-02 | .21936E+05 | .16170E+01 | .17477E+01 |
| FLUID SPEC. HEAT | VULNERABLE AREA | INTERNAL FIN EFF. | COATING WEIGHT | TUBE WEIGHT | FIN WEIGHT |
| (BTU/LB F) | (SQ FT) | ---- | (LB) | (LB) | (LB) |
| .59200E-01 | .13075E+02 | .94856E+00 | .51764E+01 | .49319E+02 | .64612E+02 |

.60000E-02

FIGURE 2-4

Step 8

The output of the summation program is presented in two forms. The first (refer to Figure 2-5) is a tabulation of one line summaries of cycle specifications and component geometry (including predicted system weight and radiator area). The second form of output is available in plot form. The initial form of the plots are the computed specified weight (including the variable weights, in $lb/kw_e$, of the BRU, recuperator, and radiator) for the system and the computed specific radiator area plotted versus gross cycle efficiency. This plotted output forms the basis for the determination of the boundary of minimum attainable system weight as a function of system performance and output. Figure 1-4 shows a typical boundary generated in this fashion. The basic philosophy employed during the study was that one can determine the point on such a boundary which best expresses the desired trade-off of cycle efficiency (fuel cost) and system weight (launch cost). Having selected a point on the boundary, one seeks to precisely define a system in this area such that no system variable can be perturbated in any manner without a resulting upward departure from the boundary. This philosophy implies that a variation of a single system parameter (referred to as a single dimension parametric study) should produce a trace (refer to Figure 2-6) of specific weight versus efficiency which is tangent to the previously defined lower boundary.

The philosophy of system selection was later expanded to include the predicted performance of a particular (fixed) system across the entire range of power output (off-design performance). This approach will be discussed in more detail later in this section.

# TYPICAL SYSTEM SUMMARY OUTPUT

| CASE | MW | PRC | RPM | ER | BETA | NSC | WCRU | VCRU | WR | VR | WRAD | ARAD | WD | VD | WT | AT | ECY |
|---|---|---|---|---|---|---|---|---|---|---|---|---|---|---|---|---|---|
| 1 | 84. | 1.50 | 52000. | .96 | .98 | .07 | 23.3 | .15 | 34.2 | .34 | 160.3 | 124.59 | 11.3 | .27 | 368.3 | 65.3 | .2652 |
| 2 | 84. | 1.50 | 52000. | .97 | .98 | .07 | 23.3 | .15 | 39.8 | .40 | 160.3 | 124.93 | 11.3 | .27 | 363.1 | 64.0 | .2711 |
| 3 | 84. | 1.50 | 52000. | .98 | .98 | .07 | 23.3 | .15 | 47.4 | .48 | 160.3 | 125.26 | 11.3 | .27 | 359.9 | 62.8 | .2773 |

FIGURE 2-5

# SINGLE DIMENSION PARAMETRIC STUDY RESULTS

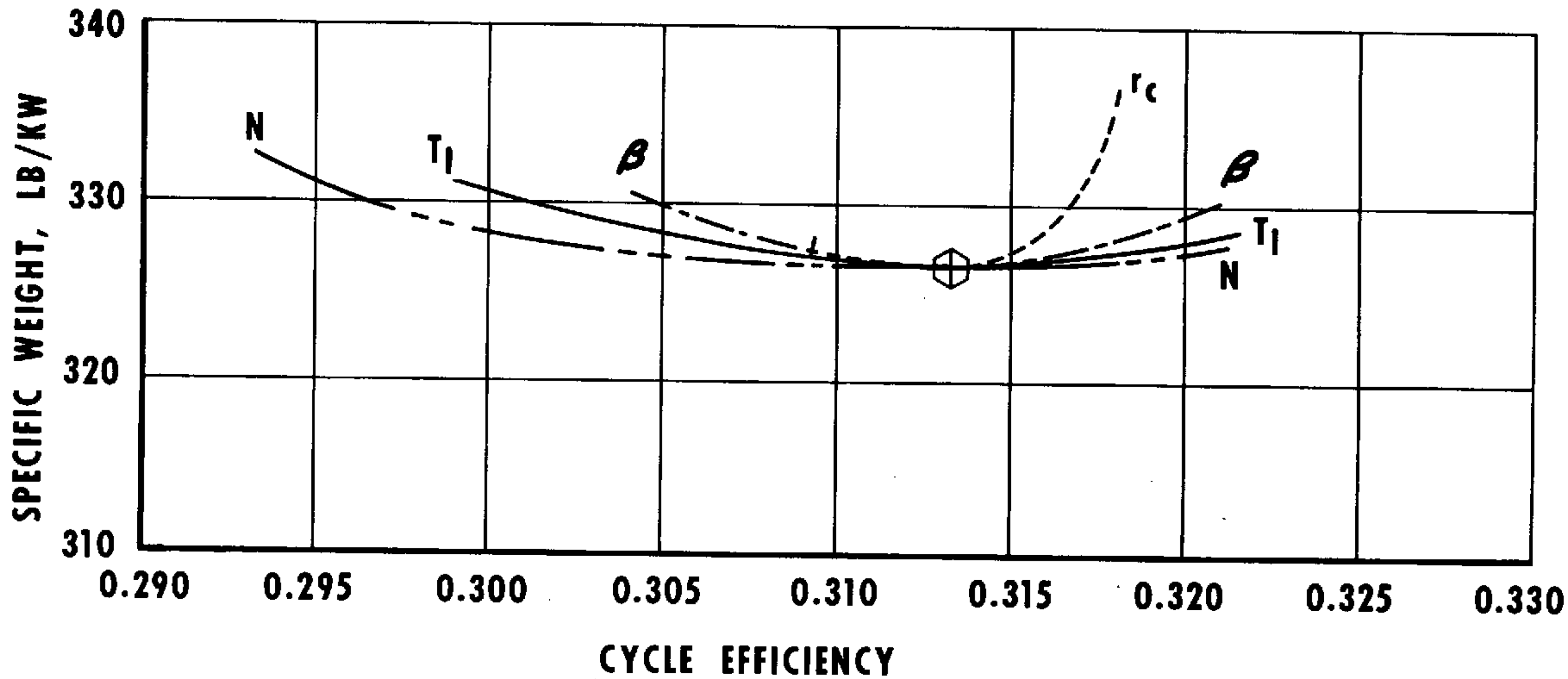


MS 3063-5

FIGURE 2-6

### 2.1.4 Reference Design Selection

In order to select the recommended reference cycle, data was generated using both system design optimization computer programs and system off-design performance computer programs. Over 8,000 completely defined systems were designed to determine general system characteristics over the power range of interest. In addition to that part of the study, several other design approaches were examined to determine which "fixed hardware" system (i.e., a particular system design) had the most favorable performance characteristics over the entire power range and how the off-design performance of a particular system compared to the systems optimized at each power level.

The trends of this investigation are summarized in Figure 2-7. The actual working curves were plotted on large (20 in. x 30 in.) graph paper and sumbitted to the study program monitor. To avoid confusion and to facilitate an explanation of the technical approach followed, the trends only are shown in Figure 2-7.

Line 1 defines the loci of minimum specific weight system designs as a function of power level. The particular designs indicated as II and III are those which are optimized (with regard to minimum specific weight) when two or three heat source capsules are used. Points III-2 and III-1 indicate the off-design performance of system III operating with two and one heat source capsules. Similarly, Points II-1 and II-3 denote the off-design performance of System II.

A similar exercise was not performed for the optimum system using one heat source because, due to the limited capability of the 0.5 $kw_e$ alternator, it could not be made to produce 2 $kw_e$ during off-design operation.

# SYSTEM SPECIFIC WEIGHT CHARACTERISTICS

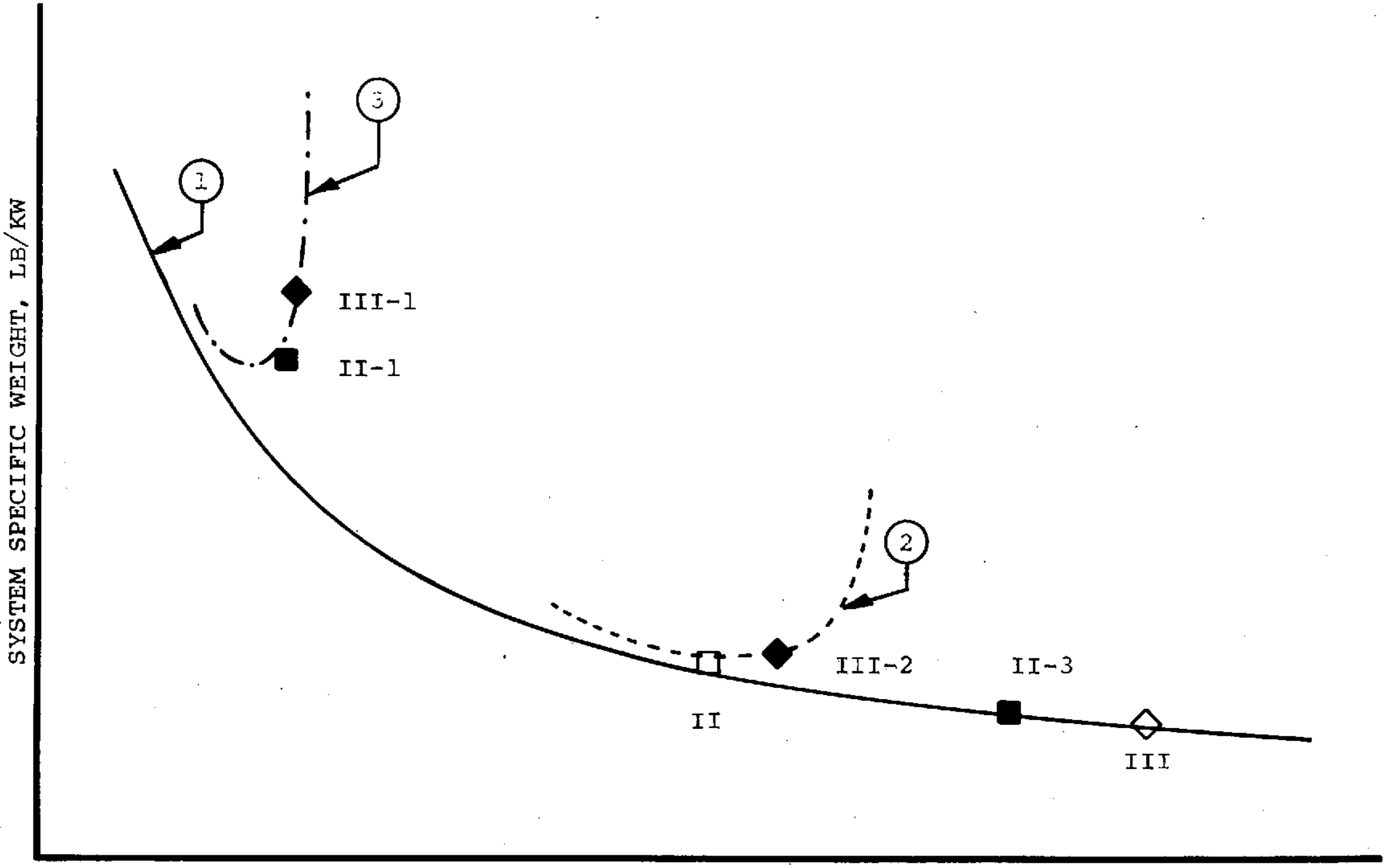


FIGURE 2-7

Another possibility studied was a system assumed to be comprised of the reference system (III) rotating unit and recuperator but with varying size radiators. Lines 2 and 3 show the trends and an inspection of the data yields ample justification for the important conclusion that one CRU and recuperator, which would be designed specifically for the 3 heat source capsule case, would be quite suitable for use over the entire power range. This is a tremendous advantage since it precludes the need of multiple development efforts on several configurations of the same basic set of hardware.

The clinching argument for selection of the system optimized for the 3 heat source capsule case as the reference system was the results of a comparison study of the reference system with three other candidate specific system designs. The system designs compared included:

(a) A system optimized for 0.5 $kw_e$. Since this system included a CRU with an alternator of limited output, multiple units would have to be employed in parallel to achieve 2.0 $kw_e$.

(b) Approach (a) modified to include an oversized alternator. However the heat exchangers, sized for the low power condition, represent a limitation.

(c) A system optimized to operate with 2 heat source capsules.

The system comparison results are shown in Table 2-1. The numbers represent an attempt to give some quantification to the comparison.

TABLE 2-1

SYSTEM COMPARISON MATRIX

| | Development Risk | ncy-over Power Range | Weight | Cost | Power Capability | Reliability | Total |
|---|---|---|---|---|---|---|---|
| A. Optimized for 1 heat source capsule (multiple systems used for higher power) | 1 △1 | 3 | 1 △2 | 1 | 1 | 3 | 10 |
| B. Optimized for 1 heat source capsule with 2.0 $kw_e$ alternator | 1 △1 | 1 △3 | 3 | 2 | 2 △3 | 2 | 11 |
| C. Optimized for 2 heat source capsules | 2 △1 | 2 | 2 | 3 | 2 | 2 | 13 |
| D. Optimized for 3 heat source capsules | 3 | 3 | 2 △4 | 3 | 3 | 2 | 16 |

Merit Scale

3 - Most advantageous

2 - In between

1 - Least advantageous

△1 The optimum 0.5 $kw_e$ system has a smaller diameter compressor than the reference system (2.1 in. versus 2.3 in.)

△2 Multiple units required to achieve 2.0 $kw_e$

△3 Heat exchanges are undersized for higher power level applications, resulting in inefficiency

△4 Larger system, somewhat oversized for low power application

# 3. TASK III - PRELIMINARY DESIGN OF ROTATING UNIT

## 3.1 Mechanical Design

The mini-BRU rotating group configuration consists of a single-stage compressor, turbine, and an alternator an a common shaft. The shaft is supported on gas-lubricated foil journal and thrust bearings with self-acting start-stop capability. The journal bearings are located in the alternator secondary air gap to minimize shaft length. Further, in order to minimize losses, the machine design specifically excludes seals; rather the journal and thrust bearings act as seals to prevent gas flow from the compressor to turbine ends.

### 3.1.1 Bearings

The general design requirements for the mini-BRU foil gas bearings are presented in Table 3-1. Based on these requirements, the bearing design was initiated by conducting a parametric analysis to determine the critical speed characteristic of the rotating group as a function of the foil bearing stiffness. Results of this analysis, presented in Figure 3-1, show that at low bearing spring rates both the first and second critical speed regimes are far below the 100 percent operating speed of 52,000 rpm. Also, the 160,000 rpm third critical is shown to be independent of spring rate and is far above even the runaway speed (limiting speed due to aerodynamic component performance characteristics) of 92,000 rpm.

Following the parametric analysis, a bearing spring rate of 3,300 lb/in. was selected, through successive iterations, as that yielding the most desirable shaft dynamics. The bearing load versus shaft speed plots are presented in Figure 3-2, for a shaft eccentricity of 0.0005 in. and journal diameter of 1.0 in. As may be noted from the figure, the first and second criticals (7,200 rpm and 9,200 rpm respectively) are significantly removed from the engine operating speed such that no critical speed problem is anticipated. The third critical lying far

GARRETT

# FOIL BEARING GENERAL DESIGN REQUIREMENTS

- DESIGN SPEED = 52,000 RPM
- OPERATING TEMPERATURE = 450°F
- WORKING FLUID - (XE-HE) M.W. = 83.8
- AMBIENT PRESSURE
  = 24 PSIA
  = 95 PSIA
- ROTOR WEIGHT = 1.68 LB.
- LOW BEARING LOSS
- LOW DRAG TORQUE

MS 3011-20

TABLE 3-1

# CRITICAL SPEED VS BEARING SPRING RATE

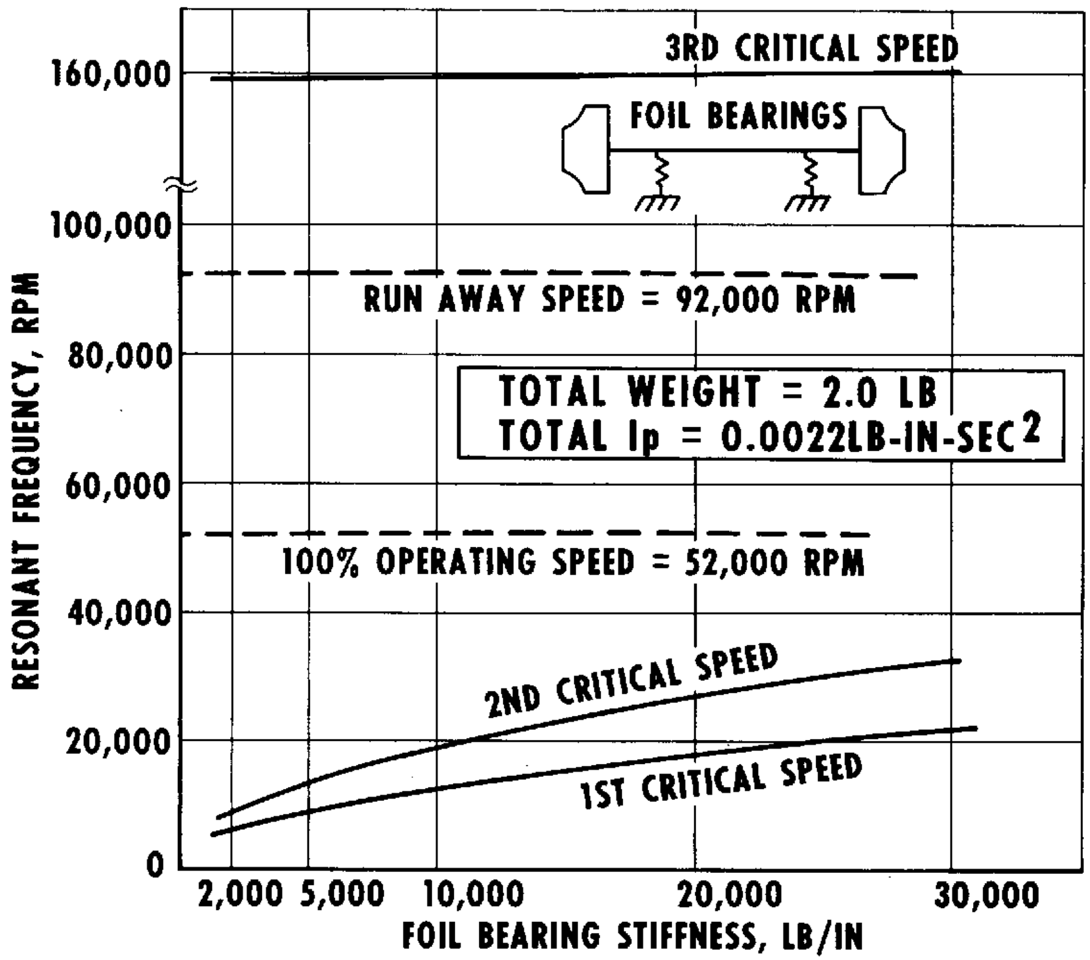


MS 3063-11

FIGURE 3-1

# BEARING LOADS

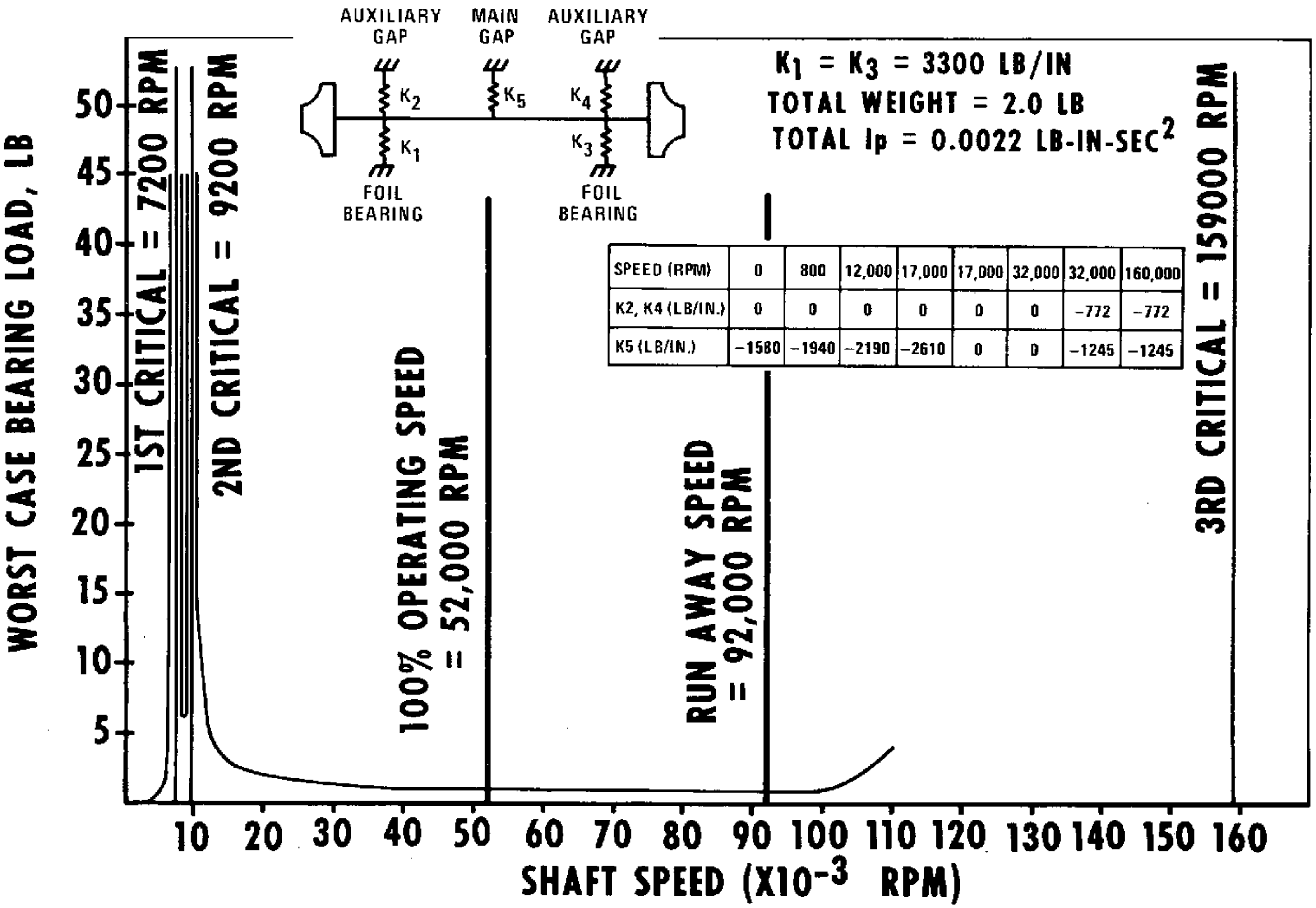


| SPEED (RPM) | 0 | 800 | 12,000 | 17,000 | 17,000 | 32,000 | 32,000 | 160,000 |
|---|---|---|---|---|---|---|---|---|
| K2, K4 (LB/IN.) | 0 | 0 | 0 | 0 | 0 | 0 | −772 | −772 |
| K5 (LB/IN.) | −1580 | −1940 | −2190 | −2610 | 0 | 0 | −1245 | −1245 |

MS 3063-12

FIGURE 3-2

above the runaway speed provides the potential for simplification of the overspeed control design. The table at the top of Figure 3-2 summarizes the unbalanced magnetic forces, expressed as "negative" bearing spring rates, for the alternator in the motor start mode (0 through 17,000 rpm), during bootstrap operation (17,000 through 32,000 rpm) and in the normal alternator mode producing electrical power (32,000 through 160,000 rpm). Data for the table was generated in the alternator magnetic unbalance analyses for motor start and alternator operation (refer to Figures 3-21 and Table 3-14, respectively).

The resulting foil journal bearing design best satisfying the load requirements and yielding minimum losses is summarized in Table 3-2.

In order to properly size the foil thrust bearing for minimum power loss, a turbine and compressor thrust balance analysis was conducted. Figure 3-3 presents the estimated turbine thrust as a function of back face slip factor and percent turbine scallop. As may be noted from the figure a wide variance in thrust may be obtained by changing the turbine shroud clearance (and hence slip factor) and/or decreasing the turbine back face area through material removal. Further, Figure 3-4 shows the effect of back face slip factor and the addition of compressor lip on net compressor thrust. Therefore, by selecting the proper combination of shroud clearances, turbine scallop and compressor lip height, an optimum system thrust balance may be achieved leading to a minimum loss thrust bearing design. This design is summarized in Table 3-3.

The journal and thrust bearing power losses were estimated for bearing cavity pressures of 24 and 95 psia (corresponding to the 1 and 3 capsule power level conditions). These results are presented in Table 3-4. Estimated performance for the journal and thrust bearings, plotted as power loss (watts) versus unit load (psi), is shown in figures following Table 3-4.

# JOURNAL BEARING DESIGN

- JOURNAL DIAMETER = 1.00 IN.
- BEARING LENGTH = 0.90 IN.
- NUMBER OF FOILS = 8
- THICKNESS OF FOILS = 0.003 IN. + COATING
- RADIUS OF CURVATURE = 0.70 IN.
- SWAY SPACE = 0.006 IN.
- PREDICTED SPRING RATE = 3300 LB./IN.

MS 3011-22

TABLE 3-2

# TURBINE THRUST CHARACTERISTICS

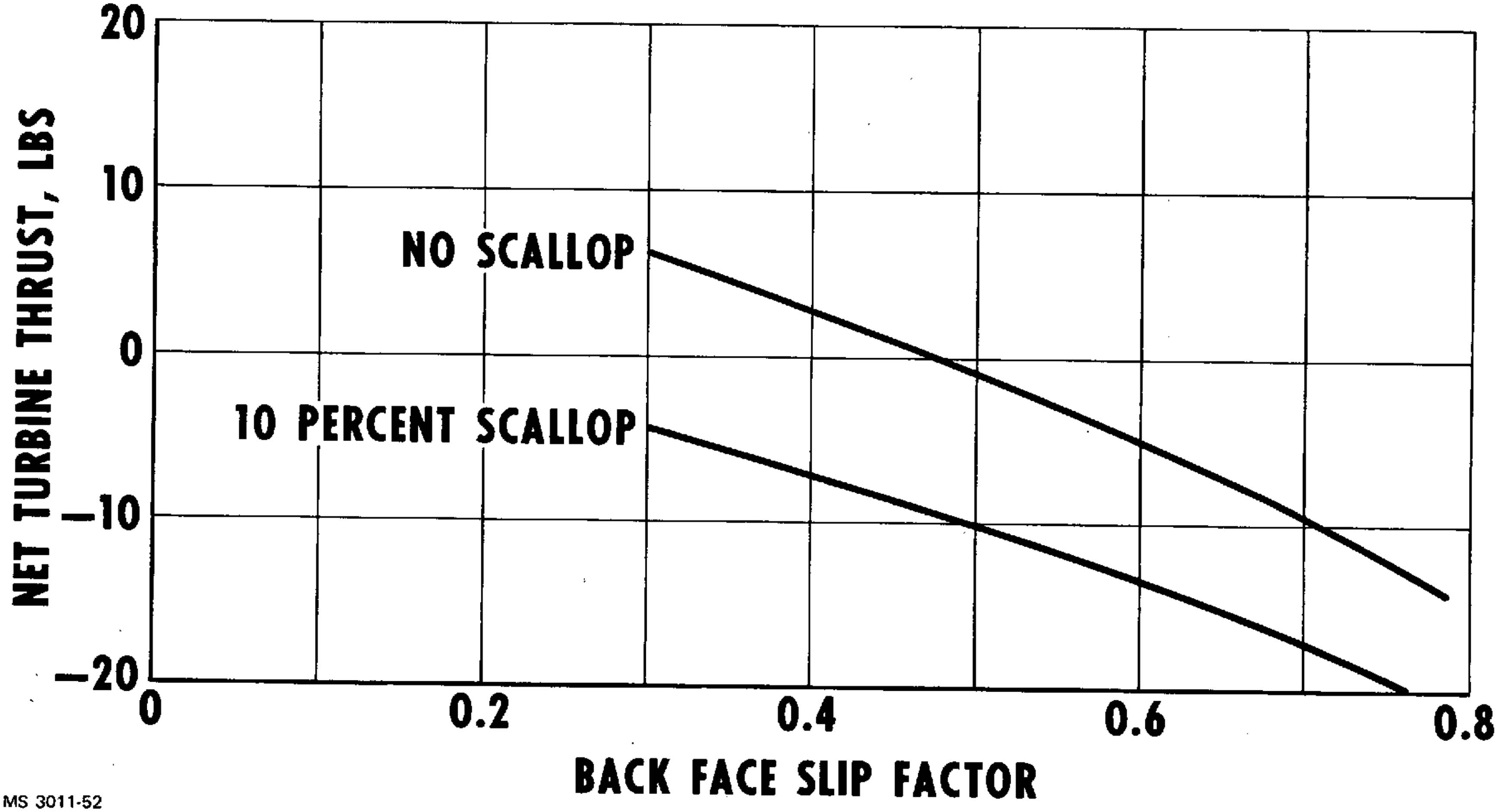


MS 3011-52

FIGURE 3-3

# COMPRESSOR THRUST CHARACTERISTICS

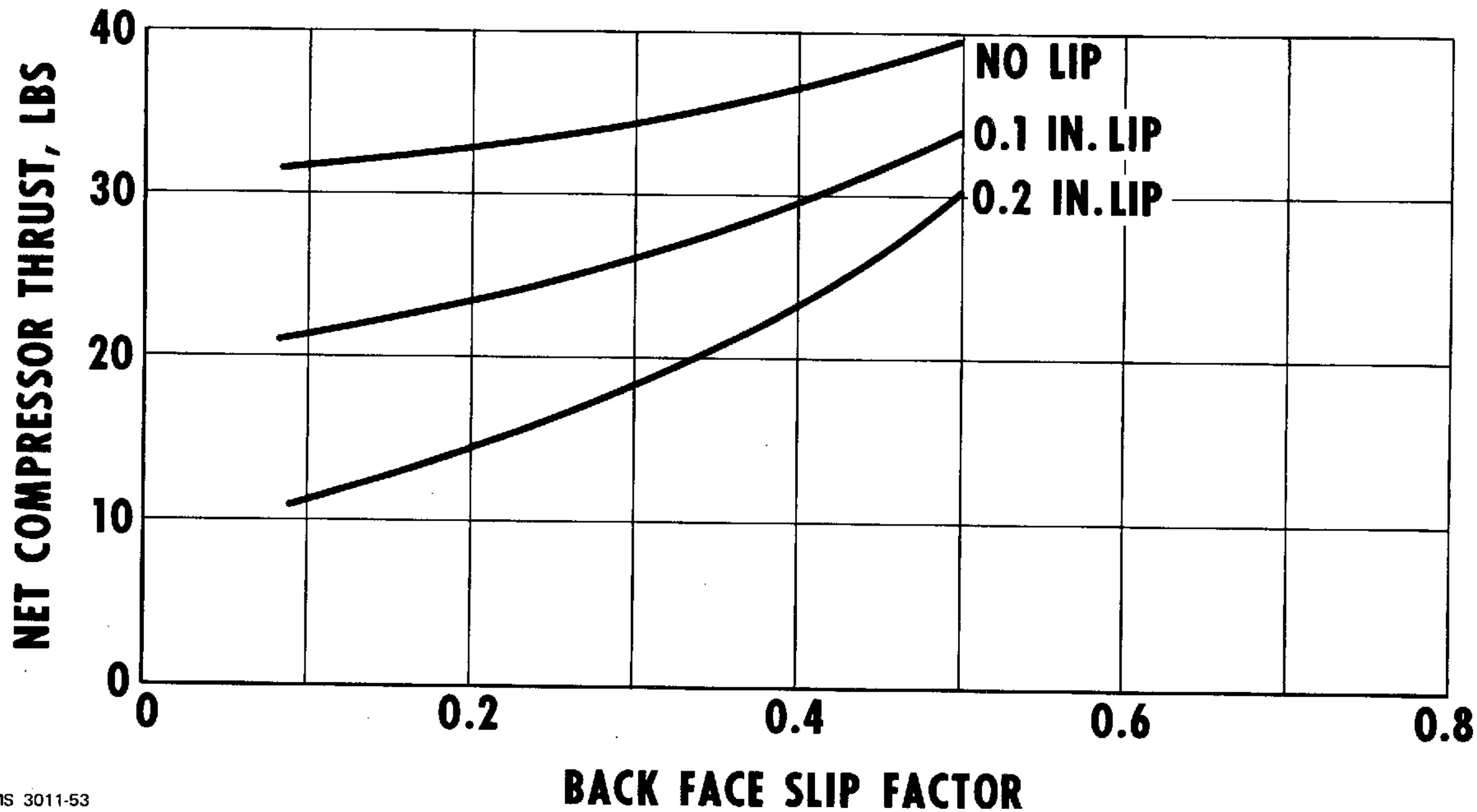


MS 3011-53

FIGURE 3-4

# THRUST BEARING DESIGN

- OUTSIDE DIAMETER = 1.75 IN.
- INSIDE DIAMETER = 1.00 IN.
- NUMBER OF PADS = 10.00
- PAD THICKNESS = 0.003 IN. + COATING
- PAD PLATE THICKNESS = 0.005 IN.
- SPRING PLATE THICKNESS = 0.005 IN.
- PRE-LOAD = 3.50 LBS.

MS 3011-21

TABLE 3-3

GARRETT

# ESTIMATED POWER LOSS SUMMARY

## LOSSES IN WATTS

| | 24 PSIA | 95 PSIA |
|---|---|---|
| JOURNAL BEARING (BOTH) | 77 | 116 |
| THRUST BEARING (LOADED SIDE) | 59 | 74 |
| THRUST BEARING (UNLOADED SIDE) | 39 | 58 |
| TOTAL | 175 | 248 |

MS 3011-23

TABLE 3-4

# JOURNAL BEARING PERFORMANCE

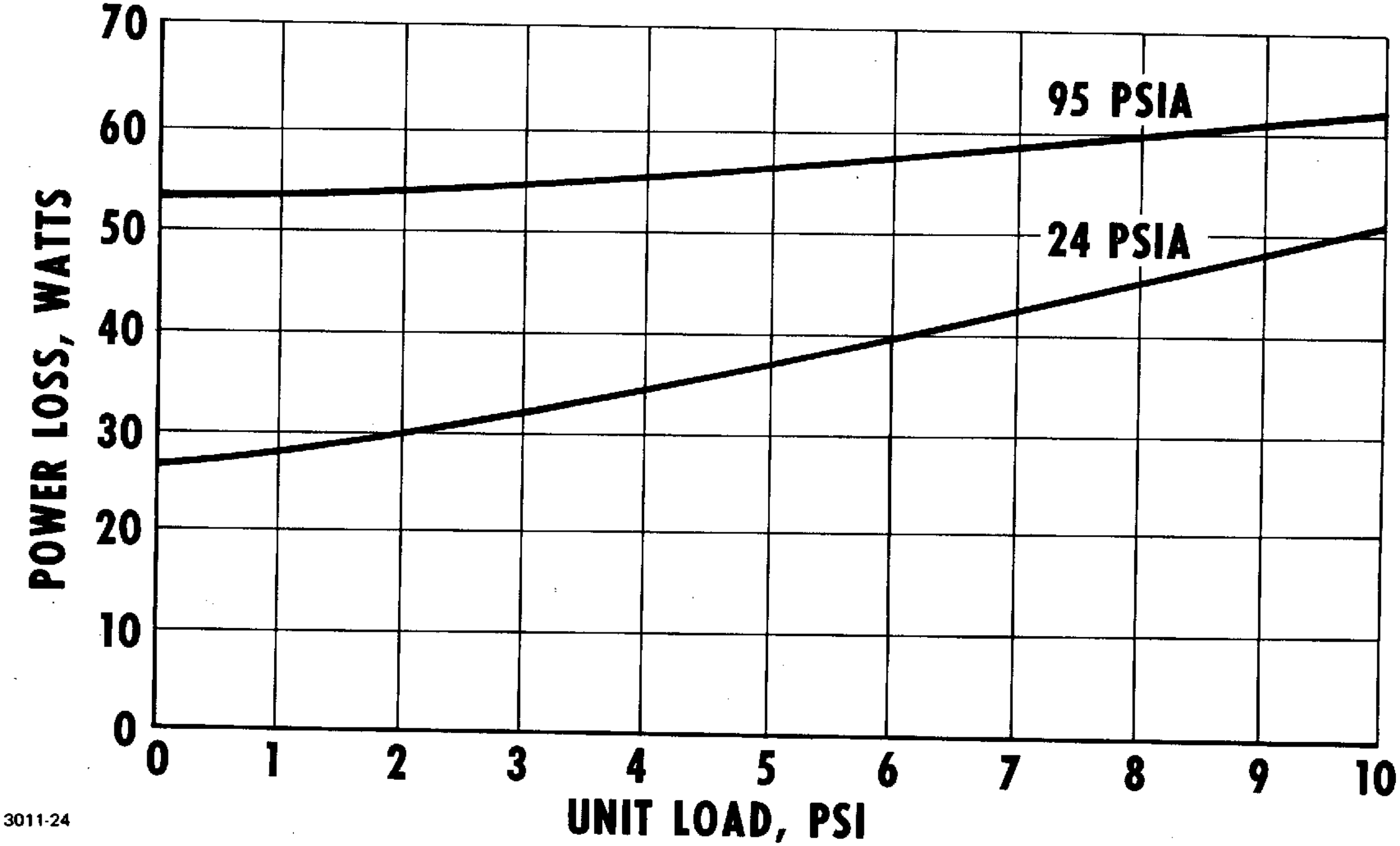


MS 3011-24

# THRUST BEARING PERFORMANCE

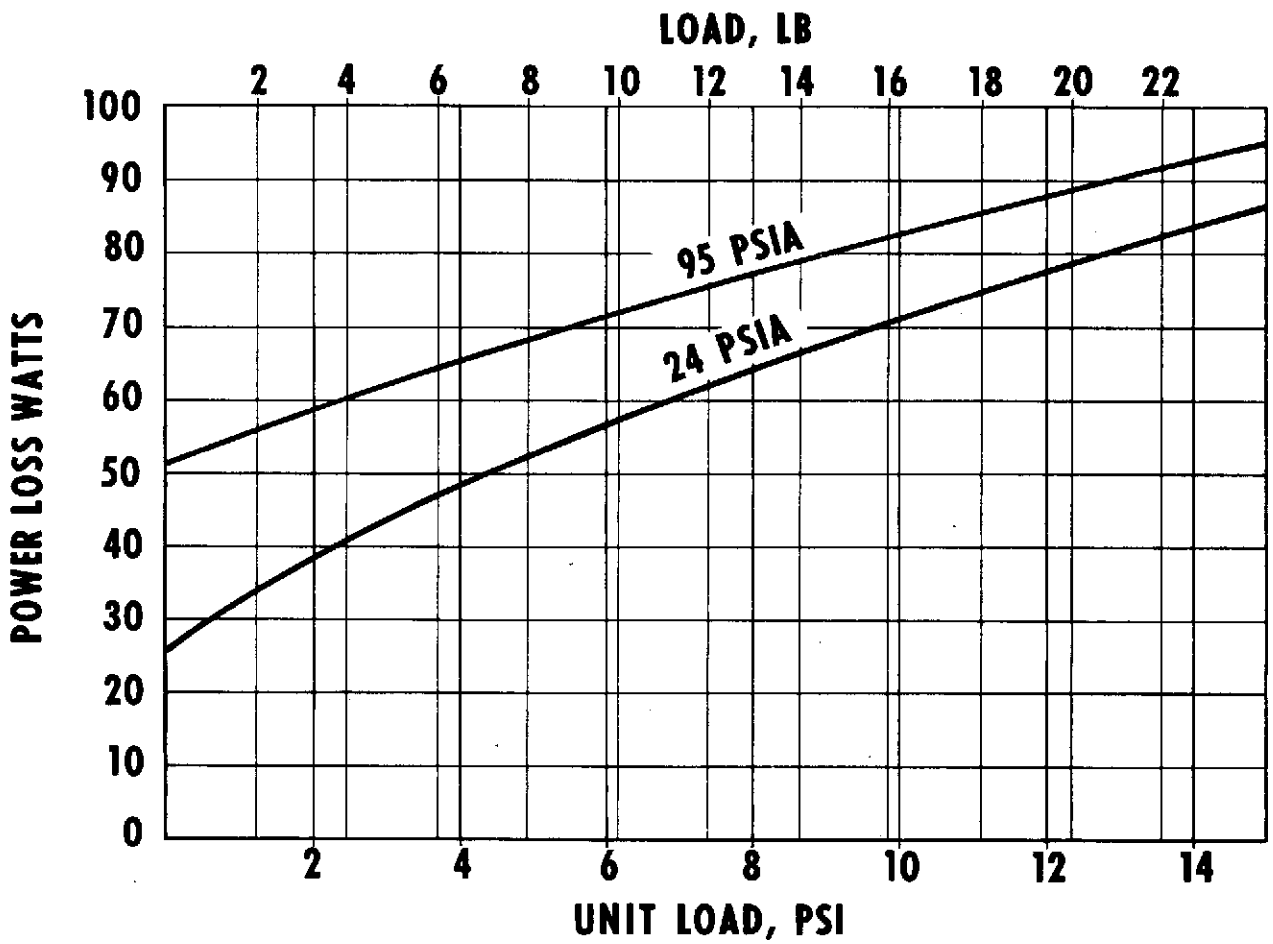


MS 3063-2

### 3.1.2 Mini-BRU Materials

The materials for the mini-BRU were reviewed with tentative selections based on experience gained from the NASA BRU and TAC programs. Although the stresses are modest throughout the machine, the design life is at least 5 years. With the exception of the turbine-end of the machine, operating life up to 10 years can be expected.

Figure 3-5 shows the material selections for mini-BRU. Stainless steel will be used extensively in the center frame, compressor end, and alternator heat exchanger for corrosion resistance. 347 CRES was selected for its good fabricability and weldability. The compressor wheel will be 17-4 PH or 410 CRES, combining the high strength and good thermal conductivity necessary to extract heat from the thrust bearing. Bearing materials were selected to be consistant with the BRU and TAC designs. The alternator materials will result in good electromagnetic performance and thermal conductivity.

The turbine nozzle will be fabricated from cast WI-52 because of this metal's high temperature strength and stability and because it has good weldability with the HS-188 sheet metal used for the turbine scroll, shroud, and diffuser. The turbine wheel will be made from an Inco 713 LC casting. This selection is based on long experience in the design, fabrication and operation of many types of turbine wheels.

# MINI-BRU MATERIALS

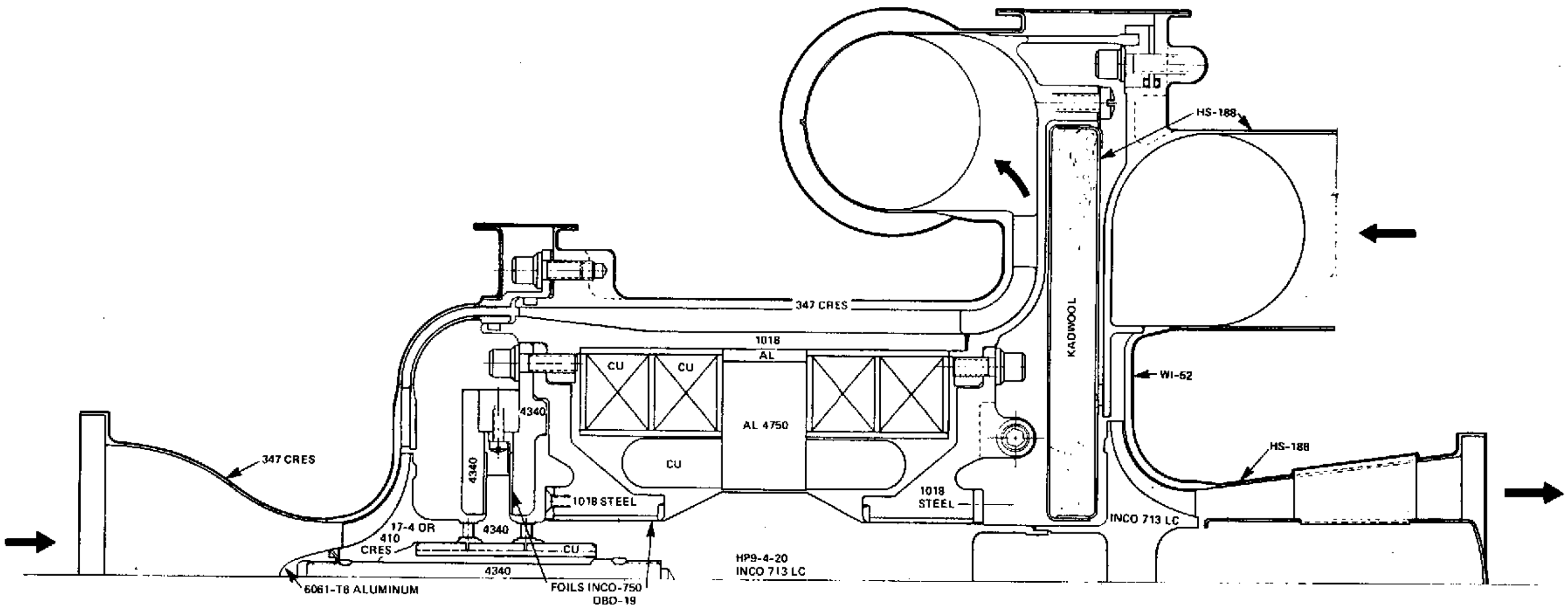


MS 3011-54

FIGURE 3-5

## 3.2 Aerodynamic Design

The aerodynamic design effort for this study focused on accurately assessing the performance of small, single stage radial compressors and turbines. Considerable attention was also given to coordinating the compressor diffuser design with the alternator heat exchanger design.

Table 3-5 summarizes the design factors which have an important effect on compressor efficiency.

Compressor pressure ratio, considered above, has direct effects on: the cycle flowrate required; the compressor size and efficiency; and the cycle pressure levels. The secondary effects of compressor pressure ratio selection include: rotating unit weight; heat exchanger/radiator heat transfer and pressure drop requirements; and cycle efficiency.

Evaluation of the combination of rotating and specific speeds selected for the aerodynamic components cannot be rigorously analyzed, excluding the remainder of the system. However, the combined effect of these two parameters can be viewed thusly: Any number of combinations of rotor and specific speeds can be found which result in a particular cycle pressure level and flowrate. With the system pressure levels and flowrates established, the system heat exchanger requirements are virtually invariant. The cycle optimization now centers on determining the particular combination of rotating speed and specific speed which results in the highest aerodynamic efficiency. High rotor speed results in small turbomachinery diameters and increasing losses due to increased blockage, surface losses and other size related phenomena. Low specific speeds eventually yield increasing losses due to increasing hub, shroud and end wall losses and clearance losses. After careful consideration of these factors and review of

# COMPRESSOR DESIGN PROBLEMS AND SOLUTIONS

| PROBLEM | RESULT |
|---|---|
| • LOW PHYSICAL SPEED IMPLIES LOW SPECIFIC SPEED | MODERATE EFFICIENCY PENALTY BECAUSE OF NON-OPTIMUM SPECIFIC SPEED |
| • SMALL SIZE | |
| (A) SMALL EXIT WIDTH + REASONABLE RUNNING CLEARANCE | HIGH CLEARANCE LOSSES |
| TYPICAL $\dfrac{\text{CLEARANCE}}{\text{EXIT WIDTH}} = 0.030$ | |
| THIS CASE $\dfrac{\text{CLEARANCE}}{\text{EXIT WIDTH}} = 0.104$ | |
| (B) TOLERANCES, FILLET RADII RELATIVELY LARGER | SUBSTANTIAL EFFICIENCY PENALTY |
| • DESWIRL-RESWIRL VANES TO ACCOMMODATE HEAT EXCHANGER | MODERATE EFFICIENCY PENALTY |

MS 3011-6

TABLE 3-5

NASA LeRC data (based on extensive testing of closed cycle machinery compressors) suitable performance penalties as a function of compressor size were defined as shown on the following page. A similar characteristic for the turbine is also shown.

The compressor design is summarized in Table 3-6 and Figure 3-6. The reference design is compared to existing component experience in Figure 3-7.

The turbine design is essentially a direct scale-down from existing single stage turbine. It is felt that there will be less difficulty in achieving the required turbine efficiency than will be the case for the compressor. The reference turbine design point is quite consistant with test data obtained on a number of radial turbines, as seen in Figure 3-8. The design point is summarized in Table 3-7 and Figure 3-9.

For reference purposes, the method of calculating inlet and mean specific speeds for the compressor and turbine is presented on Table 3-8.

## 3.3 Alternator Electromagnetic Design

### 3.3.1 Design Selection

The alternator is a four-pole Rice machine designed to have high efficiency over a wide range of load conditions. Optimum system speed was determined to be 52,000 rpm. Preliminary studies at 41,000; 52,000; and 60,000 rpm for 2, 4, 6, and 8-pole alternator designs indicated that a four-pole machine had the smallest, lightest rotor at each speed (refer to Table 3-9). Although total alternator weight was slightly less for 6- and 8-poles, efficiency of these machines was reduced by higher windage losses caused, in turn, by larger diameter rotors.

# COMPRESSOR AND TURBINE SIZE CORRECTION

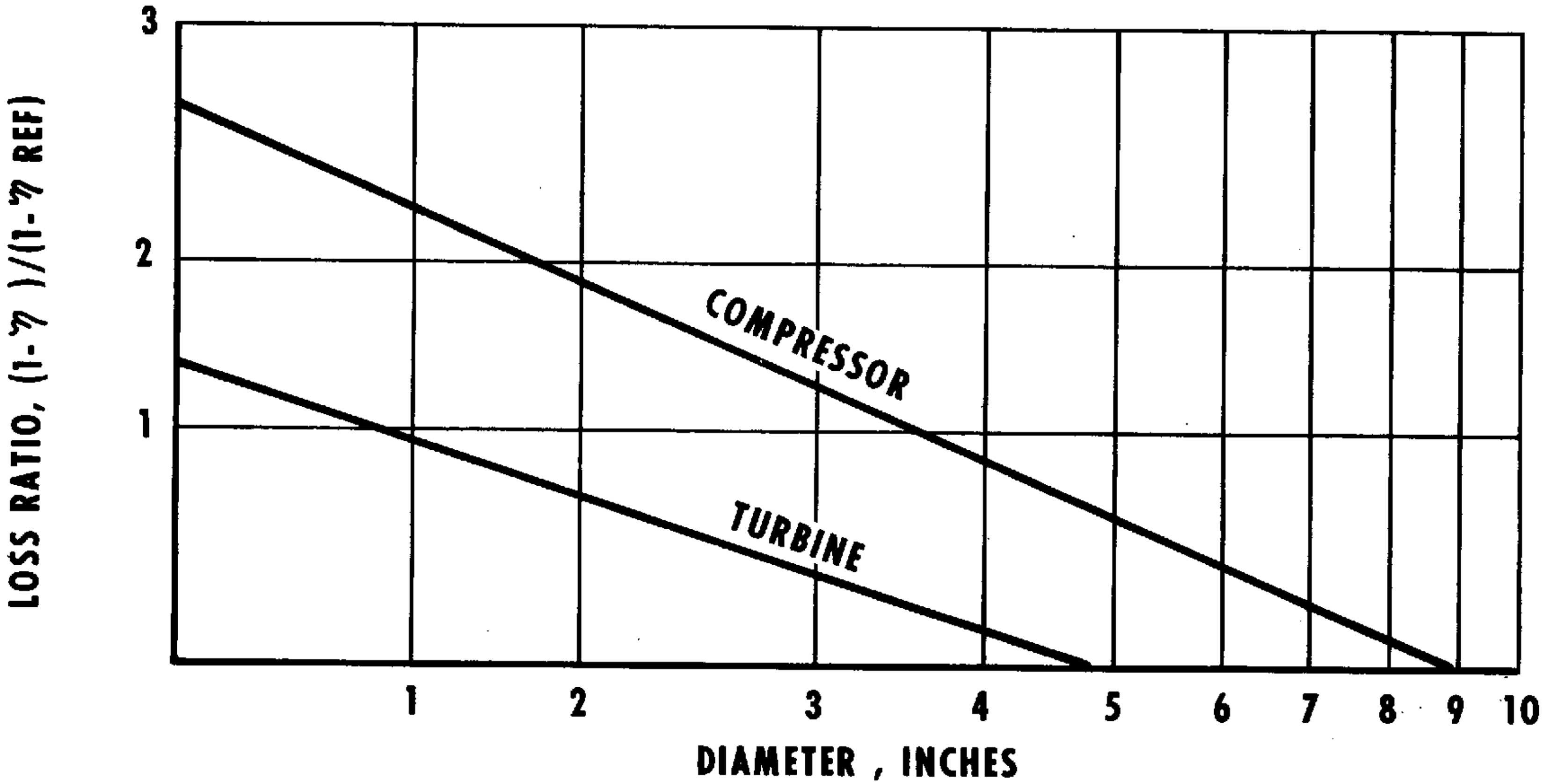


MS 3063-6

# COMPRESSOR DESIGN POINT CONDITIONS



## PRESSURE RATIO
- TOTAL TO TOTAL = 1.50

## EFFICIENCY
- TOTAL TO TOTAL = 0.76

## SPEED
- SPECIFIC SPEED* = 44.3 (MEAN); 46.6(INLET)
- RPM = 52,000

## REYNOLDS NUMBER
- $\dfrac{\rho_{T1}\ U_2\ D_2}{\mu_1} = 5.68 \times 10^6$

## INLET TOTAL PRESSURE
- $P_{IN}$ = 70.8

## INLET TOTAL TEMPERATURE
- $T_{IN}$ = 536°R

## PERFORMANCE PARAMETERS
- CORRECTED FLOW = 0.0756 LB/SEC
- CORRECTED SPEED = 51,153 R.P.M.

## MISCELLANEOUS
- AXIAL CLEARANCE = 0.008 IN.
- RADIAL CLEARANCE = 0.008 IN.
- NO. OF BLADES = 13
- VANED DIFFUSER INLET GAS ANGLE = 76.7°
- VANED DIFFUSER EXIT MACH NO. = 0.125

MS 3063-4

* SPECIFIC SPEED=(RPM)*(VOLUMETRIC FLOW RATE)$^{1/2}$*$\left(\frac{TR}{PR}\right)^{1/4}$/ $(\Delta h_{isen})^{3/4}$

TABLE 3-6

# COMPRESSOR VECTOR DIAGRAMS



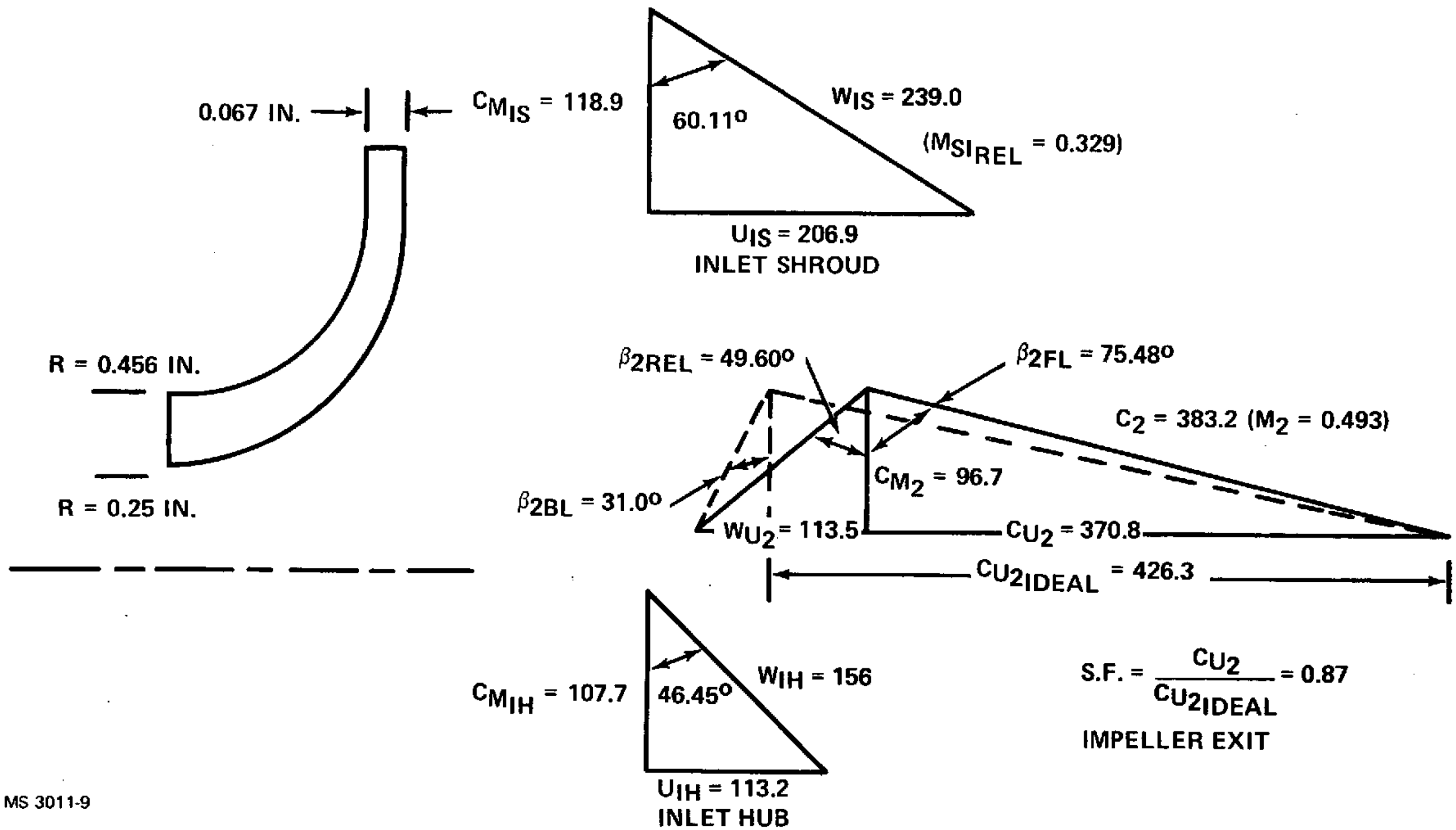


FIGURE 3-6

# RADIAL COMPRESSOR EXPERIENCE

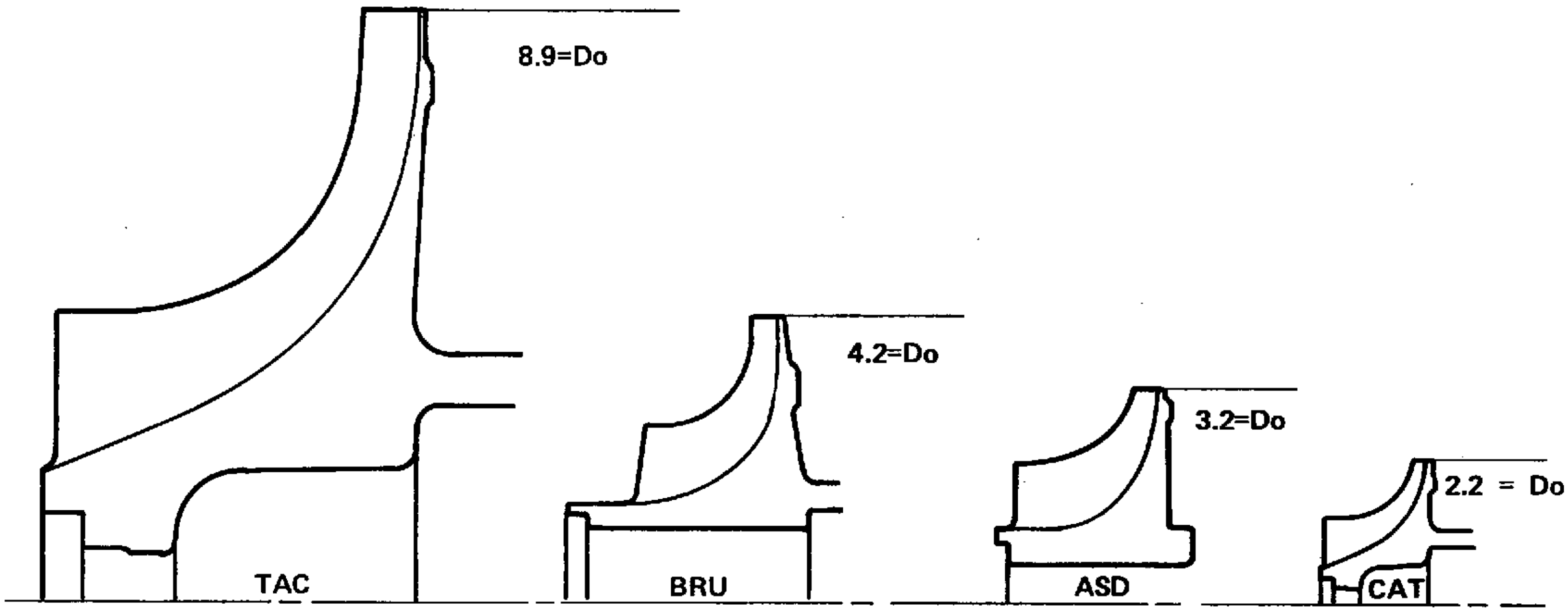


| | | | | |
|---|---|---|---|---|
| $\eta_c$ | 0.87 | 0.83 | 0.805 | 0.760 |
| $P_r$ | 1.95 | 1.9 | 2.06 | 1.50 |
| N | 24,000 | 36,000 | 64,000 | 52,000 |
| M | 39.94 | 83.8 | 39.94 | 83.8 |
| $N_{SC}$ | 0.086 | 0.105 | 0.10 | 0.070 |

MS 3011-8

FIGURE 3-7

# TURBINE EFFICIENCY EXPERIENCE (1-12-73)

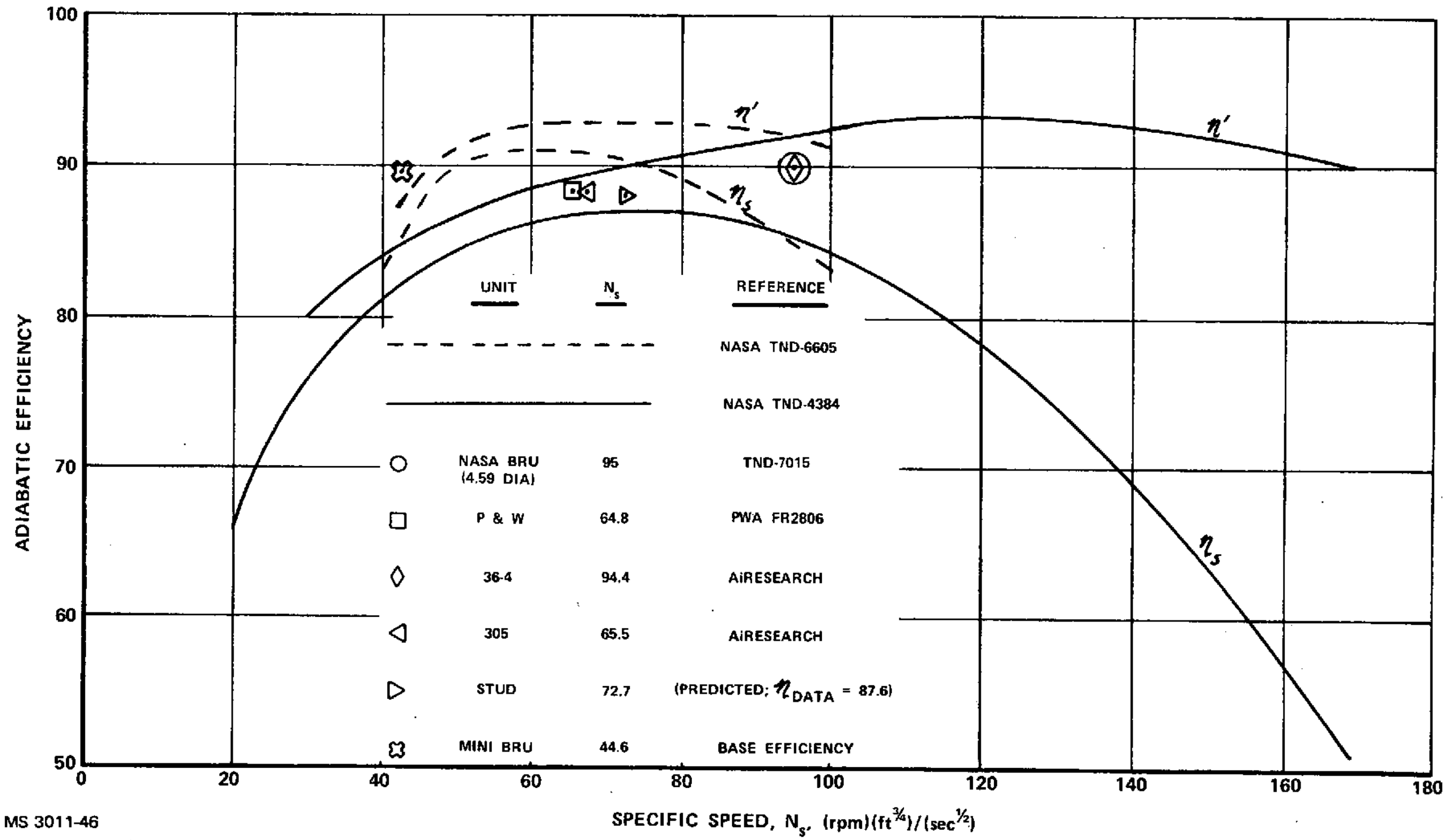


FIGURE 3-8

GARRETT

# TURBINE DESIGN POINT CONDITIONS

## PRESSURE RATIO

- TOTAL TO TOTAL = 1.47
- TOTAL TO D.E. STATIC = 1.4737

## EFFICIENCY

- BASE TOTAL TO TOTAL = 0.896
- CLEARANCE LOSS = 0.039
- DISK FRICTION = 0.021
- NET ADIABATIC = 0.832

## SPEED

- SPECIFIC SPEED* = 44.3 (MEAN); 41.5(INLET)
- RPM = 52,000.
- REYNOLDS NO. ($\dot{w}/\mu r$) = 64,500

## INLET TEMPERATURE

- $T_{IN}$ = 2060°R

## PERFORMANCE PARAMETERS**

- EQUIV. FLOW = 0.0551 LB/SEC
- EQUIV. WORK = 9.903 BTU/LB
- EQUIV. TORQUE = 1.134 IN-LB
- EQUIV. SPEED = 42,899 RPM

## MISCELLANEOUS

- WHEEL DIAMETER = 3.0 IN.
- PRESSURE RECOVERY = 0.6
- NOZZLE EXIT ANGLE = 72°
- DISCHARGE MACH NO. = 0.087
- AXIAL CLEARANCE = 0.008 IN.
- RADIAL CLEARANCE = 0.008 IN.
- NO. OF BLADES = 11

*SPECIFIC SPEED = SPEED (RPM) * (VOLUMETRIC FLOW RATE)$^{1/2}$ * $\left(\frac{TR}{PR}\right)^{1/4} / (\Delta h_{isen})^{3/4}$

** STANDARD CONDITIONS ASSUMED: T=58.67°F; P=14.7 PSIA

MS 3063-3

TABLE 3-7

# TURBINE VECTOR DIAGRAMS

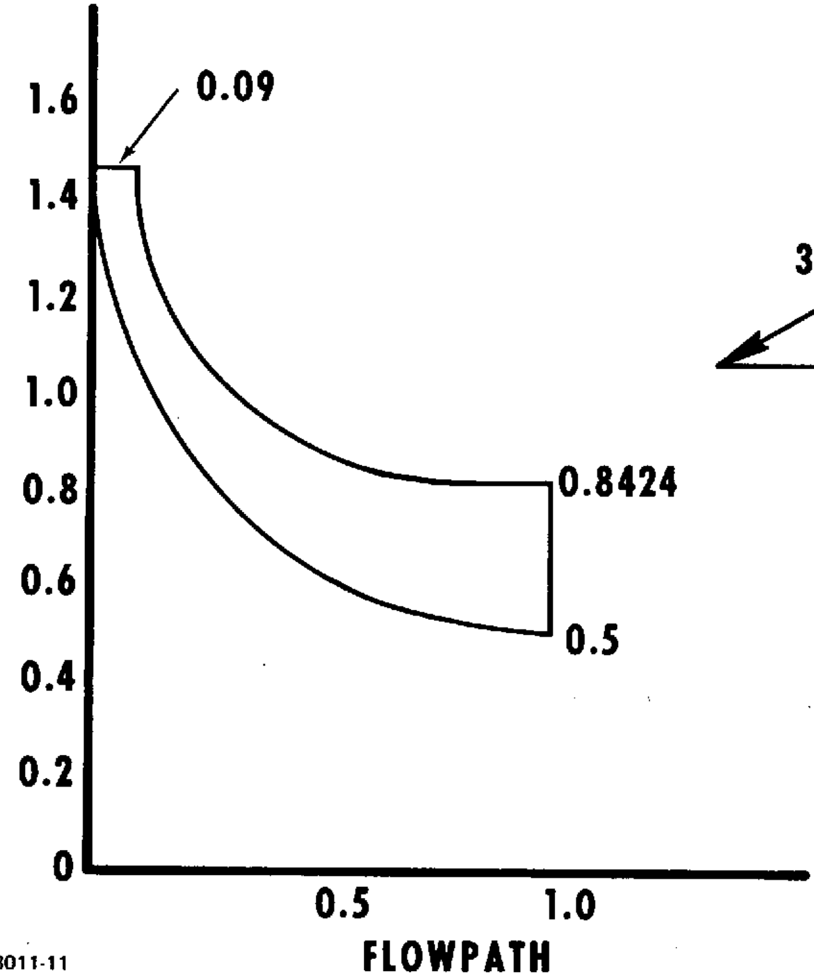


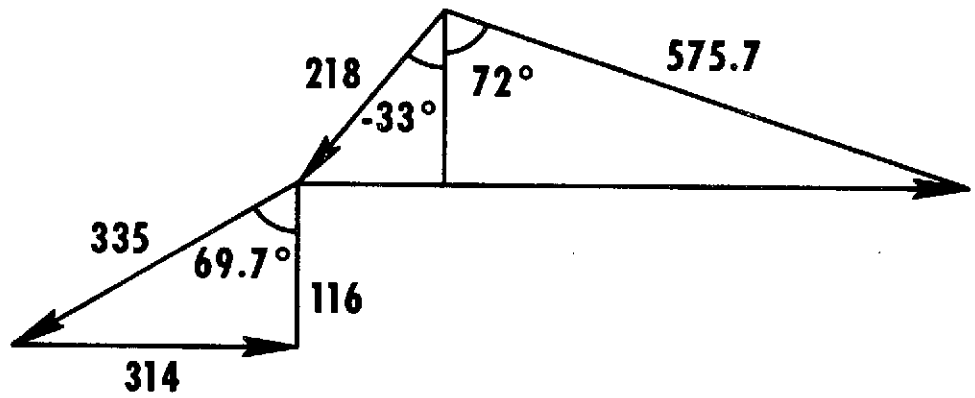


VECTOR DIAGRAM

MS 3011-11

FIGURE 3-9

TABLE 3-8

METHOD OF CALCULATING SPECIFIC SPEED

$$\text{specific speed}\Big)_{mean} = \text{rpm} * (Q1D * Q2D)^{1/4}/(\Delta h)^{3/4}$$

$$Q2D = Q1D * PR/TR$$

$$Q1D = \mathring{m}/\rho$$

$$\text{specific speed}\Big)_{inlet} = \text{specific speed}\Big)_{mean} * \left(\frac{TR}{PR}\right)^{1/4}$$

Compressor

$$\text{specific speed}\Big)_{mean} = 44.3$$

$$\text{specific speed}\Big)_{inlet} = 46.6$$

Turbine

| | | |
|---|---|---|
| $\rho =$ | $PR = 1.47$ | $P_{IN} = 105$ psia |
| $\mathring{m} =$ | $\Delta T = 244.8$ | $T_{IN} = 2060$ |
| | | $TR = 1.136$ |

$$\text{specific speed}\Big)_{inlet} = \frac{52{,}000 * (0.875\ )^{1/2}}{(0.0592 * 244.8 * 778.16)^{3/4}} =$$

$$\frac{52{,}000}{1{,}100} * (0.875)^{1/2}$$

$$\frac{52{,}000}{1{,}100} * 0.935 = 44.3$$

$$\text{specific speed}\Big)_{mean} = \text{specific speed}\Big)_{inlet} * \left(\frac{PR}{TR}\right)^{1/4}$$

$$44.3 * \left(\frac{1.136}{1.470}\right)^{1/4} = 41.5$$

# MINI-BRU SPEED AND POLE STUDY

| DATA DESIGN POINT: 2.169 KW, 66.24 VOLTS, 13.19 AMPS –0.8271 PF, $X_L$ = 0.15 PU, $Z_{BASE}$ = 5.02 OHMS | | | | | | | | LOSSES — WATTS | | | | | | |
|---|---|---|---|---|---|---|---|---|---|---|---|---|---|---|
| | SPEED RPM | FREQ Hz | N* % | Ne % | DROT INCHES | WTOT POUNDS | WROT POUNDS | STATOR COPPER | STACK | POLE HEAD | FIELD | STRAY | FRICTION & WINDAGE* | TOTAL |
| 8 POLE | 41,000 | 2733 | 86.36 | 90.10 | 1.9 | 7.060 | 1.828 | 46.25 | 81.76 | 8.97 | 97.61 | 3.81 | 104.0 | 342.5 |
| | 52,000 | 3467 | 84.25 | 89.68 | 1.8 | 5.937 | 1.532 | 40.22 | 101.1 | 8.50 | 94.7 | 5.02 | 156.0 | 405.5 |
| | 60,000 | 4000 | 82.84 | 88.96 | 1.7 | 5.433 | 1.406 | 36.39 | 125.2 | 7.58 | 92.67 | 5.66 | 179.2 | 446.8 |
| 6 POLE | 41,000 | 2050 | 87.99 | 90.95 | 1.8 | 6.750 | 1.509 | 52.99 | 59.29 | 17.20 | 83.83 | 2.65 | 80.08 | 296.0 |
| | 52,000 | 2600 | 86.42 | 90.71 | 1.7 | 5.714 | 1.278 | 45.71 | 76.37 | 16.20 | 80.78 | 2.94 | 118.80 | 340.8 |
| | 60,000 | 3000 | 85.66 | 90.47 | 1.6 | 5.170 | 1.150 | 41.25 | 91.20 | 14.35 | 78.46 | 3.24 | 134.40 | 363.0 |
| 4 POLE | 41,000 | 1367 | 88.41 | 90.67 | 1.7 | 7.090 | 1.280 | 64.09 | 41.04 | 45.59 | 71.00 | 1.40 | 61.18 | 284.3 |
| DESIGN SELECTION | 52,000 | 1733 | $\boxed{87.51}$ | 90.78 | 1.6 | 5.977 | 1.079 | 55.33 | 52.50 | 42.48 | 68.33 | 1.57 | 89.35 | 309.5 |
| | 60,000 | 2000 | 87.26 | 90.89 | 1.5 | 5.366 | 0.956 | 50.05 | 61.96 | 37.30 | 66.35 | 1.76 | 99.29 | 316.7 |
| 2 POLE | 41,000 | 683 | 87.83 | 90.77 | 1.8 | 11.03 | 1.451 | 96.52 | 27.02 | 56.93 | 39.05 | 0.98 | 80.0 | 300.5 |
| | 52,000 | 867 | 86.88 | 91.21 | 1.7 | 9.183 | 1.204 | 83.41 | 33.83 | 53.68 | 36.82 | 1.08 | 118.4 | 327.2 |
| | 60,000 | 1000 | 86.66 | 91.55 | 1.6 | 8.227 | 1.068 | 75.71 | 38.77 | 48.13 | 36.12 | 1.21 | 133.7 | 333.7 |

*INCLUDES WINDAGE LOSSES IN THE MAIN GAP AND 1/2 OF THE CONE SECTION

MS 3011-33

TABLE 3-9

Since high efficiency rather than minimum weight was a design goal, the four-pole machine was selected for further optimization and analysis. Practical considerations of fabrication also favored a four-pole machine.

The analysis employed a math model based on conventional salient-pole alternator theory. The model included the following routines:

(a) Pole and flux collector geometry; stator geometry

(b) Pole leakage

(c) Rotor windage loss

(d) End bell design and leakage

(e) Control and series field design

(f) Pole head loss

(g) Eddy factor for stator windings

(h) Apparent power factor, a-c volts and amps, d-c volts and amps, distortion factor, and rectifier losses for operation into a three-phase, full-wave rectifier load.

(i) Iteration of stator turns to achieve specified commutation reactance.

The operation of the alternator math model is such that the initial or "design" load condition synthesizes a basic geometry. Then, when subsequent load conditions are applied, performance is calculated using the initial basic geometry. The basic geometry can readily be changed either by changing the initial "design" load data or by changing initial design parameters such as pole flux density, winding reactance, or an air gap dimension.

Figure 3-10 describes the magnetic circuit used in the alternator math model. An understanding of this circuit is necessary to interpret the magnetic data presented in Table 3-10.

The math model made it possible to rapidly compare many design variations while maintaining consistent values for flux densities, winding reactance, or geometric features as appropriate. Figure 3-11 shows the effect of different designs on efficiency at various load conditions. The 1.5 in. diameter rotor design was selected to meet the maximum output requirements and provide good efficiency at part load. The design point rating of the selected machine is:

- Four pole Rice
- 65.9 volts, L-N
- 12.27 amps per phase
- 2.0 kw
- 2.43 kva
- 3 phase "Y" connected
- 52,000 rpm
- 1733 Hz

A summary of performance of the recommended design for d-c and a-c loads is presented in the following section.

### 3.3.2 Design Analysis

Table 3-10 presents magnetic circuit data for the initializing or design load case and for three different d-c load conditions corresponding to the power available from 1, 2, and 3 energy capsules.

Figure 3-12 presents the alternator wiring diagram used in this analysis and clarifies the proposed excitation system.

# RICE ALTERNATOR MAGNETIC CIRCUIT

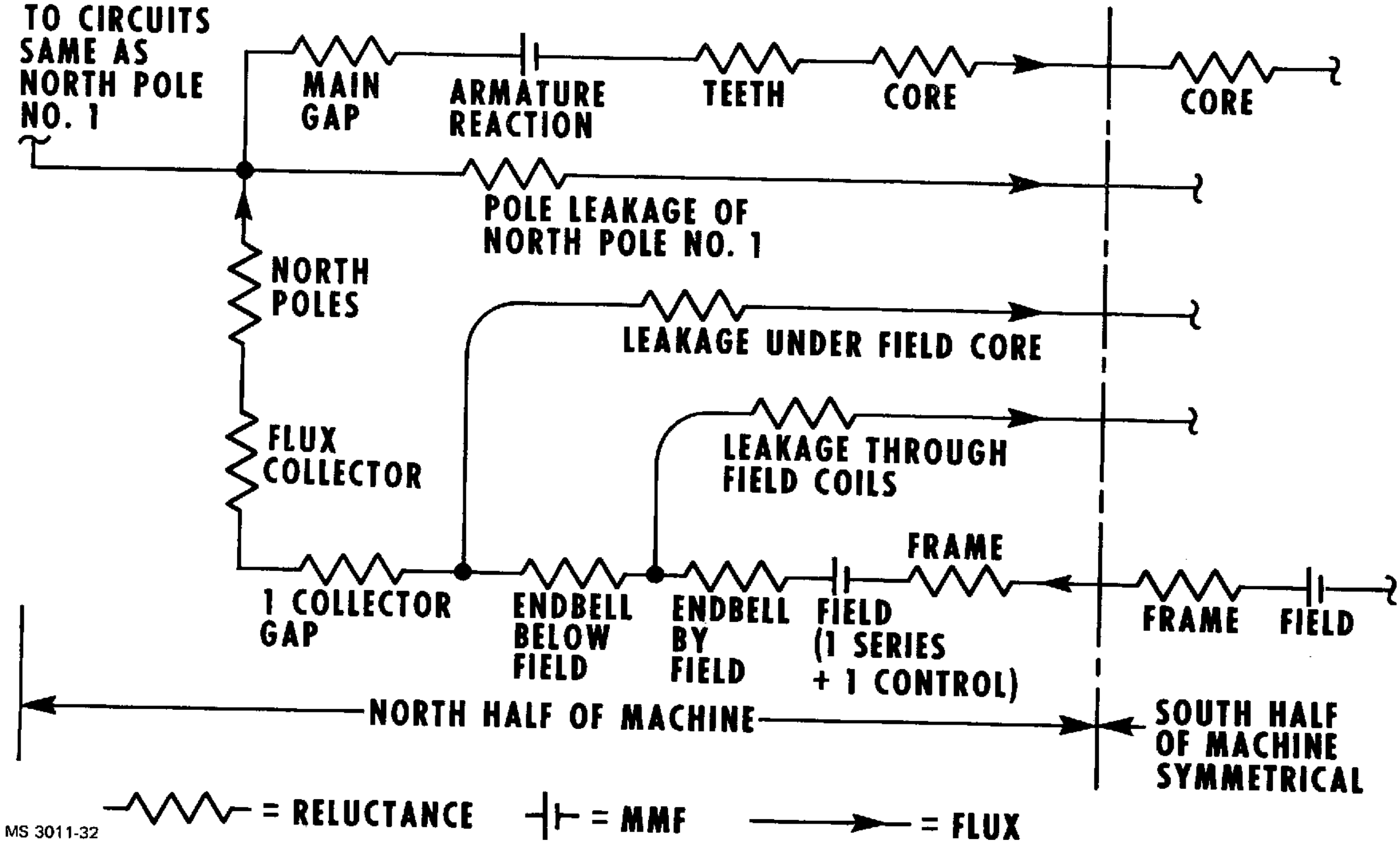


FIGURE 3-10

GARRETT

# MAGNETIC DATA

| | | | | INPUT POWER | | | | | | | | | | | |
|---|---|---|---|---|---|---|---|---|---|---|---|---|---|---|---|
| | | | | 0.883 KW (1 CAPSULE) | | | 1.805 KW (2 CAPSULES) | | | 2.16 KW (DESIGN) | | | 2.574 KW (3 CAPSULES) | | |
| | PERMEANCE LINES/AT | MAGNETIC LENGTH, IN. | AREA, $IN^2$ | KILOLINES PER POLE | KILOLINES PER $IN^2$ | MMF/POLE, AMP TURNS | KILOLINES PER POLE | KILOLINES PER $IN^2$ | MMF/POLE, AMP TURNS | KILOLINES PER POLE | KILOLINES PER $IN^2$ | MMF/POLE, AMP TURNS | KILOLINES PER POLE | KILOLINES PER $IN^2$ | MMF/POLE, AMP TURNS |
| MAIN GAP | | 0.0205 | | 22.10 | 36.85 | 236.0 | 24.64 | 41.08 | 263.1 | 25.55 | 42.61 | 272.9 | 26.70 | 44.52 | 285.0 |
| TEETH | | | | | 81.90 | 4.786 | | 91.31 | 7.624 | | 94.70 | 11.72 | | 98.96 | 30.3 |
| CORE | | | 0.4317 | | 25.60 | 0.2278 | | 28.54 | 0.2464 | | 29.60 | 0.2559 | | 30.93 | 0.260 |
| ARMATURE REACTION | | | | | | 52.53 | | | 142.4 | | | 179.6 | | | 222.0 |
| POLE LEAKAGE | 27.94 | | | 8.195 | | | 11.55 | | | 12.97 | | | 27.94 | | |
| POLES* | | | 0.8111 | 60.59 | 74.70 | 79.20 | 72.38 | 89.23 | 127.6 | 77.06 | 95.00 | 165.5 | 83.45 | 102.9 | 277.7 |
| FLUX COLLECTOR* | | | 0.7823 | 60.59 | 74.45 | 26.29 | 72.38 | 92.52 | 43.31 | 77.06 | 98.50 | 62.51 | 83.45 | 106.7 | 154.1 |
| COLLECTOR GAP* | | 0.0200 | 3.185 | 60.59 | 19.02 | 119.1 | 72.38 | 22.73 | 142.3 | 77.06 | 24.19 | 151.5 | 83.45 | 26.2 | 164.0 |
| FIELD LEAKAGE* | | | | | | | | | | | | | | | |
| UNDER COIL* | 9.73 | | | 5.05 | | | 7.07 | | | 8.21 | | | 11.04 | | |
| THRU COIL* | 10.48 | | | 5.47 | | | 7.68 | | | 8.92 | | | 12.01 | | |
| END BELL* | | | 1.066 | 65.64 | 61.58 | 4.198 | 79.45 | 74.54 | 6.339 | 85.27 | 80.00 | 7.543 | 94.47 | 88.65 | 11.48 |
| | | | 1.177 | 71.11 | 60.39 | 4.234 | 87.13 | 74.00 | 6.522 | 94.19 | 80.00 | 7.090 | 106.5 | 90.41 | 13.10 |
| FRAME | | | 22.35 | 71.11 | 60.39 | 9.580 | 87.13 | 74.00 | 14.76 | 94.19 | 80.00 | 17.89 | 106.5 | 90.44 | 29.63 |
| TOTAL AMP TURNS/1/2 MACHINE | | | | | | 536.0 | | | 754.2 | | | 877.2 | | | 1188. |

*VALUES PER 1/2 MACHINE (NOT PER POLE) IN ACCORDANCE WITH MAGNETIC CIRCUIT

MS 3063-13

TABLE 3-10

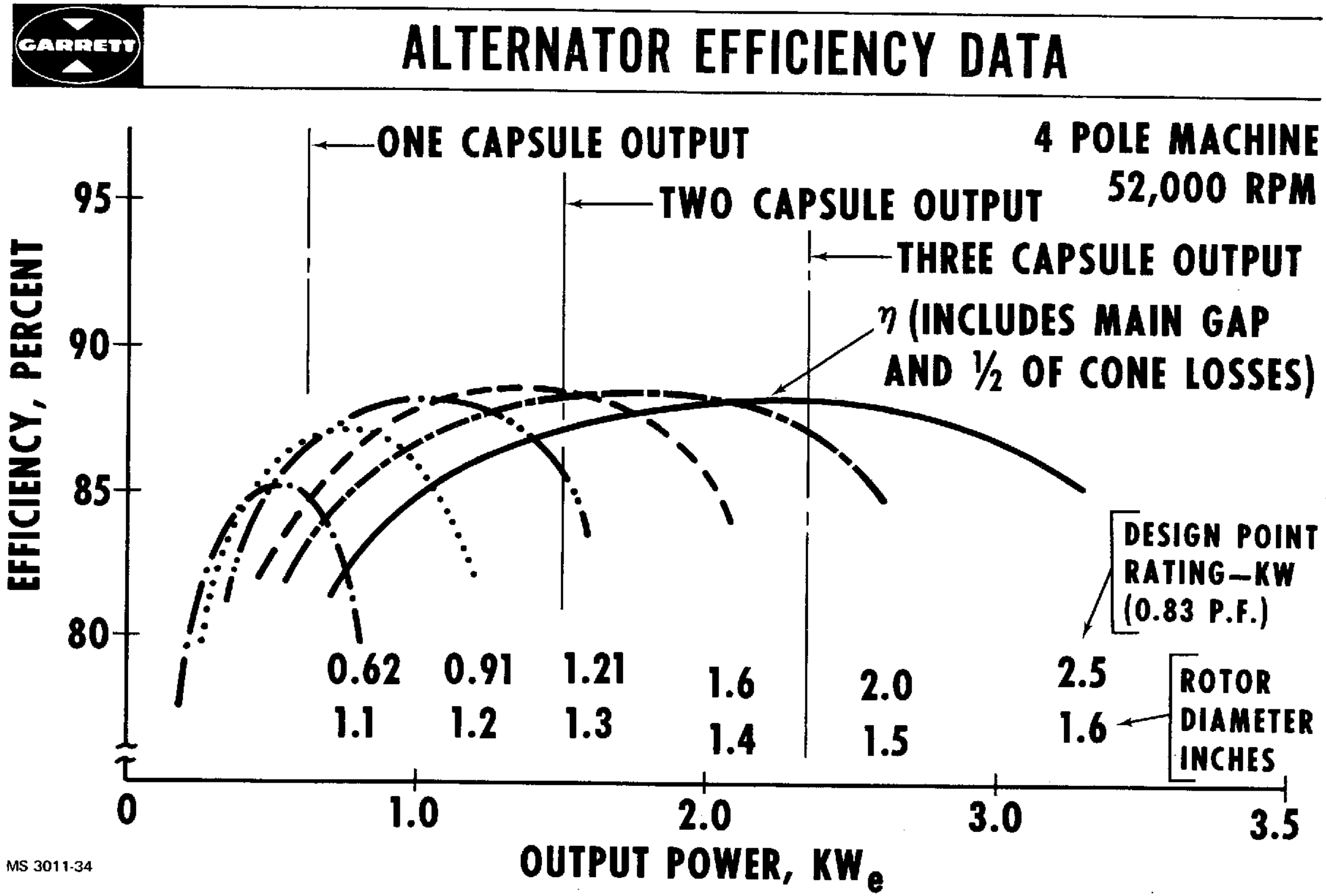
GARRETT
ALTERNATOR EFFICIENCY DATA
ONE CAPSULE OUTPUT
TWO CAPSULE OUTPUT
THREE CAPSULE OUTPUT
4 POLE MACHINE
52,000 RPM
η (INCLUDES MAIN GAP
AND ½ OF CONE LOSSES)
EFFICIENCY, PERCENT
95
90
85
80
0.62
1.1
0.91
1.2
1.21
1.3
1.6
1.4
2.0
1.5
2.5
1.6
DESIGN POINT
RATING—KW
(0.83 P.F.)
ROTOR
DIAMETER
INCHES
0
1.0
2.0
3.0
3.5
OUTPUT POWER, KWe
MS 3011-34

FIGURE 3-11

GARRETT

# WIRING DIAGRAM

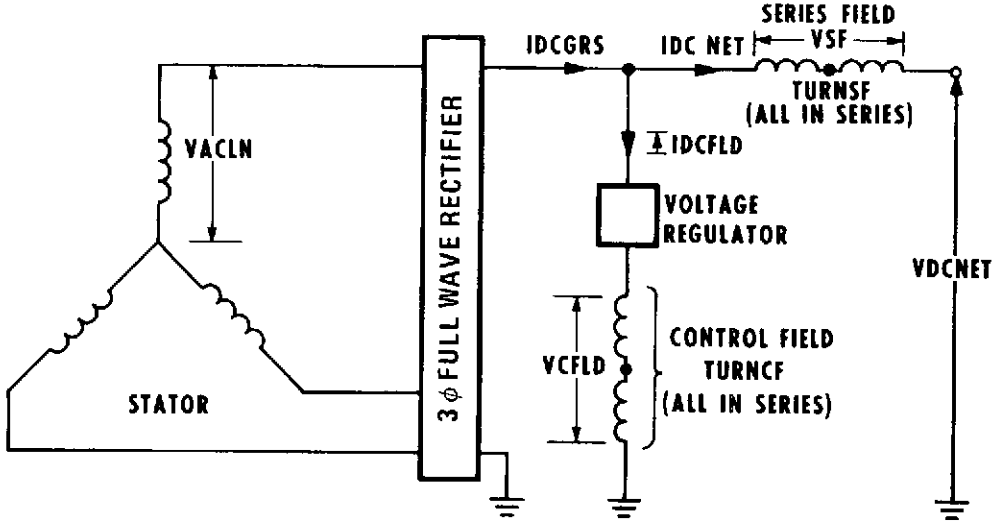


IDCGRS - TOTAL DC CURRENT FROM RECTIFIER, AMPS

IDCFLD - CONTROL FIELD CURRENT, AMPS

IDCNET - DC LOAD CURRENT, AMPS

VACLN - LINE TO NEUTRAL VOLTAGE, AC VOLTS

VCFLD - VOLTAGE ACROSS CONTROL FIELD, DC VOLTS

VSF - VOLTAGE ACROSS SERIES FIELD, DC VOLTS

VDC NET - DC BUS VOLTAGE, DC VOLTS

TURNSF - TOTAL NUMBER OF TURNS IN SERIES FIELD

TURNCF - TOTAL NUMBER OF TURNS IN CONTROL FIELD

MS 3011-29

FIGURE 3-12

Significant electrical parameters of the alternator are listed in Table 3-11. These values are based on the Design Load case in which base alternator voltage is 65.9 $V_{L-N}$; base alternator current is 12.27 amps ac, and the frequency is 1733 Hz. Since a rectifier load is specified, the subtransient reactance is a critical parameter for this application because it determines the apparent power factor of the load as a function of load current.

When the alternator is regulated to maintain a constant rectified load voltage of 120 vdc, change in load current will cause a change in apparent load power factor, alternator ac voltage and field excitation. This is depicted in Figure 3-13.

Operation at 3 pu short circuit is specified; therefore, a series field is required to provide adequate excitation for the short circuit condition. This requirement defines the slope of the series field excitation line shown in Figure 3-14. The control field curve is simply the difference between the total field curve and the series field curve. The use of a series field is not conducive to optimum efficiency at every load condition since the current density is not equal in the series and control field windings, except at certain points.

The losses in the control field and series field, the rectifier loss, and the alternator efficiency are presented in Table 3-12 and Figure 3-15.

Alternator losses at unity power factor at various ac load conditions are tabulated in Table 3-13. The corresponding efficiency and loss curves are shown in Figure 3-16.

Alternator characteristics at unity pf load conditions, no-load, and short circuit are shown in Figure 3-17. Zero pf characteristics are shown in Figure 3-18.

GARRETT

# ALTERNATOR PARAMETERS

## REACTANCE & RESISTANCE, FIELD TIME CONSTANT

| | | |
|---|---|---|
| BASE IMPEDANCE | $Z_{BASE}$ | 5.371 OHM |
| RESISTANCES | | |
| ARMATURE (@ 360°F) | $R_A$ | 0.0944 OHM |
| FIELD (@ 350°F) – 2 CONTROL FIELDS IN SERIES | $R_{CF}$ | 9.295 OHMS |
| – 2 SERIES FIELDS IN SERIES | $R_{SF}$ | 0.0669 OHMS |
| REACTANCES | | |
| DIRECT AXIS SYNCHRONOUS | $X_D$ | 1.040 PER UNIT |
| QUADRATURE AXIS SYNCHRONOUS | $X_Q$ | 0.556 PER UNIT |
| ARMATURE LEAKAGE | $X_L$ | 0.152 PER UNIT |
| FIELD LEAKAGE | $X_F$ | 0.286 PER UNIT |
| ZERO SEQUENCE | $X_0$ | 0.066 PER UNIT |
| NEGATIVE SEQUENCE | $X_2$ | 0.200 PER UNIT |
| TRANSIENT | $X_{DU}$ | 0.439 PER UNIT |
| SUBTRANSIENT DIRECT* | $\approx X''_D$ | 0.382 PER UNIT |
| SUBTRANSIENT QUADRATURE* | $\approx X''_Q$ | 0.382 PER UNIT |
| FIELD TIME CONSTANT (HOT) SHORT CCT | TPD | 0.0137 SECONDS |
| OPEN CCT | | 0.0369 SECONDS |

*ESTIMATED VALUE FOR RICE ROTOR WITH NO DAMPER CAGE

MS 3063-14

TABLE 3-11

# EXCITATION CHARACTERISTICS — DC LOAD

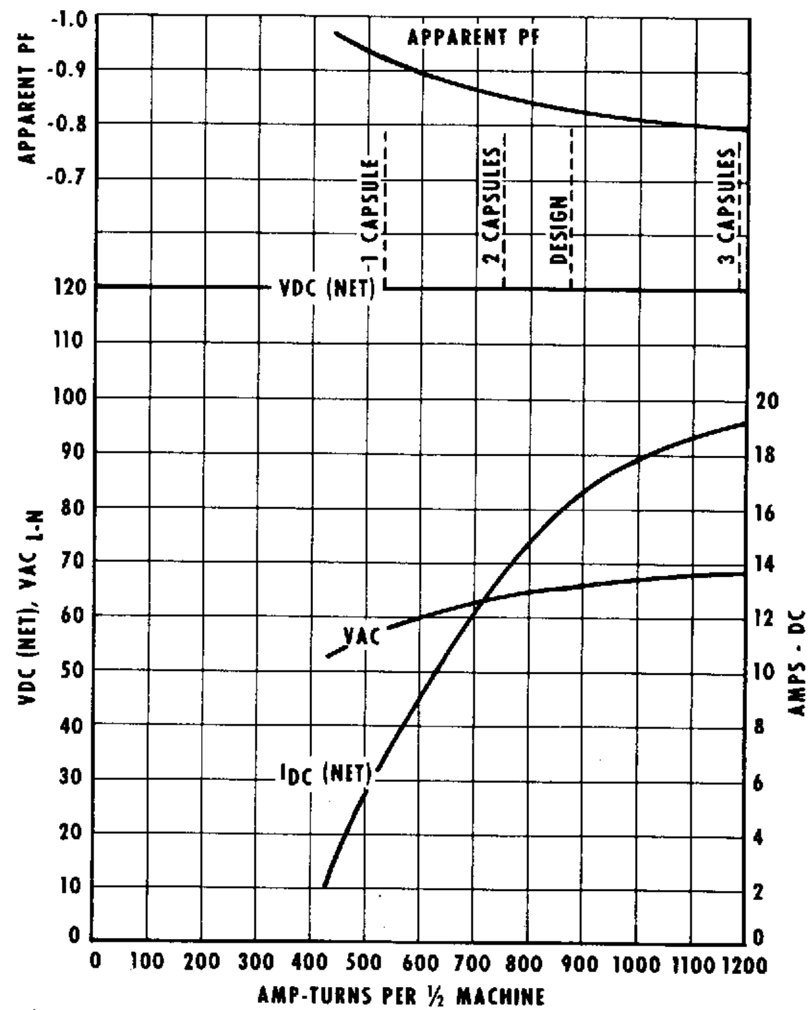


MS 3063-15

FIGURE 3-13

# FIELD CURRENT – DC LOAD

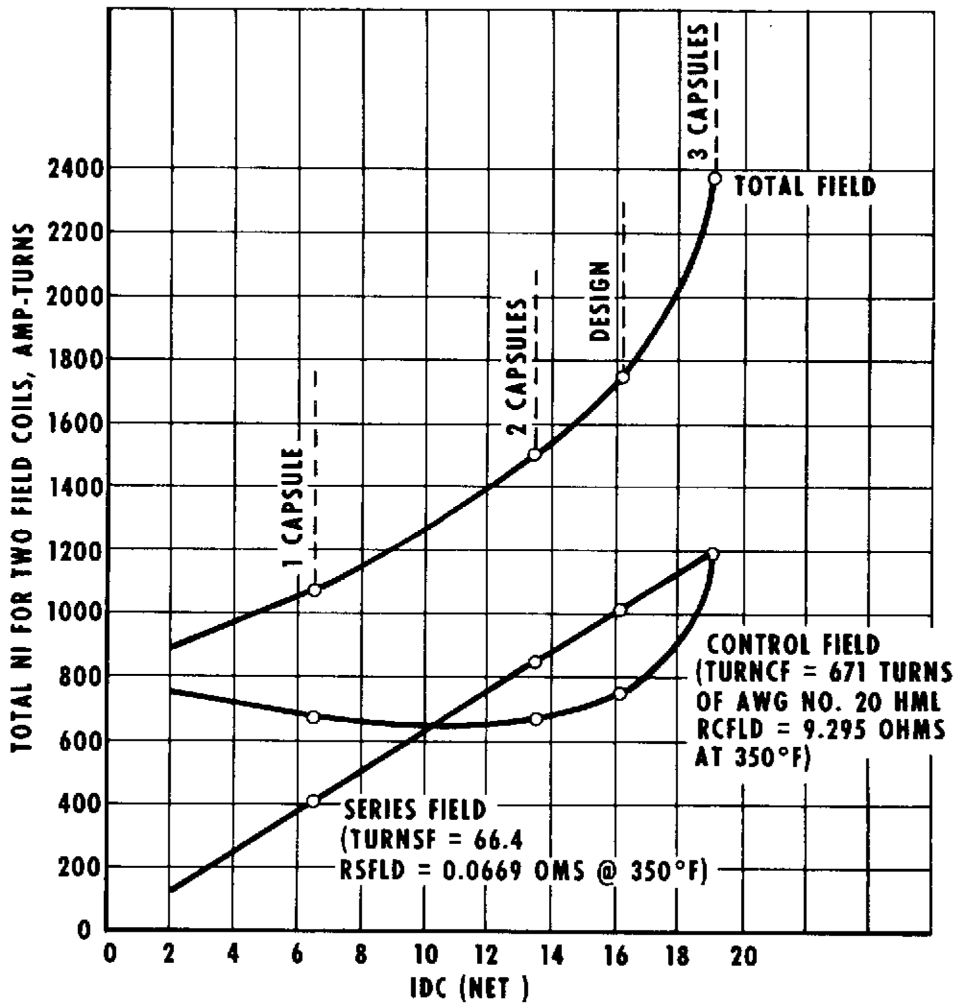


MS 3063-16

FIGURE 3-14

# ALTERNATOR AND RECTIFIER LOSSES (KW)

| | INPUT POWER | | | | | |
|---|---|---|---|---|---|---|
| | 2 AMP DC NET (0.315 KW) | 4 AMP DC NET (0.563 KW) | 1 CAPSULE (0.883 KW) | 2 CAPSULES (1.805 KW) | DESIGN (2.16 KW) | 3 CAPSULES (2.574 KW) |
| CORE | 0.00984 | 0.01050 | 0.01145 | 0.01423 | 0.01530 | 0.01671 |
| TEETH | 0.01709 | 0.01823 | 0.01988 | 0.02471 | 0.02657 | 0.02902 |
| STATOR COPPER | 0.00086 | 0.00301 | 0.00742 | 0.03025 | 0.04278 | 0.05948 |
| STRAY | 0.00004 | 0.00012 | 0.00030 | 0.00124 | 0.00175 | 0.00244 |
| POLE HEAD | 0.01418 | 0.01565 | 0.01809 | 0.02780 | 0.03249 | 0.03871 |
| CONTROL FIELD | 0.01153 | 0.01031 | 0.00921 | 0.00914 | 0.01406 | 0.02879 |
| SERIES FIELD | 0.00024 | 0.00095 | 0.00247 | 0.01077 | 0.01550 | 0.02163 |
| WINDAGE | 0.01281 | 0.02071 | 0.02962 | 0.05234 | 0.06019 | 0.06904 |
| TOTAL (ALTERNATOR) | 0.06659 | 0.07948 | 0.09844 | 0.17048 | 0.20864 | 0.26582 |
| EFFICIENCY (ALT) | 79.8% | 86.0% | 88.9% | 90.6% | 90.3% | 89.7% |
| RECTIFIER (BASED ON LOSS EQUIVALENT TO 1.5 $V_{FWD}$) | 0.00330 | 0.00625 | 0.00992 | 0.02047 | 0.02450 | 0.02908 |
| TOTAL LOSSES | 0.06989 | 0.08573 | 0.10836 | 0.19095 | 0.23314 | 0.2949 |
| EFFICIENCY (DC NET) | 77.5% | 84.8% | 87.7% | 89.4% | 89.3% | 88.6% |

MS 3063-17

TABLE 3-12

# EFFICIENCY AND LOSSES – DC LOAD

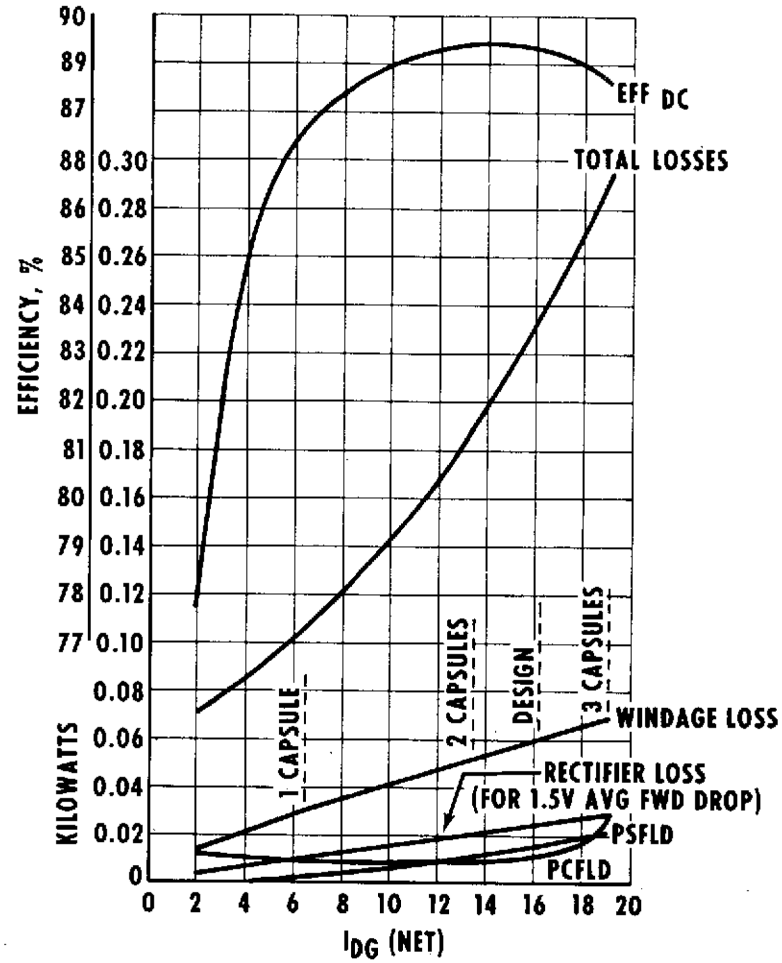


MS 3063-18

FIGURE 3-15

GARRETT

# ALTERNATOR LOSSES (KW) AT UNITY P.F.

## AC MODE: $I_{AC}$ = 12.27 AMPS $V_{AC}$ = 65.9 VOLTS

| PER UNIT CURRENT | LOAD CONDITIONS | | | | | |
|---|---|---|---|---|---|---|
| | 0 | 0.25 | 0.50 | 0.75 | 1.00 | 1.25 |
| CORE | 0.01471 | 0.01484 | 0.01485 | 0.01482 | 0.01479 | 0.01483 |
| TEETH | 0.02555 | 0.02577 | 0.02579 | 0.02573 | 0.02569 | 0.02575 |
| STATOR COPPER | 0.0000 | 0.00267 | 0.01070 | 0.02407 | 0.04278 | 0.06685 |
| STRAY | 0.0000 | 0.00011 | 0.00044 | 0.00099 | 0.00175 | 0.00274 |
| POLE HEAD | 0.02089 | 0.02175 | 0.02379 | 0.02709 | 0.03177 | 0.03788 |
| FIELD* | 0.01055 | 0.01125 | 0.01284 | 0.01536 | 0.01911 | 0.02417 |
| WINDAGE | 0.000 | 0.02376 | 0.04067 | 0.05589 | 0.07019 | 0.08386 |
| TOTAL | 0.07170 | 0.1002 | 0.1291 | 0.1639 | 0.2061 | 0.2561 |
| EFFICIENCY | | 85.81% | 90.37% | 91.73% | 92.16% | 92.21% |

*BASED ON DESIGN WITHOUT SERIES FIELD COMPOUNDING

MS 3063-19

TABLE 3-13

# EFFICIENCY & LOSSES — UNITY POWER FACTOR LOAD

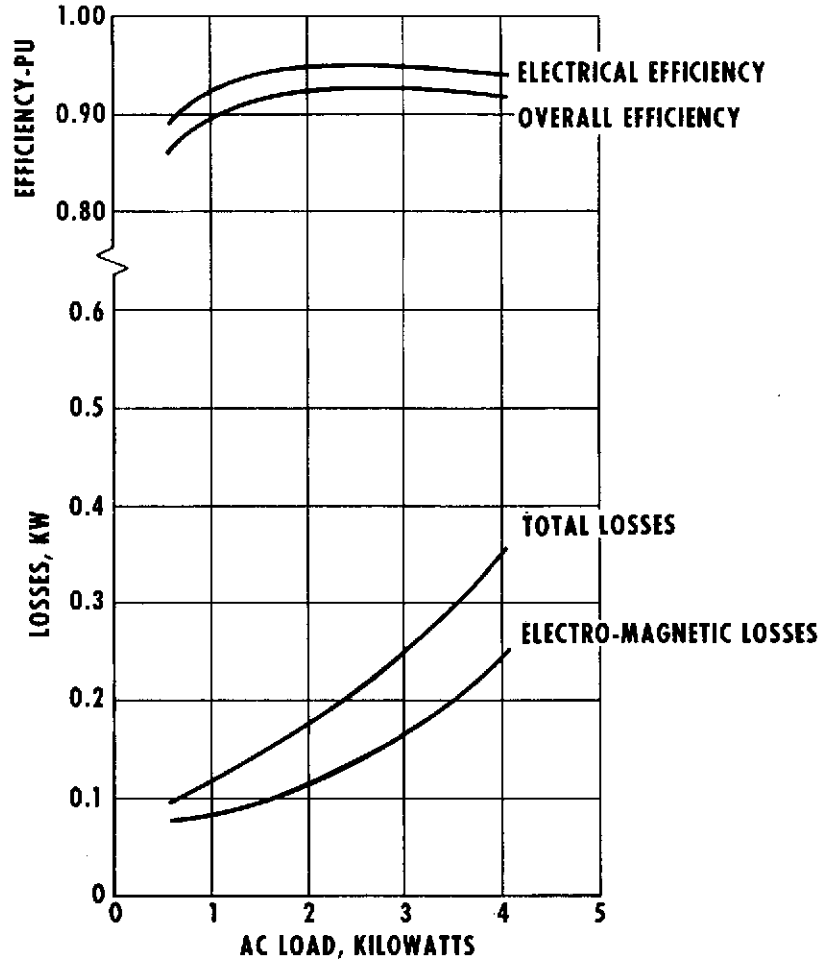


MS 3011-36

FIGURE 3-16

# EXCITATION CHARACTERISTICS NO LOAD AND SHORT CIRCUIT

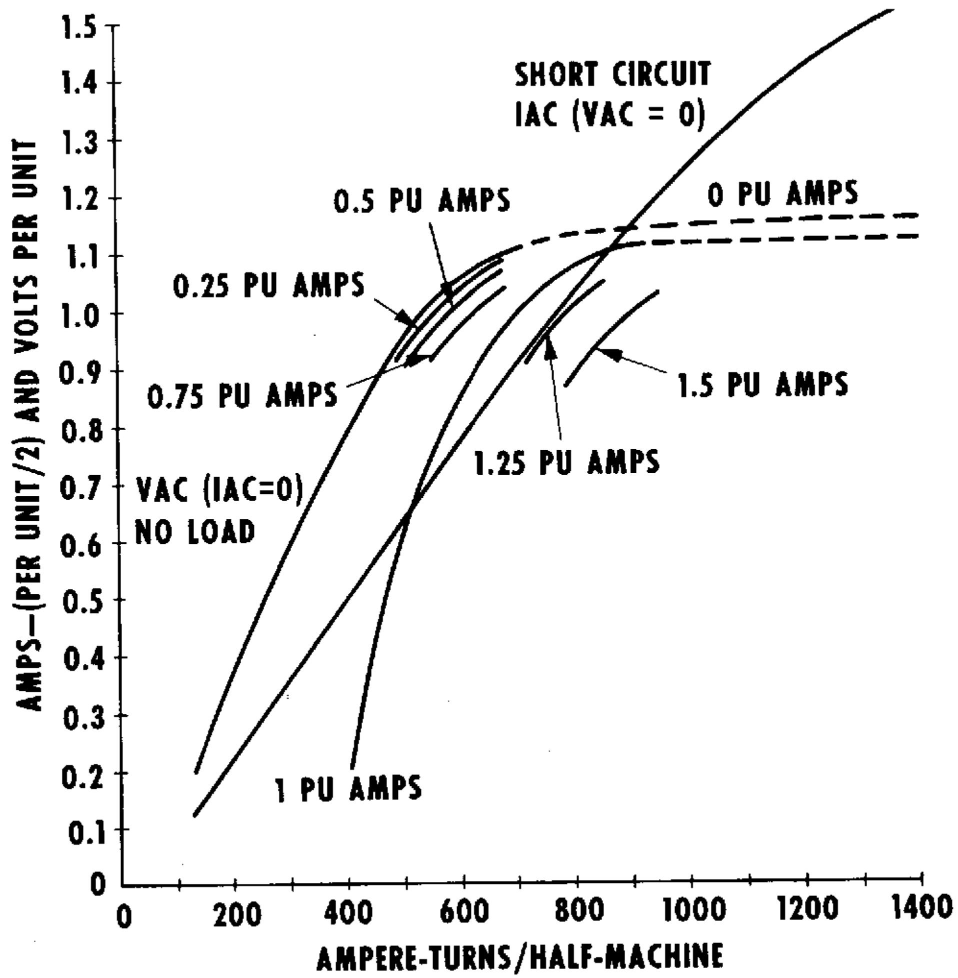


MS 3011-30

FIGURE 3-17

# ALTERNATOR CHARACTERISTICS AT ZERO POWER FACTOR

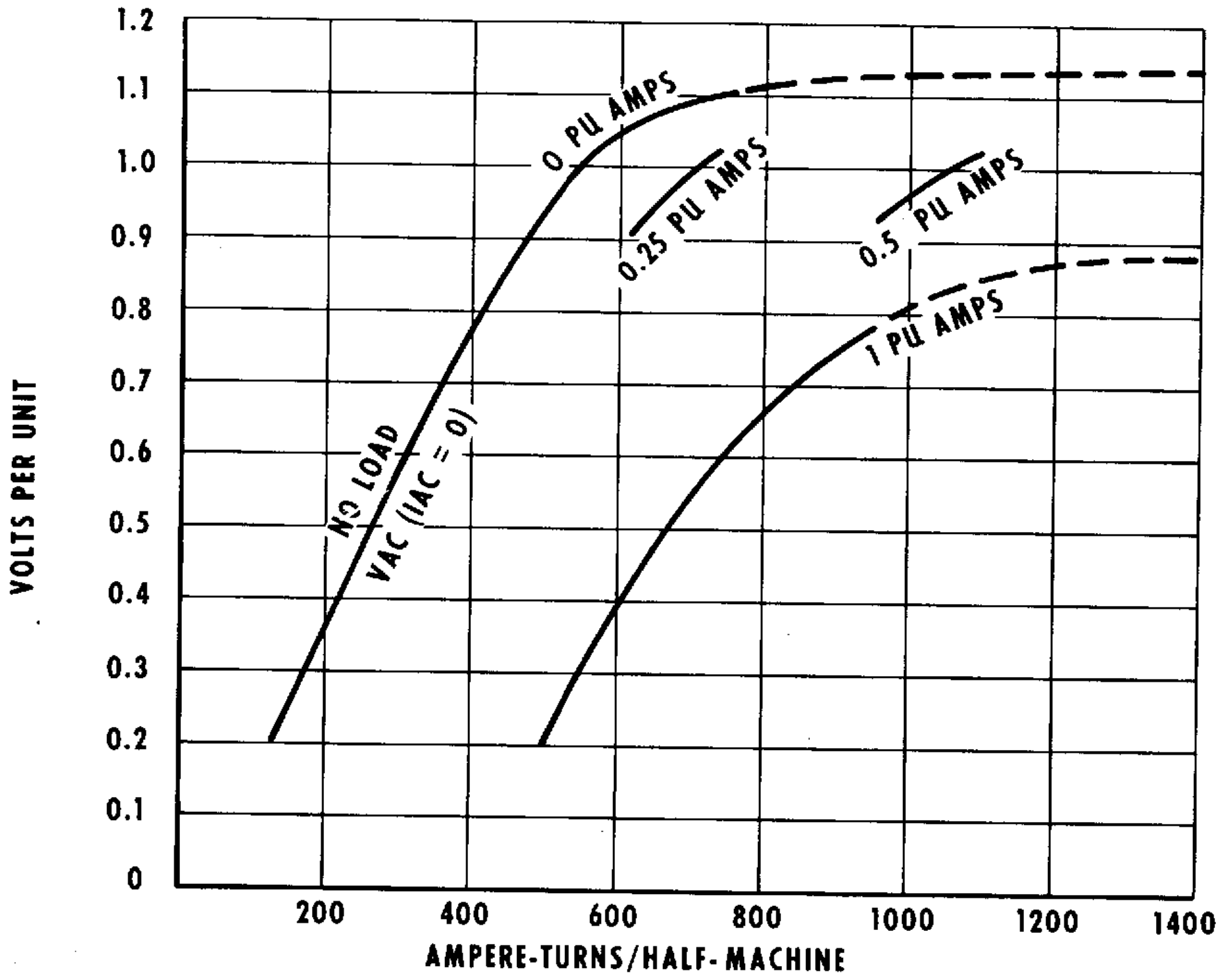


MS 3063-20

FIGURE 3-18

### 3.3.3 Motor Start Characteristics

Figures 3-19 and 3-20 show the expected performance characteristics of the alternator when operated as an induction motor.

For purposes of evaluation, the breakaway torque is estimated to be 0.22 to 0.33 Newton-meters (2.0 to 3.0 in.-lb); however, the maximum drag torque is expected to be about 0.33 to 0.45 Newton-meters (3.0 to 4.0 in.-lb) at about 4000 rpm. Using the torque/slip relationship of

$$\tau = \tau_{LR} \, S^{1/2},$$

the required stall torque to accelerate past the maximum drag torque speed is 1.58 per unit.

### 3.3.4 Magnetic Unbalance Characteristics

The standstill forces that would be developed with the rotor magnetically displaced and the unit excited for rated load and short circuit conditions are given as negative spring rates in Table 3-14. These forces were calculated using standard magnetic theory.

It has been demonstrated that the force is significantly reduced when the rotor is rotated. As reported in NASA CR-1452, the force is reduced by a factor of four in a homopolar inductor alternator. Tests with the Brayton Rotating Unit (BRU) four-pole Rice alternator demonstrated significant reduction, in that excitation at standstill locked the rotor; whereas the same excitation at a few hundred rpm only slightly affected the rotor orbit. A mathematical model of the Rice machine was developed to evaluate the effects of rotation on unbalance forces in the auxiliary gap. The results of the analysis indicated that the force was reduced by a factor of two, maximum, at speeds greater than 7000 rpm. A similar reduction in main gap force is expected.

GARRETT

# MOTOR START CHARACTERISTICS I

PER UNIT RATING

| | |
|---|---|
| 65.9 | VOLTS, L-N |
| 12.27 | AMPS PER PHASE |
| 2.0 | KW |
| 2.43 | KVA |
| 3.25 | IN.-LB (0.367 NEWTON-METERS) |
| 52,000 | RPM |
| 1733 | Hz |
| 0.038 | VOLTS/Hz |

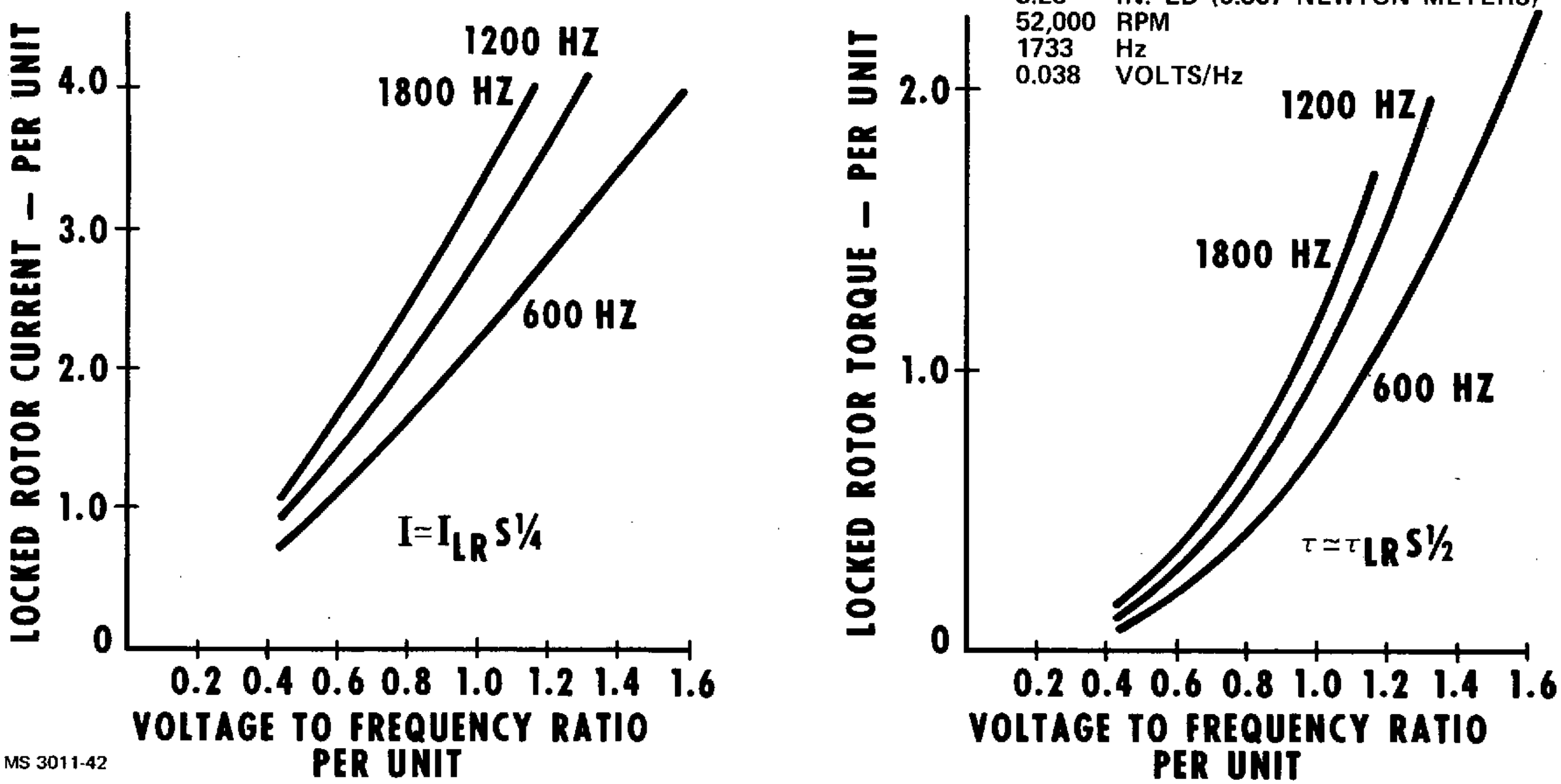


MS 3011-42

FIGURE 3-19

# MOTOR START CHARACTERISTICS II

PER UNIT RATING

| | |
|---|---|
| 65.9 | VOLTS, L-N |
| 12.27 | AMPS PER PHASE |
| 2.0 | KW |
| 2.43 | KVA |
| 3.25 | IN.-LB (0.367 NEWTON-METERS) |
| 52,000 | RPM |
| 1733 | Hz |
| 0.038 | VOLTS/Hz |

---- KVA
—— KW

**ASSUMES**
**ROTOR WT = 2.0 LBS**
**ROTOR IP = 0.0022 IN-LB-SEC$^2$**

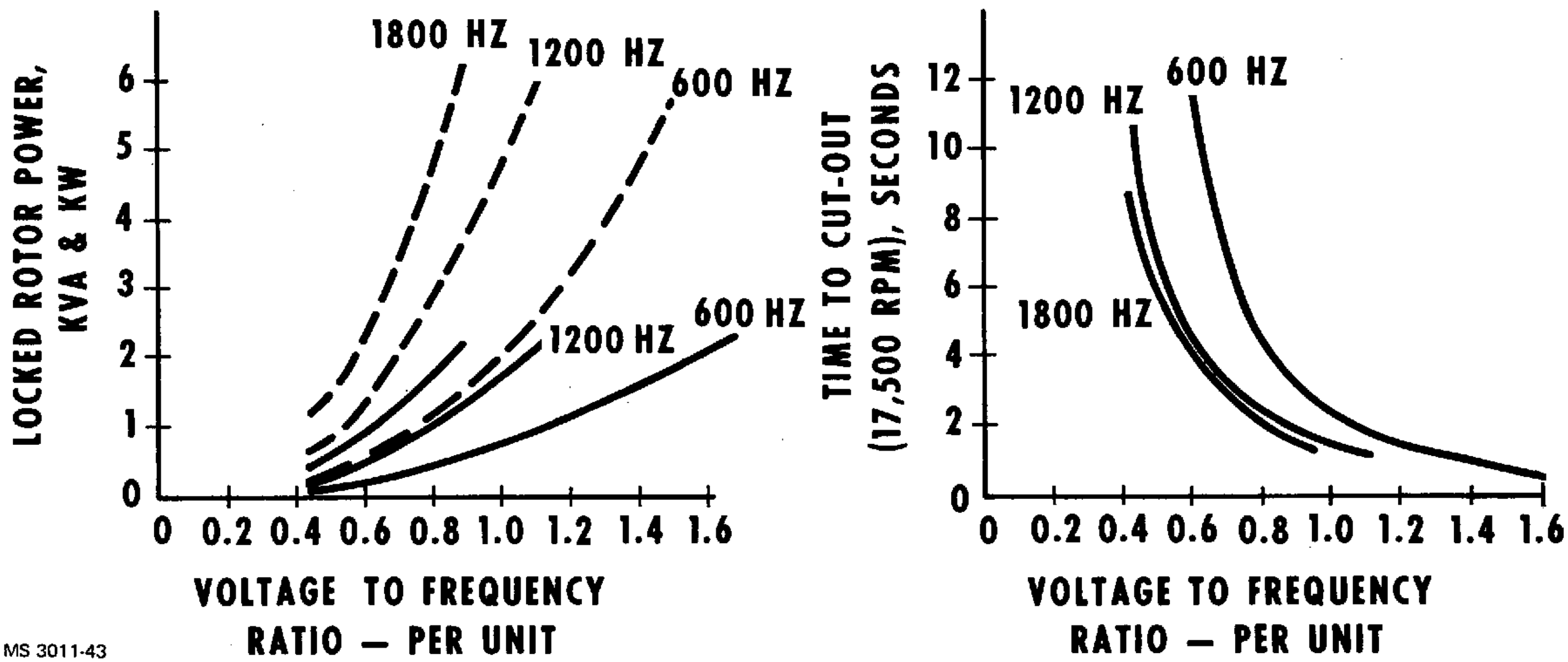


MS 3011-43

FIGURE 3-20

# MAGNETIC UNBALANCE — ALTERNATOR OPERATION

## STANDSTILL FORCE 'SPRING RATE'[1]

| LOCATION | 1 CAPSULE | 2 CAPSULES | 3 CAPSULES | 3 CAPSULES SHORT CCT (36.8 AMPS/$\phi$) |
|---|---|---|---|---|
| AUXILIARY GAP (EACH BEARING) N/CM (LB/IN.) OF DISPLACEMENT | 1424 (813) | 2033 (1161) | 2702 (1543) | 2492 (1423) |
| MAIN GAP N/CM (LB/IN.) OF DISPLACEMENT | 2988 (1706) | 3710 (2118) | 4360 (2490) | 1470 (840) |

[1]VALUES ARE IN THE DIRECTION OF MINIMUM AIR GAP.

EFFECT OF ROTATION: THE SPRING RATE WILL BE REDUCED BY A FACTOR OF 2 AT SPEEDS GREATER THAN 7000 RPM AND WILL BE DIRECTED AT AN ANGLE OF 24.5 DEGREES PRECEEDING THE MINIMUM AIR GAP.

MS 3063-21

The effect of magnetic unbalance due to field excitation is minimized by inhibiting excitation until the machine has passed through the critical speeds and the gas bearing film is established.

Displacement will also result in magnetic unbalance forces during motor starts. Figure 3-21 shows the expected "negative spring rate" as a function of speed for a motor start with 0.003 in. displacement and using a fixed 31 v, 600 Hz supply as required to provide worst case starting torque (see Section 3.3.2).

# MAGNETIC UNBALANCE – MOTOR START OPERATION

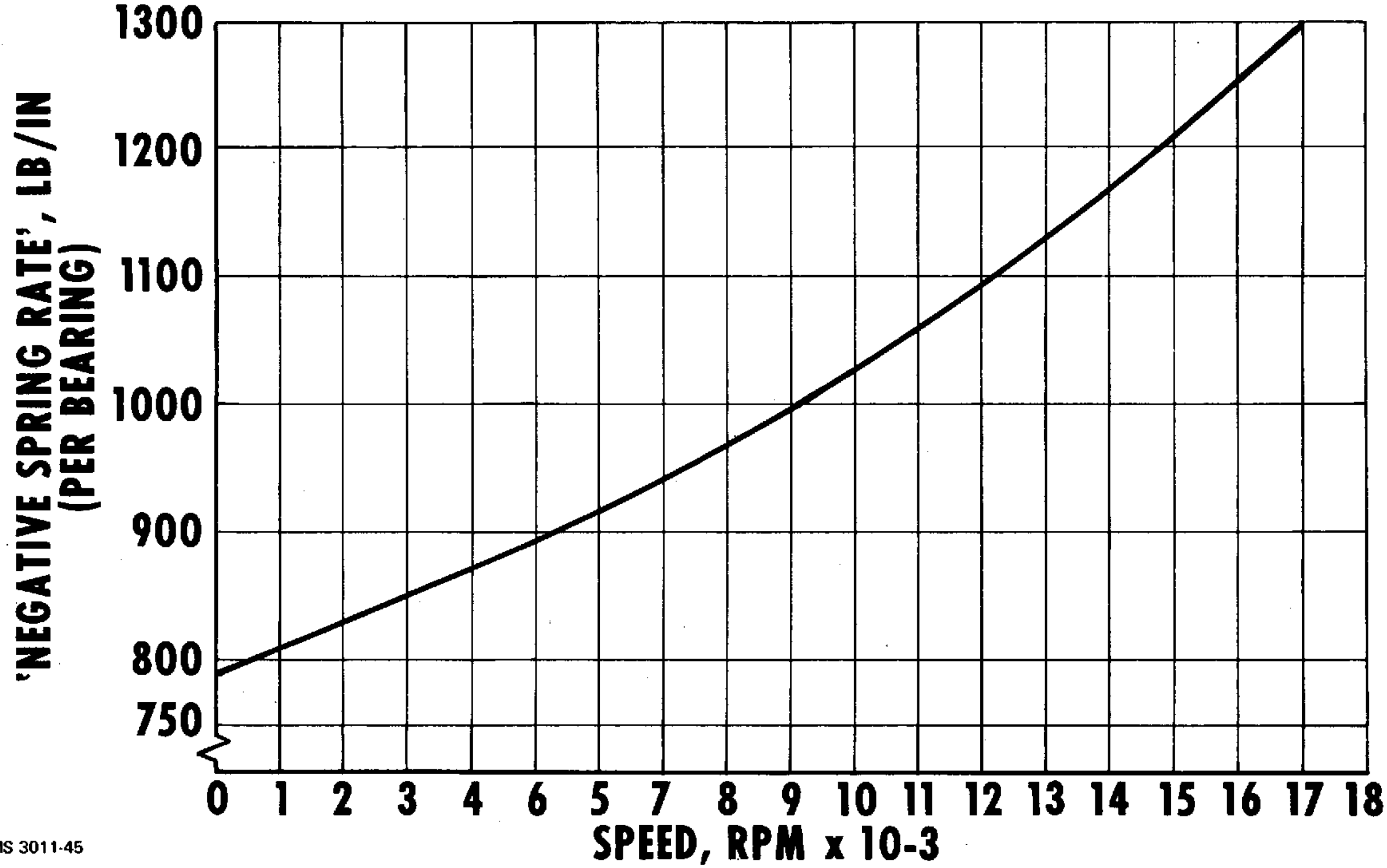


MS 3011-45

FIGURE 3-21

## 3.4 Thermal Analysis

### 3.4.1 General Approach

The rotor thermal analysis was performed in three parts. The turbine, and compressor and thrust runner were both analyzed at AiResearch, Phoenix, while the alternator portion of the rotating group was analyzed by the Los Angeles Division. This approach is shown diagrammatically in Figure 3-22.

The gas path boundary conditions for the Phoenix portion of the analysis were those specified for the three capsule reference design, shown in Figure 1-6. Several heat flexes were specified by Phoenix at the interface with the alternator (see Figures 3-23 and 3-24). Los Angeles then used these heat flux and interface temperatures as boundary conditions for thermal analysis of the alternator. The results of the combined analysis for the 3 and 1 capsule power levels are presented in Figures 3-25 and 3-26.

### 3.4.2 Turbine-End

The results of the turbine-end thermal analysis for both 1 and 2 percent cooling flows are presented in Figure 3-23. The maximum equivalent stress is less than 15 ksi which, for the 713LC turbine material, operating at metal temperatures less than 1300°F, represent a very conservative design.

### 3.4.3 Compressor-End

The compressor and thrust runner thermal analysis data are presented in Figure 3-24. The maximum heat flow rate to the compressor of approximately 120 watts is quite low compared to that of other turbomachines designed by AiResearch, and no thermal stress problems are anticipated over the design life goal of 5 yr. In addition, the radial

# THERMAL ANALYSIS PROBLEM APPROACH

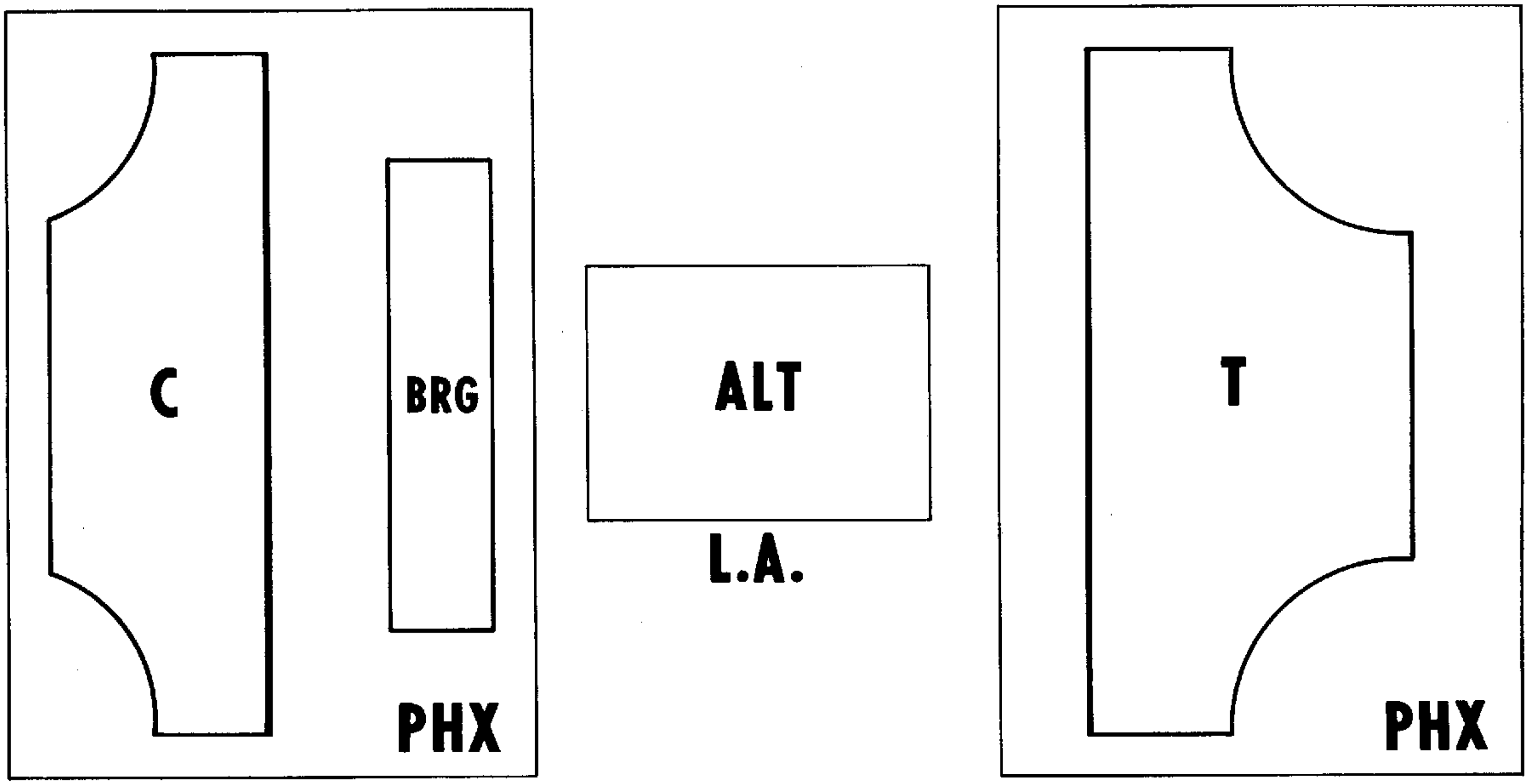


MS 3011-12

FIGURE 3-22

# TURBINE WHEEL THERMAL ANALYSIS

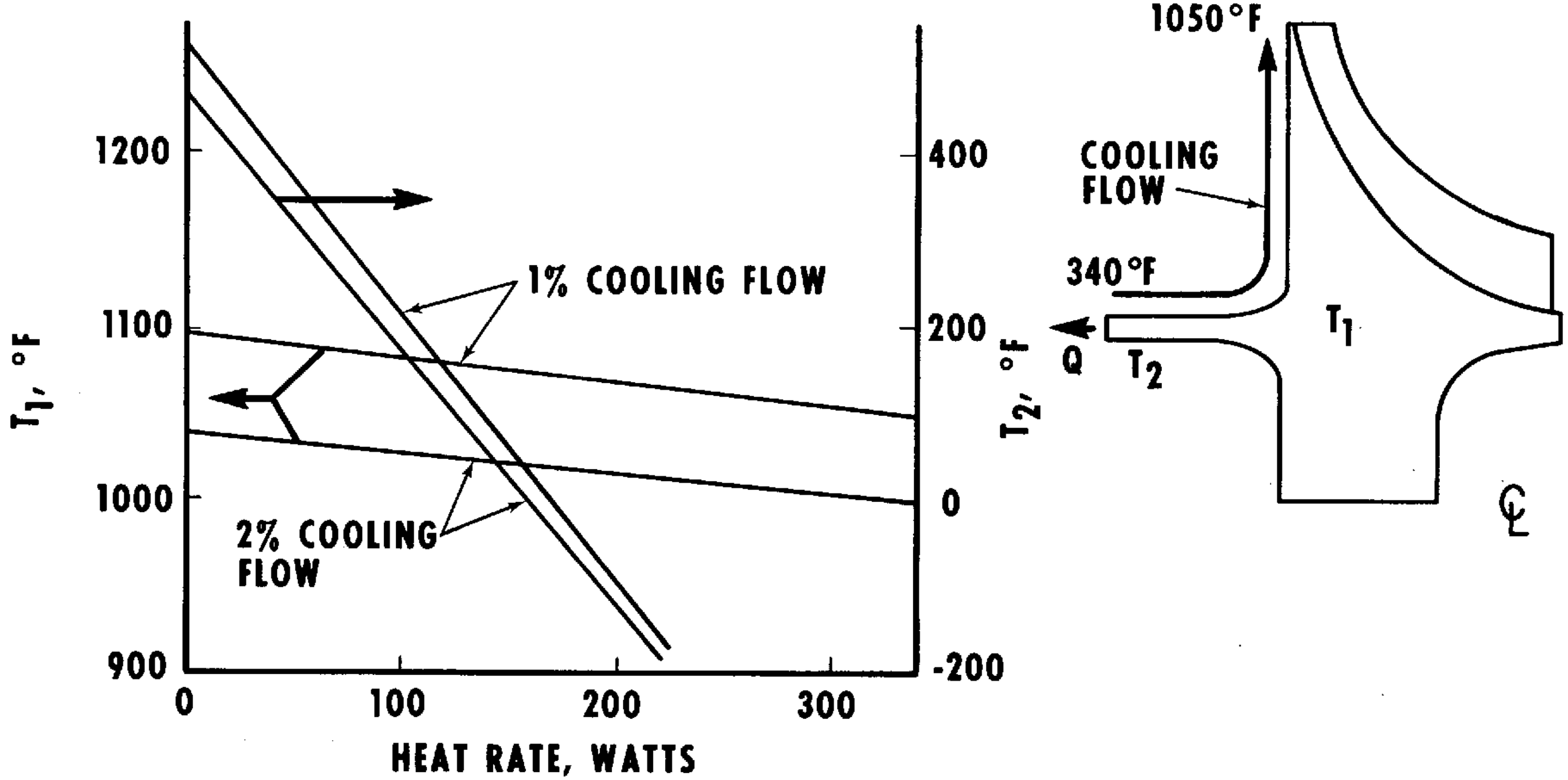


MS 3063-22

FIGURE 3-23

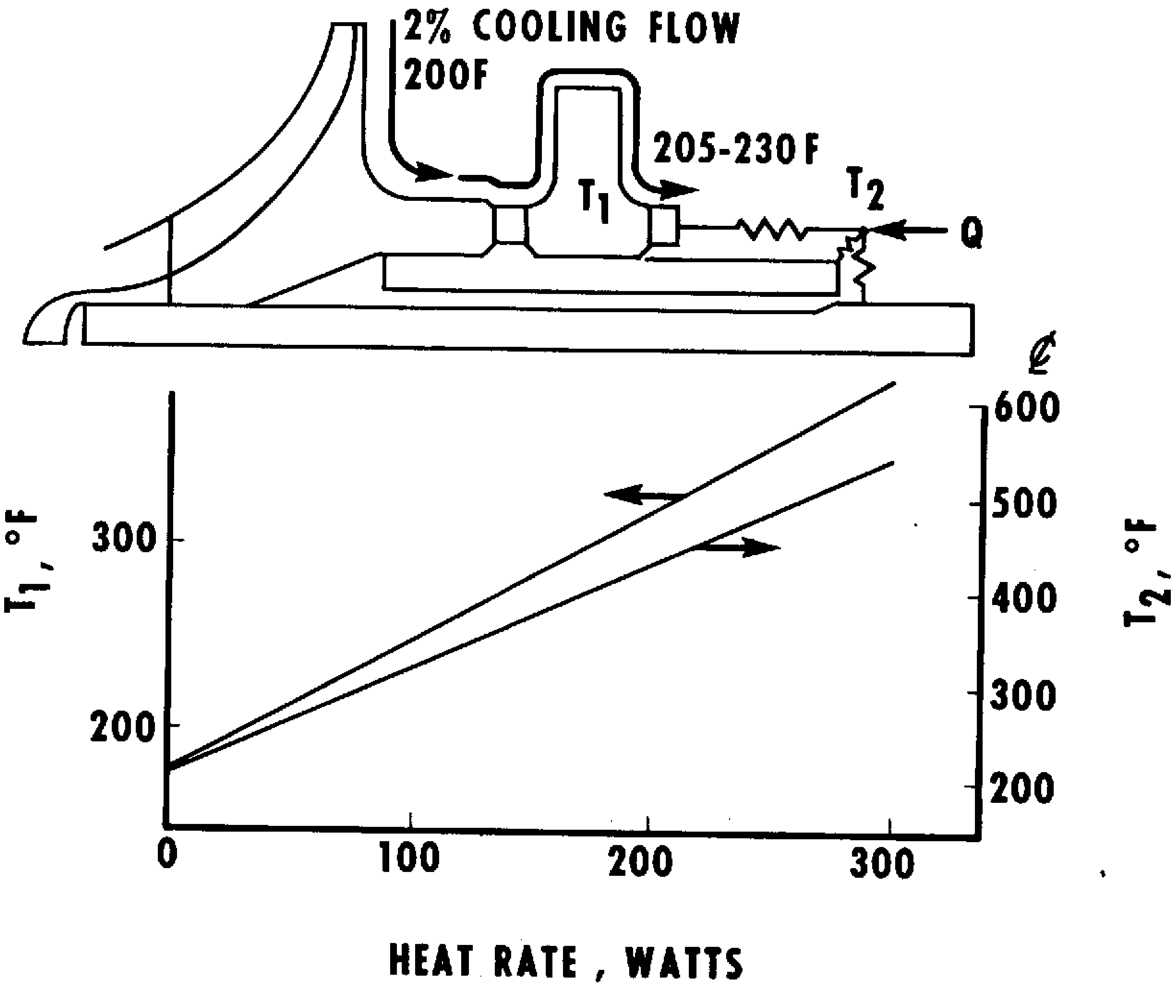


MS 3063-23

FIGURE 3-24

# THERMAL DESIGN SUMMARY – 3 CAPSULES

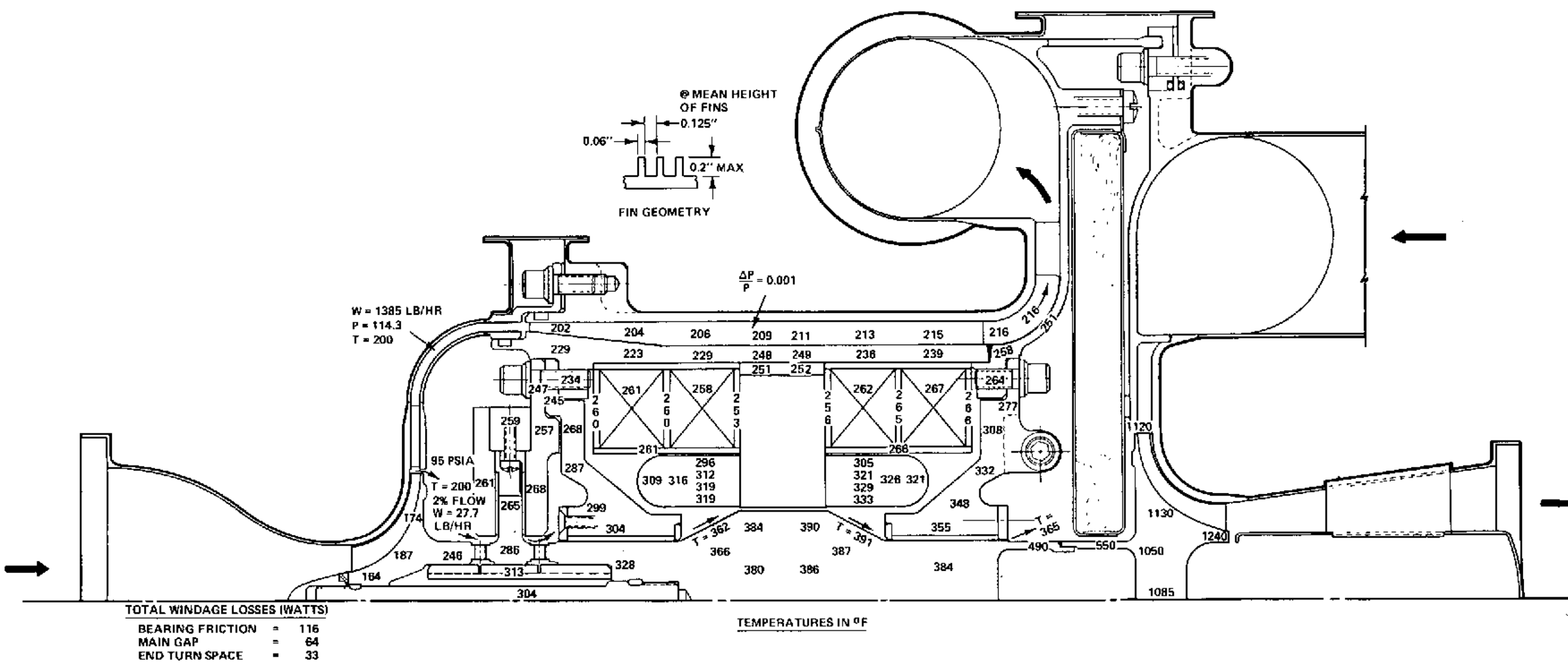


MS 3011-15

FIGURE 3-25

GARRETT

# THERMAL DESIGN SUMMARY – 1 CAPSULE

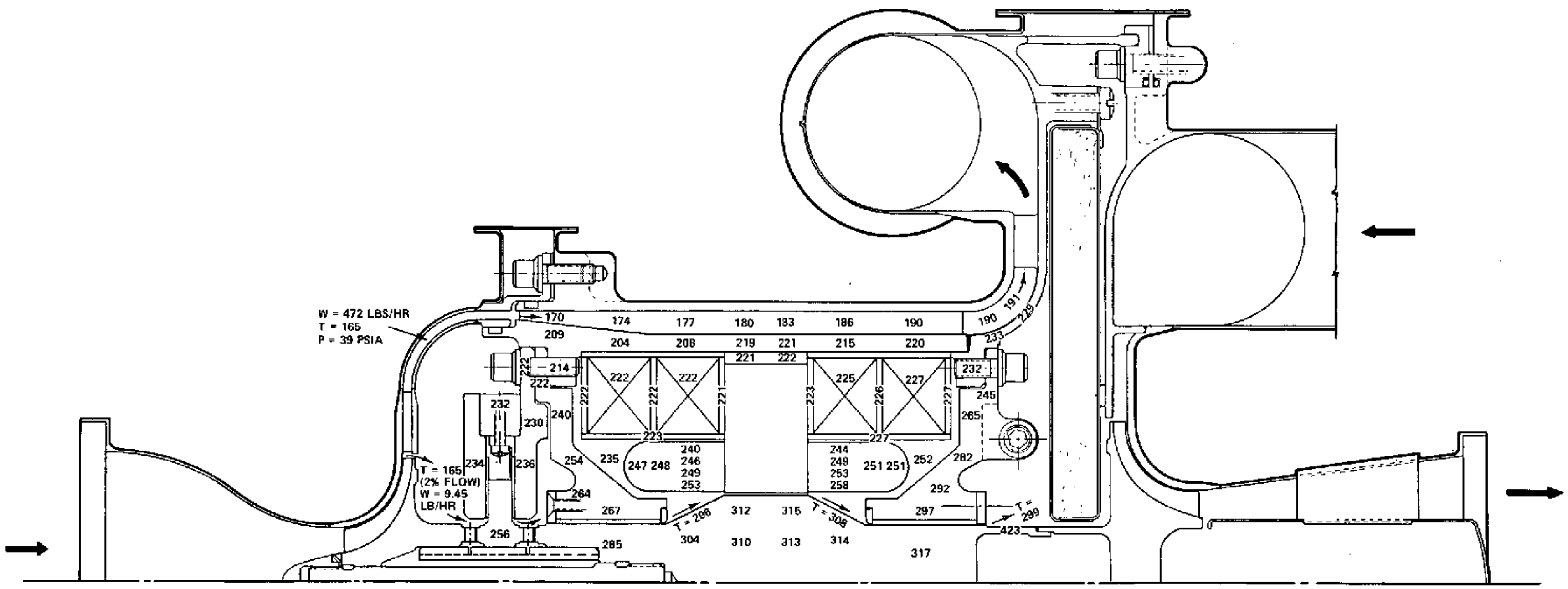


TEMPERATURES IN °F

TOTAL WINDAGE LOSSES (WATTS)

| | | |
|---|---|---|
| BEARING FRICTION | = | 78 |
| MAIN GAP | = | 29 |
| END TURN SPACE | = | 14.5 |

MS 3011-16

FIGURE 3-26

thermal gradient in the thrust rotor is small and the axial gradient even smaller. As a result, there is virtually no thermal distortion of the thrust rotor, and thrust bearing performance is unimpaired.

### 3.4.4 Alternator

The results of the thermal analysis on the final configuration of the mini-BRU alternator for 3 and 1 heat source capsules are presented in Figures 3-25 and 3-26. The heat load from the turbine was input as a heat flux (watts) versus shaft temperature. Heat generation in the foil journal and thrust bearings was also input to the analysis. A leakage flow of 2 percent was assumed to flow along the shaft from the compressor discharge to the back face of the turbine wheel. Temperatures in critical areas of the stator are seen to be well below the 400°F maximum tolerated and other temperatures throughout the machine are compatible with the materials used.

From the results of this analysis and other preliminary work, it appears that the final design selected was the most logical choice of all the schemes originally contemplated. The simple, machined rectangular fin approach employed in the final design (fin details on Figure 3-25) proved adequate without resorting to the complexity of a brazed plate fin design. The pressure drop in the rectangular fin design (0.001 $\Delta P/P$) was well below the design objective (0.005 $\Delta P/P$). The final design chosen improves cycle performance by adding heat after the compressor.

## 3.5 Heat Exchangers

### 3.5.1 Recuperator

During the course of the system optimization study, a number of alternative recuperator core configurations were investigated. The final selection was determined only after a detailed analysis, which included manufacturability, unit life expectancy, and performance considerations, was made.

Table 3-15 presents the reference recuperator design summary. The effectiveness of 0.975 and the fractional pressure drop of 0.70 percent (total both sides) represent the optimum combination with regard to minimizing total system weight.

### 3.5.2 Radiator

Many radiator configurations were investigated, and the configuration selected for the reference system is shown in Figure 3-27. The first configuration considered was steel tubes with internal fins, steel headers and ducts, and aluminum external fins and armor. Cases were run with 0, 4, 8, 16 and 32 radial fins within each tube. The bare tube case (no internal fins) showed no weight penalty over its finned counterparts. Radiators of all aluminum configuration were also investigated and presented an alternative 25 percent reduction in radiator weight, however a bimetal joining problem exists with the stainless steel ducting at two locations in the loop.

The design values for pressure drop allocation were optimized for the minimum total weight of the radiator and also for the minimum total of recuperator and radiator weight.

A summary of geometry and performance for the reference design is presented in Section 1.3.2 of this report. Throughout the analysis of the radiator, a 20 percent pressure drop margin was reserved.

# RECUPERATOR DESIGN SUMMARY

| | ORIGINAL DESIGN* | NEW DESIGN* |
|---|---|---|
| FIN CONFIGURATION: | | |
| NUMBER OF FINS PER INCH | 28. | 20. |
| FIN HEIGHT (INCHES) | 0.154 | 0.101 |
| FIN THICKNESS (INCHES) | 0.004 | 0.004 |
| FIN MATERIAL | NICKEL | HAST-X |
| PLATE CONFIGURATION: | | |
| PLATE THICKNESS (INCHES) | 0.006 | 0.008 |
| PLATE MATERIAL | HAST-X | HAST-X |
| HEADER CONFIGURATION: | | |
| NUMBER OF FINS PER INCH | 10. | 10. |
| FIN THICKNESS (INCHES) | 0.006 | 0.006 |
| FIN MATERIAL | NICKEL | HAST-X |
| GENERAL: | | |
| SPACER BAR THICKNESS (INCHES) | 0. | 0.100 |
| WRAP-UP THICKNESS (INCHES) | 0.060 | 0.060 |
| BRAZE THICKNESS (INCHES) | 0. | 0.001 |

MS 3011-47

*MATRIX FOR BOTH HIGH AND LOW PRESSURE SIDES.

TABLE 3-15

# RADIATOR MODEL

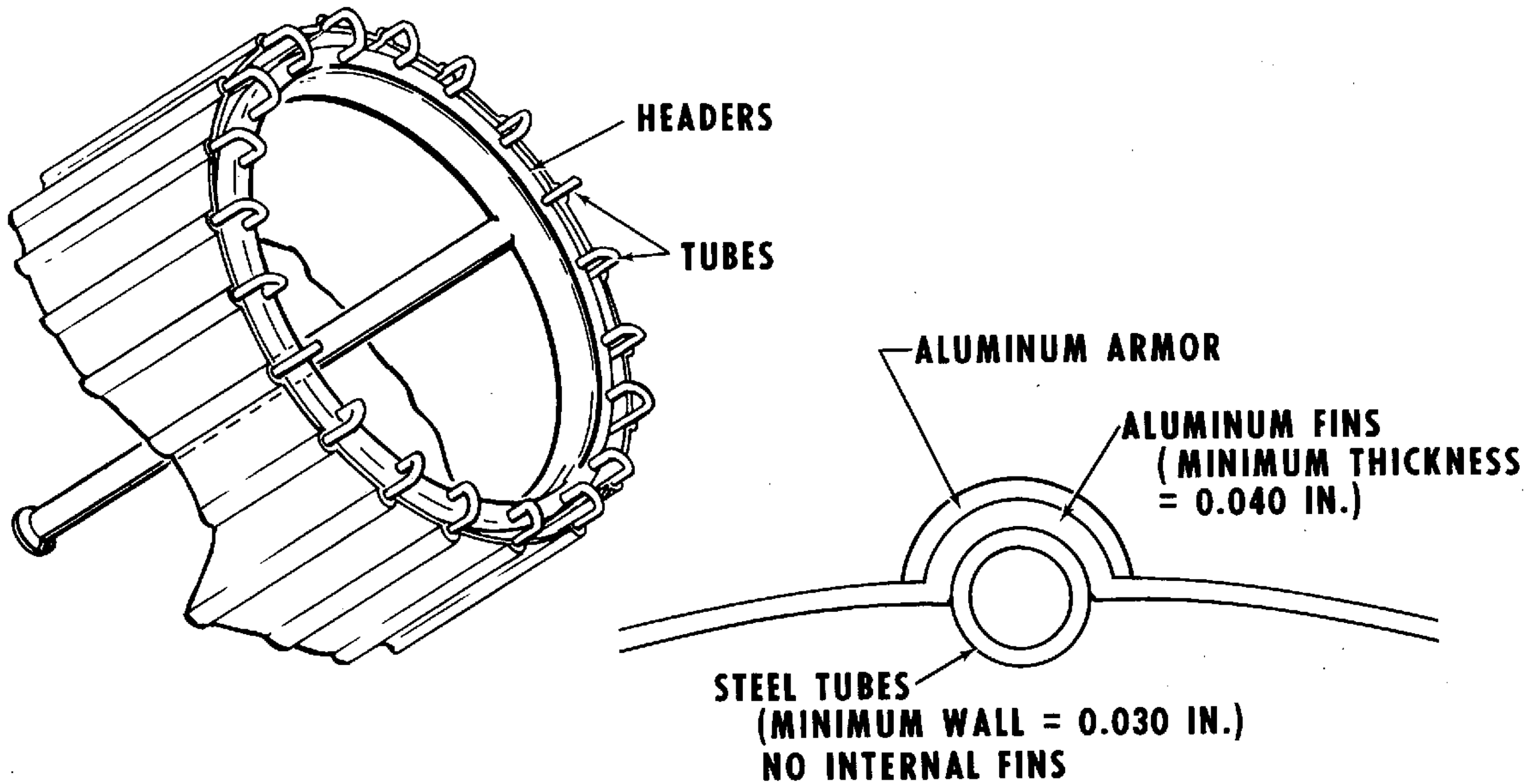


MS 3063-24

FIGURE 3-27